Enhancing Sustainability of Pollution Control with Electrochemical Oxidation Optimized by Alternating Polarity

A Thesis Presented for the

Master of Science

Degree

The University of Tennessee, Knoxville

Chenyang Wang

December 2025

DEDICATION

I dedicate my work to my family.

ACKNOWLEDGEMENTS

I would like to express my heartfelt gratitude to my advisor, Dr. Qiang He, for his invaluable guidance, encouragement, and continuous support throughout my graduate study. His expertise, patience, and insightful advice have not only directed my research but also shaped my academic and professional development.

I am sincerely thankful to my committee members, Dr. John S. Schwartz and Dr. Haochen Li, for their constructive feedback and valuable suggestions. Their guidance has been crucial in refining this thesis and broadening my perspective.

I would also like to thank my lab colleagues Dr. Clifford, Dr. Cao Liu, Richard Zhao, Rui Li and friends Mengju Yuan, Huan Wang, Liqiong Yang for their assistance and encouragement during my time at the University of Tennessee, Knoxville. Their support made my academic journey more collaborative and enjoyable.

Finally, I am deeply grateful to my family for their unwavering love, understanding, and constant encouragement. Their trust and support have always been my strongest motivation, and this accomplishment would not have been possible without them.

ABSTRACT

Electrochemical oxidation is promising for pollution control with distinctive advantages in sustainability and effectiveness, particularly in aqueous environments high in salinity and hardness. However, electrode fouling, such as scaling, is shown as a critical limitation in this application. This study investigates the potential of alternating polarity as an in-situ strategy to mitigate electrode fouling while maintaining stable oxidation efficiency. Specifically, the work evaluates the effectiveness of alternating polarity in achieving a balance among fouling control, pollutant degradation, and energy consumption.

In the first part, methylene blue was used as a surrogate in a continuous reactor to optimize parameters including different electrode configurations (anode/cathode: Boron-Doped Diamond (BDD)/ graphite (Gr), Gr/Gr), polarity modes (constant polarity, alternating polarity), and polarity-exchange frequency (0.25 hr^{-1}, 0.5 hr^{-1}, 2 hr^{-1}). With constant polarity, electrochemical treatment of methylene blue exhibited an initial removal efficiency of 95%, which, however gradually declined with prolonged treatment beyond 0.5 hr due to electrode fouling by scaling. In comparison, the use of alternating polarity resulted in sustained removal of methylene blue with the reduction in scaling by over 87% as well as the increase in the production of free chlorine as the oxidizing agent by 185%. Further testing of alternating polarity indicated that the exchange frequency of 0.5 hr^{-1} was optimal for sustained treatment efficiency and mitigation of electrode scaling. Moreover, the use of graphite as electrode material resulted in the reduction in energy consumption by 27% as compared with BDD as the electrode material.

In the second part, a hydrophobic n-alkane (n-docosane) typical of petroleum produced water, was used as the target pollutant. Batch experiments were conducted to optimize the applied voltage (2, 4, 5V) and electrode configurations (BDD/BDD, BDD/Gr, Gr/Gr). Effective degradation was achieved at applied voltages above 4 V. Graphite electrodes exhibited strong affinity toward n-docosane, which facilitated the adsorption of the pollutant onto the electrode surface and promoted its subsequent electrochemical oxidation. Adsorption experiments revealed that equilibrium was reached within 6 hours with a capacity of 0.11 g(n-docosane) $g(graphite)^{-1}$. As a result, graphite-containing configurations achieved higher overall removal efficiency. Semi-continuous tests were conducted under the optimized conditions determined in the first part. Under constant polarity, the removal efficiency of n-docosane declined from a peak of 86.3% at 48 hours to 58.7% at 120 hours, indicating progressive electrode deactivation and loss of

treatment performance. In contrast, alternating polarity using the Gr/Gr configuration improved overall removal efficiency from 72.0% (constant polarity, BDD/Gr) to 85.7% and effectively prevented performance deterioration, although electrode corrosion was observed at high current densities for the Gr/Gr setup.

Overall, this study demonstrates that sustainable application of alternating polarity–assisted EO requires an integrated strategy combining electrode material selection, optimized voltage operation, and carefully tailored polarity-exchange frequency to simultaneously achieve fouling mitigation, high degradation efficiency, and energy efficiency.

Key words: electrochemical treatment; alternating polarity; electrode material; exchange frequency; fouling mitigation; organic pollutant.

TABLE OF CONTENTS

LIST OF TABLES

LIST OF FIGURES

CHAPTER I INTRODUCTION AND LITERATURE REVIEW

Background and significance

Of the Earth's total water resources, only about 0.65% is directly available for human use, while the vast majority exist in inaccessible forms such as saline oceans and seas (97.2%) and glaciers (2.15%) (Salehi, 2022). Rapid population growth and economic development have intensified global water demand, resulting in recurrent regional and seasonal shortages and placing increasing pressure on effective water resource management and allocation. In the context of the carbon peak and carbon neutrality goals, and under the challenges posed by the global energy crisis, wastewater is now regarded not only as an alternative water source but also as a renewable energy carrier within industrial processes. Accordingly, there is an urgent need to develop efficient, sustainable, and environmentally friendly treatment technologies that enable wastewater reclamation, reduce pollutant discharge, and ultimately mitigate or eliminate adverse environmental impacts.

Salinity is a critical parameter in wastewater treatment, with high salinity typically defined as an inorganic salt content of 1–3.5% (w/w), while seawater contains approximately 3.5% (w/w) (Lin et al., 1998; Ontiveros et al., 2013). Substantial volumes of high-salinity wastewater are generated across a wide range of industrial sectors, including coal-chemical production, agricultural by-product processing, pharmaceuticals, papermaking, aquaculture, the nuclear industry, agriculture and food processing, petroleum and natural gas extraction, and leather manufacturing (Bao et al., 2023; Guo et al., 2023; Guo et al., 2018; Li et al., 2002). These effluents are characterized by complex compositions, combining large amounts of inorganic salts with recalcitrant organic pollutants (Li et al., 2021). Without adequate treatment, their discharge not only results in the loss of valuable mineral resources but also leads to severe environmental consequences, such as water mineralization, soil salinization, and eutrophication (Guo et al., 2023). Compared with conventional industrial effluents, high-salinity wastewater poses far greater treatment challenges (Li et al., 2002). Biological processes are severely limited due to the inhibitory effects of elevated salinity on microbial activity (Zhao et al., 2020). Although acclimated microbial consortia have been explored, their performance remains unsatisfactory because they can only treat relatively low COD concentrations

and require long hydraulic retention times (He et al., 2017). Traditional physical and chemical treatment methods including evaporation and membrane techniques are also difficult to generalize due to excessive chemical consumption, equipment corrosion and fouling, and high operating costs (Guo et al., 2018; Li et al., 2002). Advanced integrated chemical treatment processes, including coagulation, sedimentation, filtration, aerated biological filters, ozonation, and activated carbon adsorption, can improve effluent quality but often still fail to meet increasingly stringent discharge standards (Li et al., 2002). Therefore, the development of efficient, environmentally friendly, and sustainable treatment technologies has become an urgent priority.

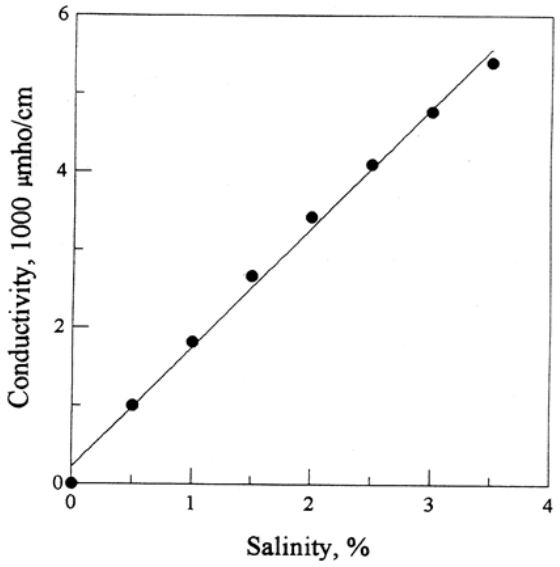

Figure 1.1: Conductivity of sample wastewater as a function of salinity (Lin et al., 1998)

Among emerging options, advanced oxidation processes (AOPs) have been extensively studied in recent years for the treatment of high-salinity wastewater (Cataldo et al., 2016). AOPs exhibit distinct advantages, including fast reaction rates, complete mineralization, absence of secondary pollution, broad applicability, the ability to induce chain reactions, and relatively simple mechanisms (Bilińska et al., 2017). Their core principle lies in the in-situ generation of hydroxyl radicals, which effectively degrade and mineralize organic contaminants. Depending on the generation pathways and reaction conditions of ·OH, AOPs can be classified into several types, including Fenton oxidation, photocatalysis,

electrochemical oxidation, ozonation and so on (Bilińska et al., 2017; Stasinakis, 2008; Yuan et al., 2014). Given the inherently high conductivity of saline wastewater, electrochemical methods represent a promising alternative for its treatment by taking advantage of this characteristic. Such methods have already been successfully applied to the treatment of various types of industrial wastewater (Li et al., 2021). Among them, electrochemical oxidation (EO) stands out, as it provides notable advantages compared with other electrochemical processes, such as high reproducibility, short operational time, clean reaction pathways, adaptability to conventional environmental conditions, and relatively low cost (Martínez-Huitle and Panizza, 2018). EO has been effectively employed for the removal of diverse pollutants, including antibiotics, herbicides, alcohols, and various non-biodegradable organic contaminants (Martinez-Huitle and Ferro, 2006; Martínez-Huitle and Panizza, 2018; Panizza and Cerisola, 2009). In addition, its effectiveness at the industrial scale has been confirmed, highlighting EO as a practical and sustainable option for wastewater treatment.

Development of EO and fundamentals

Recently, the presence of emerging and persistent pollutants such as microplastics, antibiotics and pharmaceutical compounds caused challenges in conventional biological treatment due to the barely biodegradable recalcitrant, which calls for the innovative technology (Cao et al., 2017; Li et al., 2019). Electrochemical oxidation is the most popular electrochemical procedure among the EAOPs for decontaminating organic pollutants from wastewater and is very adaptable that can blend with existing wastewater treatment (Panizza and Cerisola, 2009). The development of EO can be traced back to the late nineteenth century, when the electrochemical destruction of cyanide from mining effluents was first attempted, marking the conceptual origin of electrochemical water treatment (Martínez-Huitle and Panizza, 2018). Early patents soon followed: in 1889 the use of electricity for water purification was proposed in the UK, in 1904 Elmore patented electrolysis for mineral beneficiation, and in 1909 electrocoagulation with aluminum and iron electrodes was patented in the US, leading to the first large-scale drinking water application in 1946. However, due to high investment and energy costs, these technologies did not achieve wide adoption until stricter environmental regulations in the

late twentieth century stimulated renewed interest. Systematic research on EO began in the 1970s, with Nilsson, Mieluch, Dabrowski, and others pioneering studies on phenol oxidation and pilot-scale wastewater treatment, followed in the 1980s by Kirk, Stucki, Kotz, Chettiar, and Watkinson, who clarified the roles of electrode materials and operating conditions (Bao et al., 2023; Martinez-Huitle and Ferro, 2006). In the 1990s, Johnson, De Battisti, and Comninellis introduced the concepts of active and non-active anodes and demonstrated the exceptional properties of boron-doped diamond (BDD) electrodes for non-selective mineralization, which represented a major breakthrough in EO (Shestakova and Sillanpää, 2017). Since the 2000s, EO has expanded from model pollutants to diverse industrial wastewaters such as textile dyes, pharmaceuticals, pesticides, and petrochemicals, with research emphasizing energy efficiency, electrode stability, and hybrid process integration (Bilińska et al., 2017; Guo et al., 2018; Ontiveros et al., 2013). In recent years, advances in electrode materials, reactor design, and polarity strategies have enabled EO to address highly saline and hardness wastewater, consolidating its status as a robust and competitive advanced oxidation process for treating refractory pollutants.

The conceptual scheme of an electrochemical reactor is illustrated in Fig. 2, consisting of a power supply, a cathode, an anode, and the electrolyte. Electrochemical oxidation of pollutants generally proceeds through two distinct pathways: direct oxidation and indirect oxidation (Martinez-Huitle and Ferro, 2006; Martínez-Huitle and Panizza, 2018). In the case of direct oxidation, the reaction occurs in two consecutive steps: (i) pollutants present in the bulk solution diffuse toward the anode surface, which often represents the rate-limiting step of the process; and (ii) the adsorbed pollutants undergo oxidation through direct electron transfer between the anode and the organic molecules (Anglada et al., 2009; Bao et al., 2023; Martinez-Huitle and Ferro, 2006). The efficiency of this step is mainly governed by the electrocatalytic activity of the anode material and the applied current density. Theoretically, this direct oxidation reaction is expected to occur at anodic potentials below the onset of the oxygen evolution reaction (OER) (Eq.1.1), relying exclusively on free electrons without the involvement of external oxidizing agents (Li et al., 2019). It should be noted that the onset potential of OER varies depending on the

electrode material employed. There are two pathways for organic pollutants after direct oxidation: electrochemical conversion and electrochemical combustion. Electrochemical conversion (Eq. 1.2) means pollutants being partially oxidized and need further treatment (Panizza and Cerisola, 2009). Electrochemical combustion (Eq. 1.3) means pollutants being transformed into water, carbon dioxide and other inorganic compounds (Panizza and Cerisola, 2009).

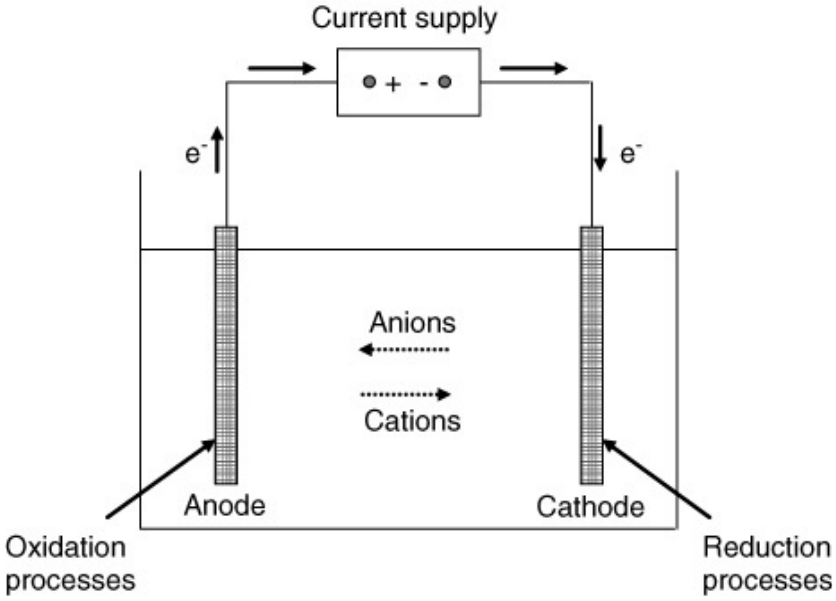

Figure 1.1: Conceptual diagram of electrochemical reactors (Anglada et al., 2009)

For indirect oxidation, pollutants are degraded by powerful oxidizing species generated in situ either at the anode surface or in the bulk solution (Panizza and Cerisola, 2009). These species include physisorbed hydroxyl radicals (M·OH), produced during the water oxidation reaction (Eqs. 1.4 and 1.5) at the electrode surface, as well as secondary oxidants such as hydrogen peroxide (H_2O_2), ozone (O_3), active chlorine species (Cl_2, $HClO/ClO^-$) (Eq. 1.6-7), and peroxydisulfate ($S_2O_8^{2-}$), which are formed through parallel electrochemical reactions of water or electrolyte ions in the solution phase (Lee et al., 2020). Unlike direct electron transfer, these oxidizing agents can diffuse into the bulk solution due to its long lifetime, thereby extending the reaction zone beyond the electrode surface and achieving higher oxidation efficiency with reduced dependence on pollutant adsorption (Anglada et al., 2009; Li et al., 2019; Martinez-Huitle and Ferro, 2006). As a

result, indirect oxidation is often regarded as the predominant pathway for the effective mineralization of refractory organic pollutants in electrochemical systems.

$$R \rightarrow P + e^- \quad \text{Equation 1.1}$$

$$R \rightarrow CO_2 + H_2O + Salts + e^- \quad \text{Equation 1.2}$$

$$M + H_2O \rightarrow M(\cdot \mathrm{OH}) + \mathrm{H}^+ + e^- \quad \text{Equation 1.3}$$

$$R + M(\cdot \mathrm{OH}) \rightarrow M + CO_2 + H_2O \quad \text{Equation 1.4}$$

$$2Cl^- \rightarrow Cl_2(aq) + 2e^- \quad \text{Equation 1.5}$$

$$Cl_2(aq) + H_2O \rightarrow HClO + Cl^- + H^+ \quad \text{Equation 1.6}$$

$$HClO \rightarrow ClO^- + H^+ \quad \text{Equation 1.7}$$

Factors influencing electrochemical oxidation performance

Electrode material

In EO technology, the electrode is the core component that governs both process efficiency and economic feasibility (Shestakova and Sillanpää, 2017). An ideal electrode must exhibit excellent physicochemical stability to withstand erosion, corrosion, and passivation; possess sufficient electrical conductivity to ensure efficient electron transfer; display high catalytic activity and selectivity to promote the oxidation of organic pollutants while minimizing side reactions; and achieve a favorable balance between cost and service life (Najafinejad et al., 2023). Among these, the anode plays a decisive role, as its catalytic activity and stability directly determine the rate, extent, and sustainability of oxidation reactions. Extensive research has focused on developing advanced anode materials through rational material selection, structural design, and optimization of fabrication methods (Mehrkhah et al., 2023). At the same time, the inherent competition between the oxygen evolution reaction (OER) and the oxidation of organics must be carefully considered, since OER not only decreases electron utilization efficiency but also compromises long-term electrode stability (Radha and Sirisha, 2018).

Historically, studies initially employed graphite and pure metal electrodes owing to their high conductivity, low cost, and operational simplicity (Periyasamy and Muthuchamy, 2018; Zhu et al., 2019b). For example, graphite electrodes demonstrated high degradation efficiency toward methyl orange and the anticancer drug cytarabine, while Al and Fe electrodes not only facilitated pollutant oxidation but also generated colloidal particles that aided in wastewater clarification (Shestakova and Sillanpää, 2017; Zhu et al., 2019b).

However, their poor corrosion resistance and limited catalytic activity significantly restricted practical applications. Metal oxide electrodes are known as dimensionally stable anode (DSA) due to its good stability and high catalytic activity, which applied in industrial over 30 years (Pikaar et al., 2011). Early oxide-based DSAs improved conductivity and corrosion resistance but suffered from poor mechanical strength, leading to the development of Ti-based coated electrodes with superior durability (Bagastyo et al., 2011; Scialdone, 2009). Recent advances, including element doping, intermediate layers, and nanostructured modifications, have further enhanced their oxidation capacity, stability, and service life (Panizza and Cerisola, 2009; Shestakova and Sillanpää, 2017). With low cost and strong performance, Ti-based DSAs remain among the most promising anode materials for EO wastewater treatment. Boron-doped diamond (BDD) electrodes, developed in the late 1990s, combine the inherent stability of diamonds with excellent electrical conductivity (Clematis and Panizza, 2021). They feature high mechanical strength, corrosion resistance, and long service life, as well as a high oxygen evolution overpotential that favors ·OH radical generation, giving them superior oxidation capacity in mineralizing persistent organic pollutants (Clematis and Panizza, 2021). Nevertheless, their high fabrication cost and limited scalability remain major barriers to widespread application. Sub-stoichiometric titanium oxide electrodes, particularly Ti_4O_7 and Ti_5O_9 of the Magnéli phase, exhibit high conductivity, wide potential window, strong corrosion resistance, and long service life, making them attractive alternatives to DSA and BDD (Wang et al., 2024). Recent studies have demonstrated their superior oxidation ability for pharmaceuticals, antibiotics, pathogens, and persistent pollutants, achieving near-complete mineralization and effective pathogen/ARG removal (Alnaimat et al., 2024). Structural modifications, including intermediate layers, porous architectures, and nanotube arrays, further enhance catalytic activity, surface area, and stability while reducing energy consumption. Owing to their strong performance and lower cost compared to BDD, Magnéli phase Ti_4O_7-based electrodes are considered highly promising candidates for wastewater treatment applications (Alnaimat et al., 2024; Mehrkhah et al., 2023; Najafinejad et al., 2023; Wang et al., 2024).

Table 1.1: Potential of oxygen evolution of different anodes

Anode	Potential (V vs SCE)	Conditions
Graphite	1.7	0.5 mol L^{-1} H_2SO_4
pt	1.3	0.5 mol L^{-1} H_2SO_4
IrO2	1.6	1 mol L^{-1} H_2SO_4
PbO2	1.9	0.5 mol L^{-1} H_2SO_4
Si/BDD	2.3	0.5 mol L^{-1} H_2SO_4
Ti/BDD	2.7	0.5 mol L^{-1} H_2SO_4
Ti/Ti_4O_7	2.16–2.44	0.1M Sodium salt solution

Current density

Current density (*i*) defined as the applied current normalized by the electrode surface area, is widely recognized as the most important operational parameter in EO because it directly controls the rate of electrochemical reactions (Fernandes et al., 2016; Periyasamy and Muthuchamy, 2018). Applied voltage is often treated as an alternative expression of current density, since the two are intrinsically related in galvanostatic systems (Lu et al., 2024). In such systems, interelectrode spacing is fixed and current is continuously supplied, making current density the primary variable that can be externally adjusted. Process efficiency is influenced not only by the applied current density itself but also by wastewater composition, electrode characteristics, and the balance between direct and indirect oxidation mechanisms (Martinez-Huitle and Ferro, 2006; Periyasamy and Muthuchamy, 2018; Radha and Sirisha, 2018). At low current densities, EO is typically under kinetic control rather than mass transport limitation. In this regime, pollutant molecules can readily diffuse to the electrode surface and undergo oxidation, so increasing current density generally enhances degradation efficiency (Martinez-Huitle and Ferro, 2006). For example, removal of dyes or phenolic compounds has been shown to increase steadily with current density in the low range, as the generation of hydroxyl radicals and other reactive intermediates is still effectively consumed by organics at the anode interface (Enache and Oliveira-Brett, 2011; Isaev et al., 2023). In contrast, at high current densities, the situation changes markedly. Once the transport of pollutants to the electrode becomes rate-limiting, the surplus current tends to favor side reactions, particularly the oxygen evolution reaction (OER). This parasitic pathway reduces current

efficiency (CE) because a larger fraction of electrons is wasted in O_2 generation rather than pollutant oxidation (Periyasamy and Muthuchamy, 2018). As a result, the energy consumption of the process increases while pollutant removal efficiency plateaus or even declines. Numerous studies have confirmed that excessive current densities lead to diminished CE and higher operating costs, especially when treating effluents with low organic loads (Fernandes et al., 2016; Saracco et al., 2000). The intermediate current density range corresponds to a mixed kinetic regime. Here, both pollutant oxidation and side reactions proceed simultaneously, leading to a trade-off between higher removal rates and lower CE. Under such conditions, the optimal current density is highly dependent on the effluent matrix. For example, in real textile wastewater treatment with a boron-doped diamond (BDD) anode, increasing the applied current density from 20 to 60 mA cm^{-2} significantly accelerated COD removal (Zou et al., 2017). This improvement was attributed not only to faster pollutant oxidation but also to the enhanced formation of reactive species such as hydroxyl radicals, which minimized mass transport limitations and partially suppressed OER.

Another important consideration is the formation of mediated oxidants. At elevated current densities, the generation of species such as active chlorine (Cl_2, HClO, ClO^-), ozone, hydrogen peroxide, persulfate ($S_2O_8^{2-}$), and peroxophosphates is favored (Periyasamy and Muthuchamy, 2018). These oxidants extend the oxidative capacity of the system beyond the electrode surface, allowing degradation of complex and bulky molecules that are otherwise resistant to direct oxidation. For instance, azo dyes and anthraquinone compounds, which are difficult to mineralize by direct electron transfer alone, can be effectively decomposed through mediated oxidation pathways involving ·OH and $S_2O_8^{2-}$ radicals generated at higher currents. However, the balance is delicate, since overproduction of oxidants may also increase secondary reactions, energy demand, and electrode wear. The influence of current density is further complicated by wastewater characteristics. Effluents with high organic loads tend to utilize oxidants more efficiently, thereby sustaining higher CE even at elevated current densities. Conversely, when the pollutant concentration is low, a large portion of electrogenerated oxidants is wasted in side reactions, which severely decreases efficiency. Similarly, the supporting electrolyte

composition, pH, and temperature can modify the speciation and stability of mediated oxidants, influencing the optimal current density window.

Case studies also illustrate the dual role of current density. During the EO of 4-chlorophenol using a BDD anode, COD removal efficiency increased at 15 and 30 mA cm^{-2} but showed little additional improvement at 60 mA cm^{-2}, where OER became dominant. In contrast, during the mineralization of dyes such as methyl orange and congo red, higher current densities promoted the accumulation of carboxylic acids initially but eventually led to complete decolorization and mineralization, with efficiencies strongly correlated to pollutant concentration and current applied. These findings confirm that current density optimization is system-specific and requires consideration of pollutant type, concentration, and operational conditions.

In summary, current density plays a decisive role in EO by dictating the balance between pollutant oxidation, oxidant generation, and parasitic reactions. Low values favor efficient pollutant utilization but may limit reaction rates; high values accelerate oxidant production but often reduce CE through OER and mass transport limitations; intermediate values present a trade-off scenario that must be optimized for each system. Moreover, the effect of current density cannot be considered in isolation—it interacts strongly with anode material properties, wastewater composition, and hydrodynamic conditions. For practical applications, careful optimization of current density is essential to maximize pollutant removal while minimizing energy consumption, ensuring that EO remains a cost-effective and sustainable technology for wastewater treatment.

Cell configuration

The configuration of the electrochemical cell is a decisive factor in governing mass transfer efficiency and the scalability of EO processes (Martinez-Huitle and Ferro, 2006). To enhance pollutant transport to the electrode surface, strategies such as gas sparging, increased fluid velocity, the use of baffles or turbulence promoters, and even sono-electrochemical methods have been investigated (Martínez-Huitle and Brillas, 2021; Rocha et al., 2012). In parallel, the rational design and fabrication of efficient electrochemical reactors play an equally important role in further improving overall process performance.

Based on electrode configuration, electrochemical reactors are generally classified into two types: two-dimensional (2D) and three-dimensional (3D) systems. Although 2D reactors are simpler in design and widely applied, they are often constrained by limited electrode surface area and relatively low current efficiency. To overcome these limitations, the concept of 3D electrodes was introduced by Bickhurst et al. in the 1960s (Backhurst et al., 1969), in which the interelectrode space of conventional 2D cells is filled with particulate materials such as activated carbon or metal granules (Arenas et al., 2019). This design significantly increases the effective electrode surface area and enhances mass transfer. Since then, 3D electrochemical reactors have been successfully applied in the treatment of landfill leachate, pharmaceutical wastewater, heavy metal ions, and various persistent organic pollutants (POPs), demonstrating their broad potential in wastewater remediation (Jajuli et al., 2020; Shi et al., 2020; Yu et al., 2020; Zhang et al., 2020).

Another important aspect is the distinction between divided and undivided cells. In divided cells, the anolyte and catholyte compartments are separated by diaphragms or ion-conducting membranes, which enable selective control of redox environments and oxidant production. This separation can suppress undesired side reactions between anodic and cathodic products. Bensalah et al. (2021) compared the EO of 2-chloroaniline in divided and undivided cells and found that the divided configuration enhanced treatment efficiency and reduced energy consumption. The performance of such systems, however, relies heavily on the choice of membrane, which must simultaneously provide high ionic conductivity and maintain mechanical and chemical stability. Despite these advantages, divided cells are often avoided in practice due to their higher cost, mechanical complexity, and corrosion issues associated with narrow electrode gaps (Martinez-Huitle and Ferro, 2006). Undivided cells, in contrast, are simpler, more cost-effective, and easier to operate, making them more common in EO wastewater treatment applications (Martínez-Huitle and Panizza, 2018).

Electrolyte

The electrolyte is a critical parameter in EO because it governs solution conductivity, influences oxidant generation pathways, and determines the suitability of reactor configurations such as divided or undivided cells (Periyasamy and Muthuchamy, 2018). In laboratory studies, synthetic wastewaters are often prepared by dissolving target pollutants in solutions containing large amounts of NaCl or Na_2SO_4 to ensure sufficient conductivity (Pikaar et al., 2011; Scialdone et al., 2009). Such systems facilitate mechanistic investigation and identification of degradation intermediates, but the pollutant and salt concentrations are typically much higher than in real effluents, which limits the extrapolation of results to practical applications. In practice, industrial wastewater is more complex, and electrolyte composition is determined by the process that generates the effluent (Li et al., 2021; Pikaar et al., 2011). High salinity wastewater naturally possesses high conductivity, which reduces cell voltage and energy demand, making EO particularly advantageous (Lin et al., 1998). The presence of chloride ions promotes the formation of active chlorine species (Cl_2, HClO, ClO^-), which enhances mediated oxidation but may also lead to chlorinated byproducts and secondary pollution. In contrast, sulfate-rich electrolytes can produce persulfate ($S_2O_8^{2-}$), a powerful oxidant considered a cleaner alternative with lower risk of halogenated byproducts (Lee et al., 2020). However, high-hardness wastewaters, containing large amounts of Ca^{2+} and Mg^{2+}, present additional challenges. These divalent cations readily combine with anions such as CO_3^{2-} or SO_4^{2-} to form insoluble scales on electrode surfaces, which block electron transfer, reduce effective active area, and accelerate electrode deactivation (Asaithambi et al., 2020; Chow and Pham, 2021).

Electrolyte composition also influences reactor design. In divided cells, membranes allow efficient and selective production of oxidants such as persulfates or perphosphates, which can be introduced into wastewater in a two-stage treatment approach (Lee et al., 2020; Yuan et al., 2014). The advantage of this strategy is that oxidant generation conditions (e.g., temperature, solution composition) can be optimized independently from the wastewater matrix. However, separating oxidant generation from pollutant degradation sacrifices the benefits of in situ activation, which is critical for generating highly reactive

radicals such as ·OH. To overcome this limitation, hybrid systems combining electrogenerated oxidants with UV irradiation, ultrasound, or H_2O_2 have been investigated to enhance process efficiency (Chuang et al., 2017; Wang et al., 2024; Yuan et al., 2014). Overall, electrolytes in EO play a dual role: they provide conductivity for the electrochemical process and serve as precursors of mediated oxidants that extend oxidative capacity.

Other factors

In addition to electrode materials, operating conditions, cell configuration, several engineering parameters such as flow rate, inter-electrode gap, temperature, and initial concentration of pollutants, also strongly affect EO system (Scialdone et al., 2009). The mass transfer coefficient of an EO system is governed by flow rate, hydrodynamic conditions, and reactor geometry. The inter-electrode gap plays a crucial role by directly influencing electrical resistance and diffusivity of reactive species, narrow gaps reduce ohmic losses and improve COD removal efficiency (Mandal et al., 2017). Temperature influences EO primarily through its effect on mass transfer and oxidant reactivity. Higher temperatures improve diffusion rates and can accelerate oxidation between organics and active chlorine (Liu et al., 2017).

EO challenges in real applications

Despite its advantages, the practical application of EO still encounters several challenges that hinder its large-scale implementation. High energy consumption and cost remain critical barriers, requiring innovations such as flow-through 3D reactors, improved electrode stability, and advanced materials to enhance efficiency and reduce expenses (Martínez-Huitle and Brillas, 2021; Zhu et al., 2025). Another key issue is the formation of toxic by-products (e.g., AOX, chlorate, perchlorate) in halide-rich wastewater, requiring careful monitoring under realistic wastewater conditions where contaminants are often present at low concentrations and subject to mass transfer limitations (Yang, 2020). For highly hazardous wastes, robust anodes such as BDD and Ti/SnO_2 offer promise, though integration with granular activated carbon may be necessary to minimize halogenated by-products (da Silva Santos et al., 2022).

In addition, maintaining stable performance during long-term operation remains a significant challenge for EO applications. In high salinity and high hardness wastewater, electrode deactivation caused by fouling and scaling becomes particularly severe. Organic fouling at the anode, often due to polymeric by-products from phenolic or aromatic pollutants (Liu et al., 2021b). Cathodic scaling arises from the precipitation of Ca^{2+} and Mg^{2+} as carbonates or sulfates under locally alkaline conditions, forming dense inorganic deposits that hinder electron transfer, increase ohmic resistance, and accelerate electrode passivation (Lu et al., 2024). Over prolonged operation, these processes not only reduce treatment efficiency but also shorten electrode lifetime, making the development of effective anti-scaling strategies essential for practical deployment of EO in high salinity and high hardness water environments (Guo et al., 2023). Various strategies have been explored to mitigate scaling. Conventional approaches include optimizing operating conditions such as lowering current density, adjusting pH, or enhancing hydrodynamics to minimize local supersaturation; applying chemical softening or antiscalants to remove hardness ions prior to electrochemical treatment; and periodic chemical or mechanical cleaning of electrodes to dissolve or detach deposits (Zhou et al., 2022). In addition, electrode material designs such as protective coatings, surface modifications, or the use of stable conductive ceramics can also delay scale formation and improve tolerance (Hanssen et al., 2016). However, these strategies are often costly, introducing secondary pollutants, or failing to provide continuous protection under real wastewater conditions (Hanssen et al., 2016). An alternative and increasingly attractive approach are the use of alternating polarity operation, in which periodic reversal of electrode polarity promotes the dissolution of scale deposited on the cathode, thereby preventing accumulation and maintaining stable electrochemical performance (Chow and Pham, 2021; Jang et al., 2024; Liu et al., 2021a). This method offers a simple, chemical-free, and energy-efficient pathway to mitigate scaling, making it particularly suitable for EO treatment of high-salinity and high-hardness waters.

Research gap and objectives

Alternating polarity has been extensively studied in electrocoagulation and water-softening applications (Chow et al., 2021; Chow and Pham, 2021; Fuladpanjeh-Hojaghan

et al., 2023; Jin et al., 2019). In electrocoagulation, sacrificial metal anodes dissolve to release ions (e.g., Al^{3+}, Fe^{2+}), which hydrolyze and form oxides that act as coagulants for pollutant removal (Chow et al., 2021). However, the localized alkaline environment near the cathode promotes precipitation of inorganic species, leading to the formation of a fouling layer on the electrode surface. This layer progressively deactivates the electrode, lowers treatment efficiency during long-term operation, and increases energy consumption and operational costs (Fuladpanjeh-Hojaghan et al., 2023). By periodically reversing electrode polarity, alternating polarity alters the dominant electrochemical reactions at each electrode and enables in situ dissolution of fouling deposits, thereby sustaining treatment performance (Chow et al., 2021). The effectiveness of AP is influenced by solution chemistry, electrode material and configuration, and operating parameters such as current density and polarity exchange frequency (Abdollahi et al., 2025; Chow and Pham, 2021; Fuladpanjeh-Hojaghan et al., 2023; Jang et al., 2024). For example, when treating dry wastewater using electrocoagulation, NaCl is a more favorable electrolyte than Na_2CO_3, as it enhances energy efficiency and facilitates partial depassivation of the electrodes (Mandal et al., 2020). This effect corresponds to the ability of high chloride ion concentrations to promote localized pitting, which disrupts passive layers and maintains electrode activity (Feng et al., 2023). Alternating polarity diminished the fouling and increased Faraday efficacy (the coagulant production efficiency per unit of electric charge passed through the system) of Al electrode but not Fe electrode (Chow and Pham, 2021). The mechanism by which alternating polarity mitigates electrode passivation in electrocoagulation is analogous to its role in water-softening processes, where it facilitates the detachment of inorganic scale formed during electrochemical precipitation, thereby preventing cathodic deactivation and the associated increase in electrical resistance (Jin et al., 2019). These parallels collectively demonstrate the broad potential of alternating polarity for mitigating electrode fouling and enhancing the stability of electrochemical systems.

Beyond fouling control, alternating polarity has also been applied for resource recovery, bipolar synergistic catalysis and electrochemical reaction pathways regulation in environmental remediation and environmental electrocatalysis. Lei et al. (2022) used

alternating polarity to ensure a large cathode surface area for electrochemically mediated calcium phosphate precipitation (ECaPP) for phosphorus removal and recovery from cheese wastewaters. Zhang et al. (2025) used biochar based alternating polarity to alter heavy metal speciation to improve the efficiency of plant extraction. Chow et al. (2021) demonstrated that a higher current density does not necessarily translate into improved Faradaic efficiency, since the outcome is strongly dependent on electrode material and the frequency of alternating polarity frequency. These findings collectively underscore the versatility of alternating polarity but also reveal its complex and context dependent behavior.

Despite these advantages, most studies have focused on either fouling mitigation or pollutant removal efficiency in isolation. For instance, research on the electrochemical degradation of per- and polyfluoroalkyl substances (PFAS) or antibiotics under alternating polarity often reported diminished electrode fouling, but the primary emphasis remained on improving degradation efficiency (Li et al., 2024a; Yang et al., 2022). In such systems, water hardness was not considered a key factor limiting performance. Although these studies acknowledged that constant polarity could lead to cathode precipitation, the hardness levels in their experimental matrices were relatively low compared with those of real high-hardness wastewaters. Consequently, electrode scaling was not regarded as a critical limitation, and research efforts largely concentrated on enhancing degradation efficiency. Integrated investigations that systematically examine the coupling between electrode passivation control and treatment performance remain scarce, representing an important knowledge gap for advancing the practical application of alternating polarity in complex wastewater systems. This study investigates alternating polarity operation as a strategy to mitigate scaling and enhance the long-term performance of EO. First, methylene blue (MB) was employed as a model pollutant to systematically evaluate the effects of prolonged operation, electrode material choice, and polarity reversal on degradation efficiency and scaling behavior. The optimal polarity exchange frequency was further determined to balance pollutant removal and energy consumption. Building upon these findings, the study was extended to the treatment of n-alkane (n-docosane) in synthetic petroleum produced water. The adsorption behavior of

n-docosane on graphite, degradation performance under varying voltages and electrode configurations, and comparative evaluation of batch versus semi-continuous reactors under constant and alternating polarity were comprehensively examined.

The overall objectives of this work are therefore to:

1. Elucidate the impact of long-term EO operation on degradation efficiency and electrode scaling under high-salinity/high-hardness conditions.
2. Assess the effectiveness of alternating polarity in mitigating cathodic scaling and maintaining stable pollutant degradation.
3. Optimize polarity exchange strategies to maximize degradation efficiency while minimizing energy input.
4. Extend the applicability of alternating polarity-assisted EO to petroleum produced water, with a focus on n-alkane degradation and realistic wastewater complexity.

Through this approach, the study aims to provide mechanistic insights and practical guidance for improving the efficiency, stability, and scalability of EO systems in high salinity and high hardness wastewater treatment.

CHAPTER II OPTIMIZATION ELECTROCHEMICAL TREATMENT OF ORGANIC POLLUTANT IN HIGH HARDNESS / SALINITY WASTEWATER TREATMENT

Abstract

Electrochemical oxidation is promising for pollution control with distinctive advantages in sustainability and effectiveness, particularly in aqueous environments high in salinity and hardness. However, electrode fouling, such as scaling, is a critical limitation in this application. This study aimed to evaluate the potential of alternating polarity in mitigating electrode fouling with sustained efficiency in electrochemical oxidation of methylene blue as the surrogate. Performance of the electrochemical process was evaluated under various configurations of electrode material (boron-doped diamond or BDD vs graphite), polarity (constant vs alternating), and polarity alternation frequency (0.25- 2 hr^{-1}). With constant polarity, electrochemical treatment of methylene blue exhibited an initial removal efficiency of 95%, which, however gradually declined with prolonged treatment beyond 0.5 hr due to electrode fouling by scaling. In comparison, the use of alternating polarity resulted in sustained removal of methylene blue with the reduction in scaling by over 87% as well as the increase in the production of free chlorine as the oxidant by 185%. Further testing of alternating polarity indicated that the alternation frequency of 0.5 hr^{-1} was optimal for sustained treatment efficiency and mitigation of electrode scaling. Moreover, the use of graphite as electrode material resulted in the reduction in energy consumption by 27% as compared with BDD as the electrode material. These findings highlight the potential of alternating polarity in mitigating electrode fouling and enhancing the sustainability of electrochemical treatment for pollution control.

Key words: electrochemical treatment; alternating polarity; electrode fouling; graphite; boron-doped diamond.

1. Introduction

Electrochemical oxidation (EO) is an emerging advanced oxidation process that generates strong oxidizing species *in situ* without the addition of external chemicals (Hoseinzadeh and Rezaee, 2015; Pikaar et al., 2011). Owing to its operational simplicity and environmental compatibility, EO has demonstrated great potential for the complete mineralization of diverse organic pollutants, particularly in high-salinity wastewaters, such as petroleum produced water, seawater desalination brine, and chemical production effluents (Dey et al., 2024; Liu and Wang, 2017). The high conductivity as a result of high salinity provides favorable conditions for EO application in these waste streams (Zhu et al., 2022). Specifically, the abundance of chloride ions in these waste streams provides precursors for reactive chlorine species (e.g., Cl_2, HOCl, ClO^-) during electrolysis, which serve as powerful oxidants to enhance the degradation of organic pollutants, many of which are recalcitrant (Dey et al., 2024; Guo et al., 2022; Zhu et al., 2022).

However, localized alkaline environment near the cathode promotes precipitation of sparingly soluble minerals and the formation of scale layers on the electrode surface, which may progressively hinder electron transfer, increase ohmic resistance, and accelerate electrode passivation(Asaithambi et al., 2020; Sarfo et al., 2023). Over prolonged operation, these processes not only reduce treatment efficiency and shorten electrode lifespan but also increase energy consumption and operational costs(Li et al., 2022; Martínez-Huitle and Brillas, 2009). Therefore, developing effective anti-scaling strategies is crucial for the practical implementation of EO under high-salinity and high-hardness aqueous conditions.

Various strategies have been proposed to mitigate scaling, including optimizing current density, pH, and hydrodynamic conditions to reduce local supersaturation; applying softening chemicals or anti-scalants to remove metal ions contributing to scale formation; and using ultrasound treatment to dislodge the scaling layer(Ayoub et al., 2018; Chow and Pham, 2021; She et al., 2022). In addition, electrode material designs such as protective coatings, surface modifications, or the use of stable conductive ceramics can also delay scale formation and improve tolerance(Hanssen et al., 2016; Li et al., 2022).

However, these strategies are often costly due to added material and equipment, introducing secondary pollutants, or ineffective in providing sustained protection from scaling.

An attractive approach involving simple operational modification is alternating polarity, where the anode and cathode are periodically switched, allowing each electrode to alternate function as the anode and neutralize alkalinity generated previously as the cathode, thus mitigating the root cause of scale formation(Chow and Pham, 2021; Jang et al., 2024; Luo et al., 2023). Therefore, this approach has the potential for sustained prevention of scale formation with minimal additional costs.

Recent studies evaluated the utility of alternating polarity in electrochemical systems such as electrocoagulation and water softening for the mitigation of electrode fouling(Chow and Pham, 2021; Severin and Hayes, 2019); however, few efforts were focused on electrochemical pollutant degradation. Therefore, with the goal to evaluate the potential of alternating polarity in enhancing the sustainability of electrochemical treatment of pollutants, the specific aims of this study were to (i) characterize the effects of alternating polarity on electrode fouling, treatment performance, and energy consumption; (ii) compare the performance of electrode materials, and (iii) optimize polarity alternation frequency to maximize treatment efficiency.

2. Material and method

2.1 Water composition

To examine the electrochemical degradation of organic pollutants in water with high salinity and hardness, a synthetic produced water was prepared to simulate the ionic composition of petroleum produced water. Analytical-grade salts were used, consisting of sodium chloride (68.0 g/L), calcium chloride (21.5 g/L), magnesium sulfate (2.0 g/L), and calcium carbonate (1.0 g/L), resulting in the water composition shown in Table 1. To adjust the pH to 6.5, 0.5 mL of 1.0 M sulfuric acid was added to per liter of synthetic water, which resulted in a total alkalinity of 300 mg/L as $CaCO_3$ and a total hardness of 21,900 mg/L as $CaCO_3$ (Table 1). In addition to the ionic composition of the water, methylene blue (MB) was tested as an organic pollutant surrogate due to the ease of measurement and presence of functional groups characteristic of aromatic pollutants

frequently encountered in petroleum produced water (Panizza et al., 2007). A stock solution of MB (4.0 g/L) was dosed at a rate of 2.48 mL/L of synthetic water, resulting in a methylene blue concentration of 9.92 mg/L in the synthetic water (5.96 mg/L of TOC).

2.2 Configurations of the electrochemical reactors

Tests of electrochemical treatment were carried out in both batch reactors (BRs) and continuous reactors (CRs). Batch experiments were carried out over varying time scales, where the reactor volume was 100 mL. The configuration of the CRs was similar to that of the BRs but being operated with a continuous flow at a hydraulic detention time of 2 hours, which was based on results from batch experiments indicating 99% MB degradation with 2 hours of electrochemical treatment.

The reactor configuration consisted of two electrodes, which were placed 10 mm apart in the reactor chamber. Two different electrode materials were tested: boron doped diamond (BDD/Nb 2500ppm neoCoat, La Chaux-de-Fonds, Switzerland), referred to as BDD, and graphite (9121K64 McMaster-Carr, Elmhurst, IL, USA). BDD has become a widely used electrode material for the production of reactive oxidizing species such as free chlorine, hydroxyl radicals, and sulfate radicals while limiting the hydrolysis of water and the formation of dissolved oxygen (Eq.1) (Wang and Xu, 2012). Graphite is a neutral electrode material commonly used as an economical alternative to BDD (Sivodia and Sinha, 2020).

$$2H_2O \rightarrow 4e^- + 4H^+ + O_2 \qquad \textit{Equation 2.1}$$

For all experimental conditions a voltage between 3.5V and 4.0V was applied such that the absolute current did not exceed 1.0A for system safety. This voltage was chosen based on cyclic voltammetry analysis (CV), where the voltage was scanned from 0V up to 8V and back to 0V at a rate of 100mV/s. In general, the initiation of electrochemical reactions is marked by a shift in the current. By examining the derivatives of the applied current, significant inflection points can be identified, corresponding to the onset of specific electrochemical reactions. CV analysis was carried out on a suite of chemical species being introduced into synthetic water including chloride ions, sulfate ions, and pure water to identify the voltages associated with the initiation of potential oxidizing agent formation. It is expected that chloride will readily electrochemically be converted

into free chlorine (Eq. 2.2) due to it being the most abundant anion (Table 2.1). Additionally, with the presence of other candidate anions it was anticipated that sulfate will be converted into sulfate radicals (Eq. 2.3), that hydroxide ions are formed from electrolysis of water (Eq. 2.4) and then further converted into hydroxyl radicals (Eq. 2.5). This had revealed that under the experimental conditions that Cl^- and SO_4^{2-} were the mainly active ions that will have electrochemical reactions happened above 3.1V and 2.17V, respectively (Fig. S2.1). While both chloride and sulfate can be converted into oxidizers, due to significantly higher concentration of chloride ions, chlorine was expected to be the main oxidant.

$$2Cl^- \rightarrow Cl_2 + 2e^- \qquad \textit{Equation 2.2}$$

$$SO_4^{2-} \rightarrow SO_4 \cdot^- + e^- \qquad \textit{Equation 2.3}$$

$$2H_2O + 2e^- \rightarrow H_2 + 2OH^- \qquad \textit{Equation 2.4}$$

$$OH^- \rightarrow OH \cdot^- + e^- \qquad \textit{Equation 2.5}$$

Two schemes of electrode polarity were tested: constant polarity and alternating polarity, both implemented by a potentiostat (Model SP-150eZ, BioLogic, Seyssinet-Pariset, France). Constant polarity was established with BDD as the constant anode and graphite as the constant cathode. In comparison for alternating polarity, the anode and cathode were exchanged periodically. A series of alternating frequency, ranging from 0.25 to 2 $hour^{-1}$, were tested.

2.3 Analytical Methods

Methylene blue was quantified spectrophotometrically at a wavelength of 663 nm (Panizza et al., 2007). Water quality parameters, such as pH and chloride, were monitored over the course of each experiment. Free chlorine is considered the predominant oxidant in this system, as the high chloride concentration favors its electrochemical generation during anodic oxidation, which was colorimetrically measured using the standard DPD method as previously described (Zheng et al., 2015). Electrochemical conditions, i.e., applied voltage or current, were set and actively monitored using a potentiostat (Model SP-150eZ, BioLogic, Seyssinet-Pariset, France).

2.4 Data Analysis

One potential concern with waters with high salinity and hardness is that if pH is allowed to increase, scaling can readily occur. As seen earlier, with the potential for electrolysis of the water to occur hydroxide ions can increase the pH (Eq. 2.4), leading to the event of scaling within the reactor which may impede treatment efficacy. As such the electrode fouling rate was used to describe the formation of electrode scales (Eq. 2.6).

$$\text{Electrode fouling rate } (\text{g}/m^2 \cdot \text{day}) = \frac{M_{t-} M_{t0}}{A*(t-t_0)} \qquad \textit{Equation 2.6}$$

Where M_t was the mass of the electrode at time t in grams, M_{t0} was the mass of the electrode initially in grams, and A was the surface area of the electrode exposed in the reactor in m^2.

Another parameter examined was the total energy input of the electrochemical system, which was based on the instantaneous power input (Eq. 2.7). Integrating this over the experimental time yields equation 2.8, which provides the total energy input for each experiment.

$$P = V * i \qquad \textit{Equation 2.7}$$

$$E = \frac{\int P\ dt}{A} \qquad \textit{Equation 2.8}$$

Where V is the applied voltage in volts; and I is the applied current intensity in amperes for each experiment. P is the instantaneous power in watt; E is the normalized total energy input in kilowatt-hours per square meter.

While energy input can lend insights into the energy efficiency for each experiment, to more specifically determine the efficiency of producing the oxidizing agent the coulombic efficiency was determined. Here the coulombic efficiency was based on the production of free chlorine, where a 100% efficiency would be caused by all current going to the formation of chlorine, as described previously (Yao et al., 2024).

$$CE\ = \frac{2*F*\int C\ dt}{\int i dt} \qquad \textit{Equation 2.9}$$

CE is coulombic efficiency in percentage; F is the Faraday constant in coulombs per mole; C is the concentration of free chlorine in M.

3. Results

3.1 Effect of electrode scale formation on electrochemical treatment

The performance of the electrochemical system was evaluated for 72 hours (36 HRTs) in CRs under constant polarity, using BDD as the anode and graphite as the cathode. Initially, MB degradation had shown to increase significantly as the reactor approached steady-state conditions, reaching a degradation rate of over 95% degradation in 0.5 hr, continuing this high level of degradation up to 48hrs (Fig. 2.1a). However, degradation efficiency gradually declined after 48 hours, falling below 90% by 72 hours. Concurrently, the applied current decreased over time (Fig. S2.2), indicating increased system resistance.

Visual inspection revealed substantial scaling on the cathode surface, likely due to localized pH elevation due to the electrolysis of water (Eq. 2.4), while the anode had negligible scaling that occurred (Fig. 2.2b). This accumulation on the cathode was seen to impact the rate of methylene blue degradation, despite the free chlorine concentration maintaining a high level of over 700 ppm (Fig. 2.1c). To quantify the impact of scaling on degradation kinetics, batch experiments using electrodes with varying degrees of fouling were conducted. The first-order decay rate decreased from 1.83 min^{-1} down to 0.93 min^{-1} after 12 hours of scaling and 0.76 min^{-1} after 36 hours of scaling (Fig. 2.2a), confirming that scaling significantly impaired pollutant degradation. These results highlight the critical need to address electrode fouling for sustained electrochemical performance.

3.2 Effect of alternating polarity on electrochemical treatment

The problem arising from scaling on the cathode was hypothesized to be related to pH increases at the cathode due to anodic electrolysis of water producing hydrogen ions (Eq. 2.1). So it was envisioned that by alternating the electrodes between cathodic and anodic states, thereby cyclically shifting the local pH from alkaline to acidic, could mitigate or reverse scaling. Under the same reactor conditions, i.e. CRs with BDD and graphite electrodes (referred to “BDD/Gr”), alternating polarity was conducted at an exchange frequency 0.5 hr^{-1}. Results showed that both constant and alternating polarity achieved comparable MB degradation (Fig. 2.3a), indicating that alternating polarity maintained a consistent level of treatment for MB.

However, a notable difference was observed in the effluent pH: the alternating polarity exhibited a significantly higher value of approximately 8.5, whereas the constant polarity configuration had a pH around 7.8 (Fig. 2.3b). This increase in pH is potentially concerning, as it suggests that alternating polarity may promote scaling under more alkaline conditions.

Given that the pH trend under alternating polarity was more conducive to scaling while the degradation efficiency remained consistent, the effect on free chlorine production was further examined. Free chlorine generation under alternating polarity was substantially higher than under constant polarity, reaching approximately 2000 ppm, which represents an increase of about 185% (Fig. 2.3c). This enhancement indicates a higher potential for degrading organic pollutants under alternating polarity.

Given the concerning pH trend under alternating polarity, the fouling rates were examined. The electrode fouling rate of graphite electrode decreased from 201.3 $g \cdot m^{-2} \cdot day^{-1}$ under constant polarity to 26.2 $g \cdot m^{-2} \cdot day^{-1}$ under alternating polarity, representing a reduction of approximately 87% (Fig. 2.3d). Meanwhile, in the alternating-polarity BDD/Gr configuration, the BDD electrode periodically acted as the cathode and exhibited a small amount of deposit accumulation (14 $g \cdot m^{-2} \cdot day^{-1}$), whereas negligible deposition occurred under constant polarity. This observation contrasts with expectations based on the effluent pH trend, suggesting that although the bulk solution exhibited a higher pH, the localized pH at the electrode surfaces alternated between acidic and alkaline conditions during polarity reversal. Consequently, the overall fouling rate under alternating polarity was significantly reduced compared with constant polarity.

To assess the energy performance, normalized total energy input was also analyzed. Alternating polarity reduced the overall resistance of the electrochemical reactor by mitigating electrode fouling, resulting in a higher current output at the same voltage input. As a result, the total energy input under alternating polarity reached 2.69 $kWh \cdot m^{-2}$, representing an increase of 122% compared with 1.21 $kWh \cdot m^{-2}$ of constant polarity (Fig. 2.4). This finding motivated the exploration of more cost-effective and energy-efficient electrode materials capable of maintaining high treatment performance.

3.3 Effect of electrode material on electrochemical treatment

Graphite is characterized by high electrical conductivity, ease of fabrication, and low cost, making it an attractive electrode material for practical electrochemical applications. Therefore, graphite was employed as both the anode and cathode (Gr/Gr configuration) to optimize system performance under alternating polarity. The Gr/Gr configuration maintained a consistent MB degradation efficiency under alternating polarity, comparable to that of the BDD/Gr system.

A slight difference was observed in the effluent pH between the two configurations. Under alternating polarity, the BDD/Gr system exhibited a higher effluent pH of approximately 8.5, whereas the Gr/Gr configuration showed a slightly lower pH of around 8.0 (Fig. 2.3b). The lower effluent pH is advantageous for suppressing scaling and maintaining long-term electrode stability in wastewater high in salinity and hardness. Free chlorine production in the Gr/Gr configuration was well maintained and comparable to that of the BDD/Gr system, with both stabilizing at approximately 2000 ppm under alternating polarity (Fig. 2.3c).

The Gr/Gr configuration also demonstrated a strong ability to mitigate electrode fouling under alternating polarity conditions. The total mass accumulation on the electrodes was comparable between the BDD/Gr (40.2 $g \cdot m^{-2} \cdot day^{-1}$) and Gr/Gr (40.53 $g \cdot m^{-2} \cdot day^{-1}$) configurations, indicating similar fouling resistance. A slight difference was observed, however: in the Gr/Gr system, one graphite electrode that served as the anode at the end of the experiment exhibited negligible mass accumulation (0.13 $g \cdot m^{-2} \cdot day^{-1}$), whereas both electrodes in the BDD/Gr configuration showed small but measurable deposit formation.

When the electrode configuration was optimized by using graphite as the anode under alternating polarity, the normalized total energy input decreased from 2.69 $kWh \cdot m^{-2}$ for the BDD/Gr configuration to 1.95 $kWh \cdot m^{-2}$ for the Gr/Gr configuration, corresponding to a 27.5% reduction in energy consumption. This improvement indicates enhanced energy efficiency and greater economic feasibility.

3.4 Optimization of polarity exchange frequency

With the improved scaling offered by alternating polarity, as well as maintained level of

methylene blue, a major factor that is to be further optimized is exchange frequency. Here different exchange frequencies were tested in the same continuous reactor configuration by using Gr/Gr electrodes, where exchange frequencies of 2 hr^{-1}, 0.5 hr^{-1}, and 0.25 hr^{-1} were compared. It was seen that all three showed consistent performance with methylene blue degradation (Fig. 2.5a).

While the degradation had remained at a consistent rate, the pH was distinguishable between each exchange frequency where the 2 hr^{-1} exchange frequency had a pH of about 7.5, the 0.5 hr^{-1} exchange frequency had a pH of about 8, and the 0.25 hr^{-1} exchange frequency had a pH of about 8.4 (Fig. 2.5b).

With chlorine production, it was seen that 0.5 hr^{-1} exchange frequency had the highest achieved level with 2,200 ppm of free chlorine, compared to the 1900 ppm produced by the 0.25 hr^{-1} exchange frequency, and the 500ppm produced by the 2 hr^{-1} exchange frequency (Fig. 2.5c). This indicated an optimal point for free chlorine production, though overall degradation could not indicate this effect.

Continuing with this, the scaling rates also indicate that there was an optimal exchange frequency. Specifically, the 2 hr^{-1} exchange frequency resulted in the highest scaling rate at 139.6 g/m^2/day, followed by the 0.25 hr^{-1} exchange frequency with a scaling rate of 73.9 g/m^2/day for both electrodes (Fig. 2.5d). The lowest scaling rate came from 0.5 hr^{-1} exchange frequency with a scaling rate of 40.4 g/m^2/day for one electrode and virtually undetected scaling on the other, for a 20.3 g/m^2/day as an average (Fig. 2.6). From this it can be seen that exchange frequency impacts this scaling, where too high may not allow for enough time for dissolution and too low will allow more extent of scaling. This trend was inversely related to the production of free chlorine, suggesting that electrode fouling may inhibit the formation of free chlorine. Normalized total energy input showed 0.5 hr^{-1} exchange frequency have significantly higher normalized total energy input 1.95 KWH/m^2 than the other two 2 hr^{-1} and 0.25 hr^{-1} were 1.34 KWH/m^2 and 1.29 KWH/m^2 respectively, while didn't have significant decrease, indicating a trade-off between fouling control and energy efficiency.

4. Discussion

4.1 Electrode fouling impedes electrochemical performance

Electrochemical degradation showed its great efficiency to treat organic pollutants in high hardness/salinity water, above 95% Methylene blue can be degraded within 0.5hr. The pathway of electrochemical degradation occurs through direct anodic oxidation and chemical reactions with electrogenerated species, with pollutant removal primarily driven by chemical reactions, as direct anodic oxidation typically provides limited decontamination (Arias et al., 2022; Ates, 2011; Panizza et al., 2007; Sarfo et al., 2023). Free radicals such as hydroxyl radical ($^{\bullet}OH$) and sulfate radical ($SO_4^{\bullet-}$) are not being considered as main reactive agent to conduct organic degradation in this high chloride electrochemical system due to radical scavenging by Cl^- and consequential loss of the process efficiency of free radical (Eq. 2.10&11) (Lee et al., 2020; Luo et al., 2020). So, the main oxidized reagent was considered as free chlorine generated by chemical reactions, and subsequently in form of hypochlorous acid or hypochlorite ions, which already showed great efficiency to mineralization and decolorization of methylene blue in former studies due to the high bleaching properties (Panizza et al., 2007; Sarfo et al., 2023; Wang and Xu, 2012; Yu et al., 2024). Reported first-order decay rates range from 0.46 to 0.57 min^{-1} at initial pH 3–11 in 0.1 M Na_2SO_4 (Panizza et al., 2007), whereas our system achieved a significantly higher rate of 1.83 min^{-1}, attributable to the elevated chloride concentration. This result is consistent with previous findings that higher chloride concentrations accelerate the first-order decay rate (Panizza et al., 2007).

$Cl^- + OH^{\bullet} \leftrightarrows ClOH^{\bullet-}$ *Equation 2.10*

$SO_4^{\bullet-} + Cl^- \rightarrow Cl^{\bullet} + SO_4^{2-}$ *Equation 2.11*

$Cl_2 + H_2O \rightarrow HOCl + H^+ + Cl^-$ *Equation 2.12*

$HOCl \rightarrow H^+ + OCl^-$ *Equation 2.13*

However, prolonged operation of electrochemical process would result in gradual deterioration in performance along with precipitation accumulated around cathode. This is because electrochemical reactions happened on cathodes increase localized pH, which subsequently cause Ca^{2+} and Mg^{2+} to form $CaCO_3$ and $Mg(OH)_2$ so that impede degradation efficiency. Similar result that electrode fouling deteriorated sulfanilic acid

degradation was also observed by (Tian et al., 2022). Fouling layer on electrode took up the sites that electrochemical reactions were used to happen, Liu et al. (2021a) showed that fouling layer decreased the electrochemically active surface area by 81.26%. Meanwhile fouling also decreased the current density which the impact rate of electrochemical reaction, caused lower kinetics of electrochemical reaction. Kinetic analysis of the decreased first order decay rates directly validated this.

4.2 Alternating polarity: a strategy to control fouling and enhance degradation

Alternating polarity involves the periodic reversal of electrode polarity, a strategy that mitigates scale formation and significantly enhances electrochemical degradation efficiency (Martínez-Huitle and Brillas, 2021; Valdes et al., 2021). During each exchange polarity, cathode switched into anode, scaling produced by previous stage started to dissolve and localized pH went down impeding new scaling formation, and the evolution of H_2(g) and Cl_2 (g)produced at cathode also can dislodge the fouling layer after each time swap polarity, which significantly reduced the electrode fouling rate (Bian et al., 2019; Liu et al., 2021a). Alternating polarity also improved mass transfer and increased the utilization of electrons, as confirmed by coulombic efficiency analysis. Specifically, under constant polarity, coulombic efficiency achieved steady state at 0.68 after 6hr, alternating polarity improved the coulombic efficiency up to 0.88 after 4hr in Gr/Gr configuration, which showed a significant improvement of electrons utilization. In addition, polarity switching balances chloride oxidation across both electrodes, producing a narrower concentration gradient than constant polarity and thereby facilitating more efficient chloride utilization through shorter mass-transfer distances. Moreover, alternating polarity maintains higher average current input due to reduced impedance from fouling, which accelerates electron transfer and improves reaction kinetics (Jang et al., 2024). However, these benefits come at the cost of increased energy consumption. Similar observations were reported by Asaithambi et al. (2020), who noted that alternating polarity in electrochemical degradation does not always result in reduced energy demand.

4.3 Graphite electrodes: a cost-effective alternative to BDD

Alternating polarity optimal for contaminant removal appeared to be dependent on electrode type (Jeong et al., 2009; Sivodia and Sinha, 2020). Chow and Pham (2021) optimized the electrode type to mitigate electrode fouling showed that current reversal diminished fouling of Al electrode but not Fe electrode, which likely due to iron (hydr)oxides accumulated on electrode are several orders of magnitude less conductive than metallic Fe. In this study, using BDD or graphite as the anode both reduced electrode fouling, primarily due to the inertness of both materials, preventing reacts with the solution so won't inhibiting the dissolution of precipitates. Meanwhile, optimizing electrode type from BDD to graphite kept degradation efficiency of methylene blue high. This is mainly because chloride ions significantly dominated in this electrochemical system, and both BDD and graphite are feasible for chemical reaction to generate free chlorine, which illustrated the similar degradation efficiency between BDD electrode and graphite. Using graphite electrode also showed high columbic efficiency and lower energy input, which is likely due to the better conductivity of graphite (Chen et al., 2023; Haider et al., 2023; Qi et al., 2021; Sivodia and Sinha, 2020). So as for treating high salinity wastewater, graphite offered a cost-effective electrode for alternative.

4.4 Role of exchange frequency in balancing efficiency and fouling

Exchange frequency is an important factor when it comes to the application of electrochemical degradation combined with alternating polarity (Blasco-Gomez et al., 2017; Chow and Pham, 2021; Martínez-Huitle and Brillas, 2021; Sarfo et al., 2023). Different exchange frequencies result in variations in stabilized effluent pH, free chlorine production, and electrode fouling rates, which means there is an imbalance in anode and cathode reactions. Ingelsson (2021) operated the exchange time (1/exchange frequency) from 1s to 10 min using BDD electrode, result showed that exchange time less or equal to 2.5s will produce 2-4 times more H_2O_2. A possible explanation for the imbalance would be that longer exchange frequencies lead to slower compensation for changes due to reduced reaction kinetics caused by electrode fouling. However, more frequent polarity exchanges do not necessarily enhance performance as well as decrease the electrode fouling rate. Barba et al. (2017) used 1, 2, 3, and 6 d^{-1} four different exchange frequency

to evaluate the remediation of oxyfluorfen polluted soil, it was seen that 2-3 d^{-1} was the optimum value. Similar results were also observed in this study. Results indicate that a exchange frequency of 0.5 hr^{-1} yields the highest free chlorine production and the lowest electrode fouling rates compare to 2 hr^{-1} and 0.25 hr^{-1}, which is likely due to sufficient reaction contact time (Martínez-Huitle and Brillas, 2009; Sarfo et al., 2023). Higher exchange frequencies prevent maximum reaction rates, while lower exchange frequencies hinder mass transfer because of electrode fouling. In summary, optimizing exchange frequency is essential for maximizing the efficiency of electrochemical systems using alternating polarity.

5. Conclusion

This study evaluated the performance of the application of electrochemical systems to treat organic pollutants in high/salinity water by using continuous reactors, and systematically optimized the electrode material, electrode polarity and exchange frequency to mitigate electrode fouling and enhance electrochemical degradation. Methylene blue was selected as a surrogate pollutant, degradation efficiency, electrode fouling rate and oxidizing reagent production were used as parameters to identify the performance of the system, coupled with calculation of energy input and columbic efficiency. Several insights were gained.

- Long-term operation of electrochemical systems under constant polarity, using BDD as the anode and graphite as the cathode, leads to a decline in degradation efficiency due to electrode fouling.
- Alternating polarity combined electrochemical degradation can effectively address electrode fouling and improve the utilization of electrons as well as generate more oxidizing agents, showing higher degradation potential, however, increase the energy input of the electrochemical system.
- Optimizing BDD to graphite as anode remained the high performance of the system as well as lower the energy input.
- Incorporating alternating polarity requires consideration of exchange frequency to ensure optimal performance.

Overall, findings from this study show that electrochemical degradation combined with alternating polarity could be a promising option for the effective abatement of aquatic contaminants *in situ*. Further investigations are needed to evaluate the degradation of more recalcitrant pollutants.

Table 2.1: Stimulated produced water composition

Ionic species	Concentration (mg/L)
Ca^{2+}	8,100
Na^{+}	27,000
Mg^{2+}	400
Cl^{-}	55,000
SO_4^{2-}	1,600
CO_3^{2-}	0.01M
Hardness	21,900 mg/L as $CaCO_3$
Alkalinity	300 mg/L as $CaCO_3$
pH	6.5

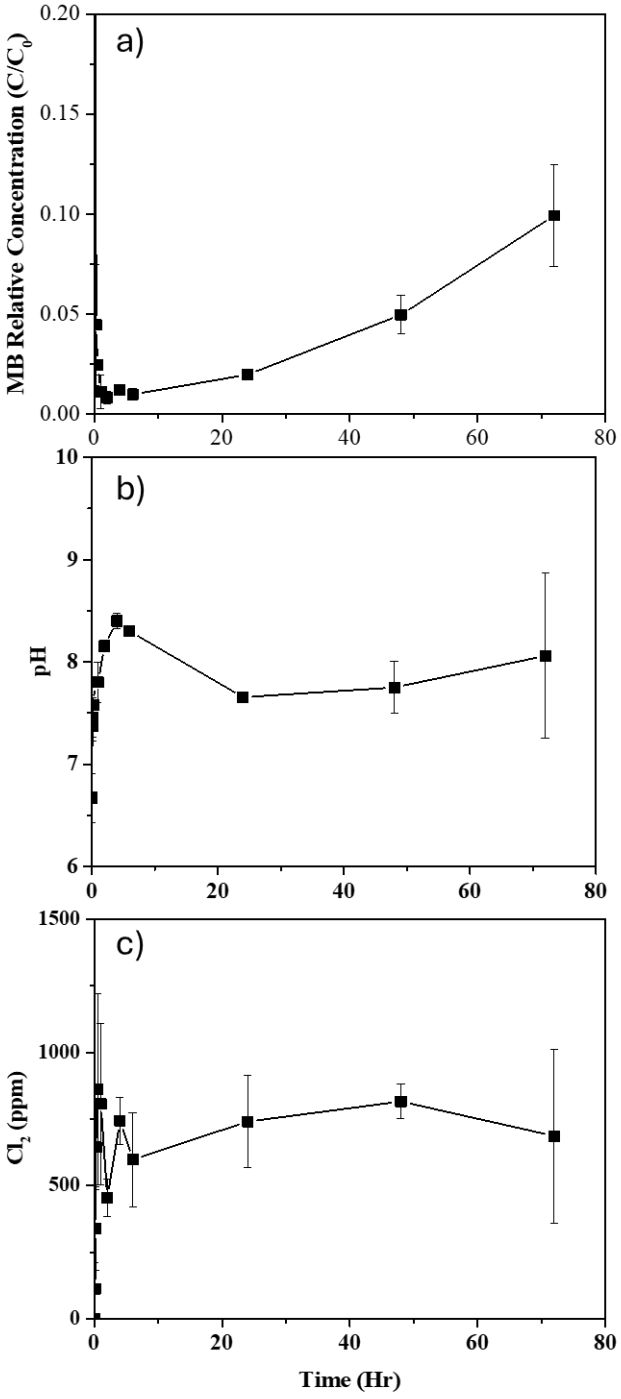

Figure 2.1: electrochemical system performance under constant polarity, methylene blue degradation(a), effluent pH change (b), and free chorine production(c)

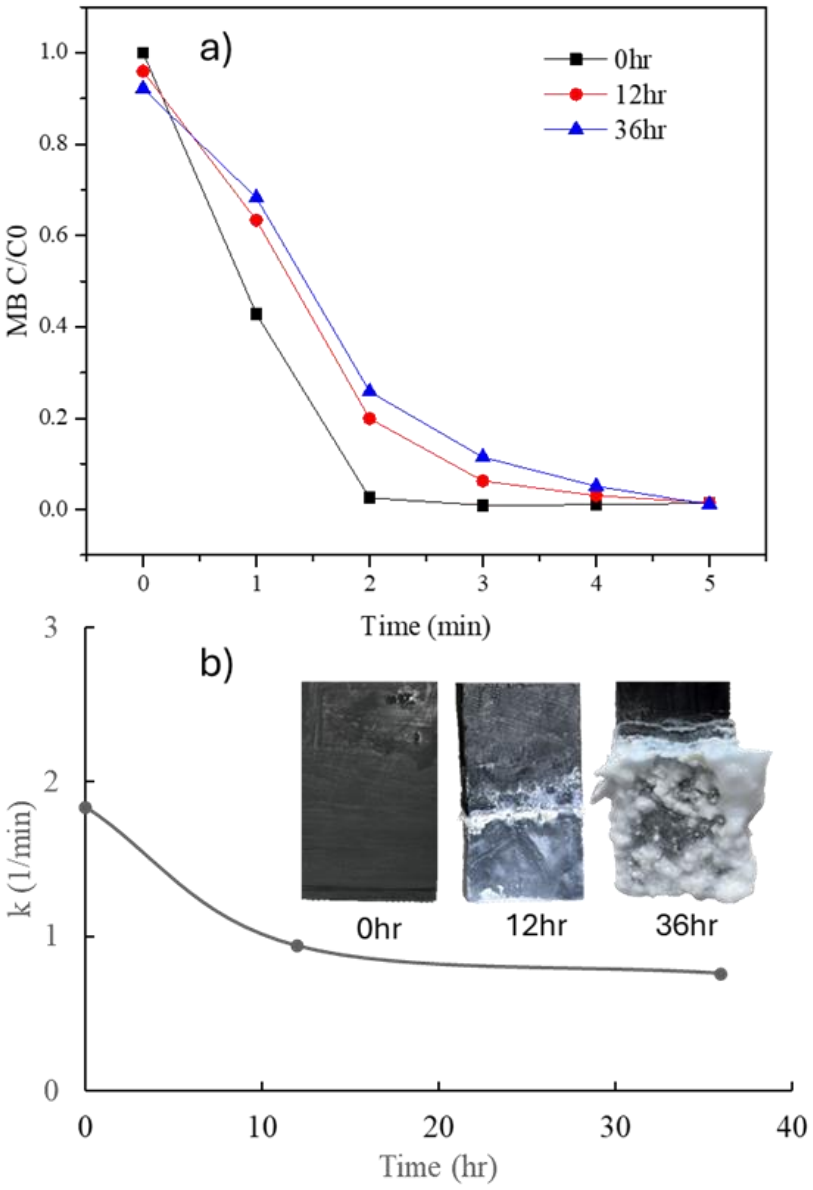

Figure 2.2: Batch reactor to show electrode fouling impedes degradation (a) MB degradation at different times, (b) First order kinetics constant under different time and real image of electrode fouling at different times

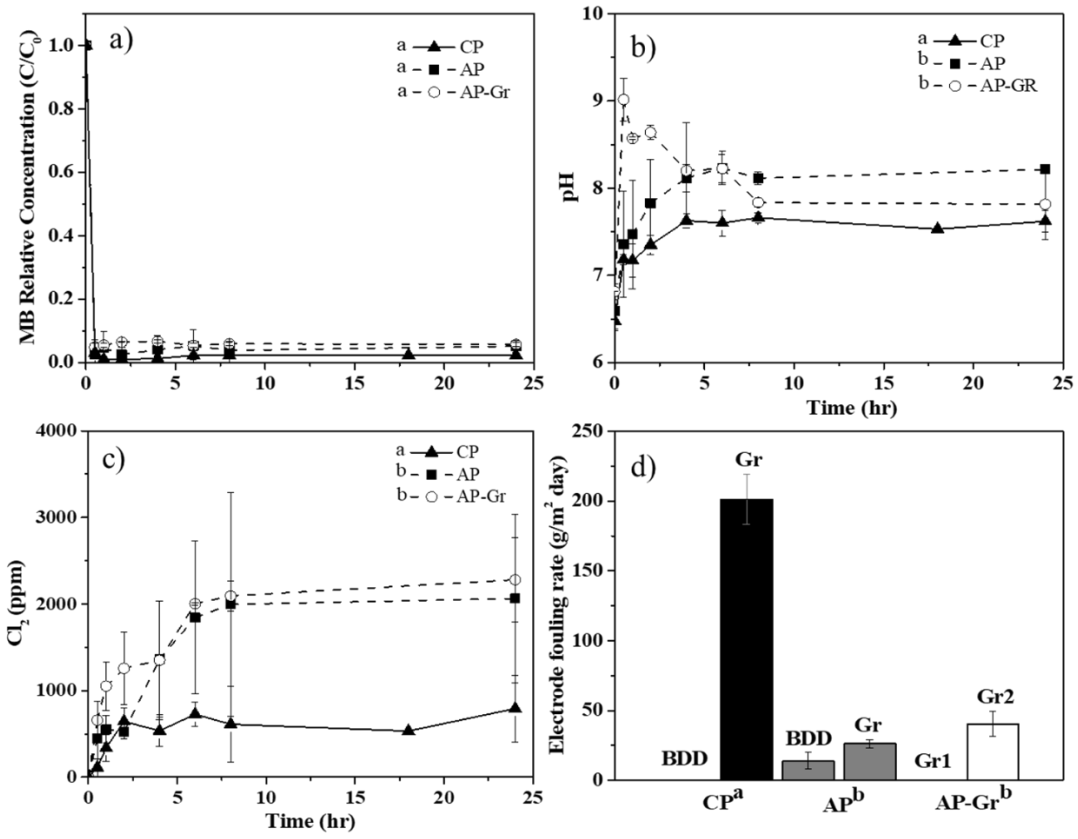

Figure 2.3: Electrochemical system performance under different polarity and electrode (methylene blue degradation(a), effluent pH change (b), free chorine production(c) and electrode fouling rate (d).

Note: CP: constant polarity; AP: alternating polarity; AP-Gr: use graphite as both electrodes; Electrode fouling rate=precipitation weight/ (electrode surface*time)

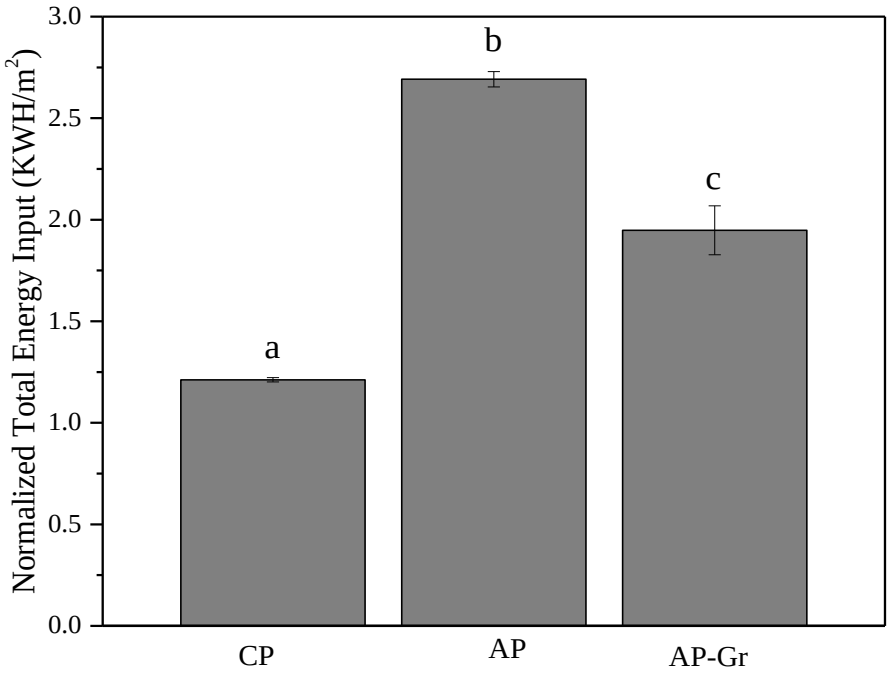

Figure 2II.4: Normalized total energy input under different polarity and electrodes

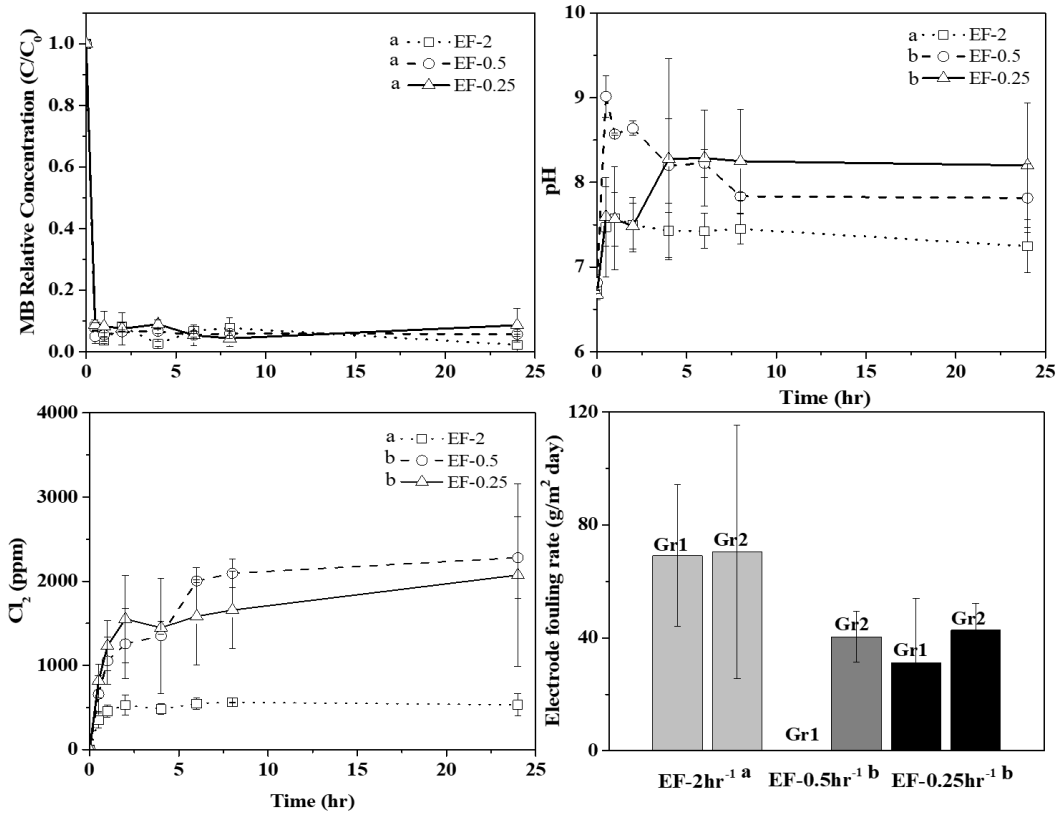

Figure 2.5: Electrochemical system performance under different exchange frequencies, methylene blue (MB) degradation(a), effluent pH change (b), free chorine production(c) and electrode fouling rate (d).

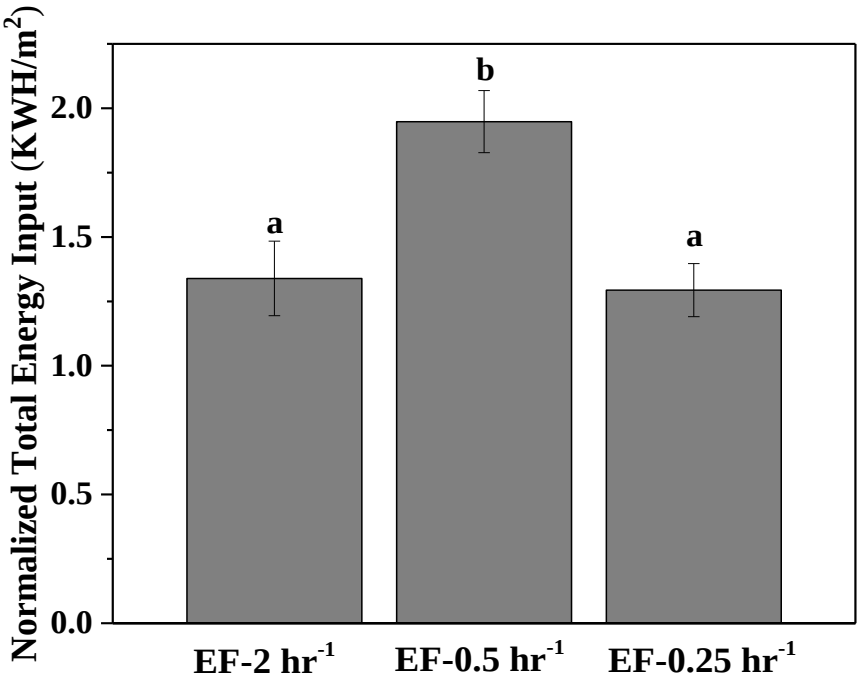

Figure 2.6: Normalized total energy input under different exchange frequencies

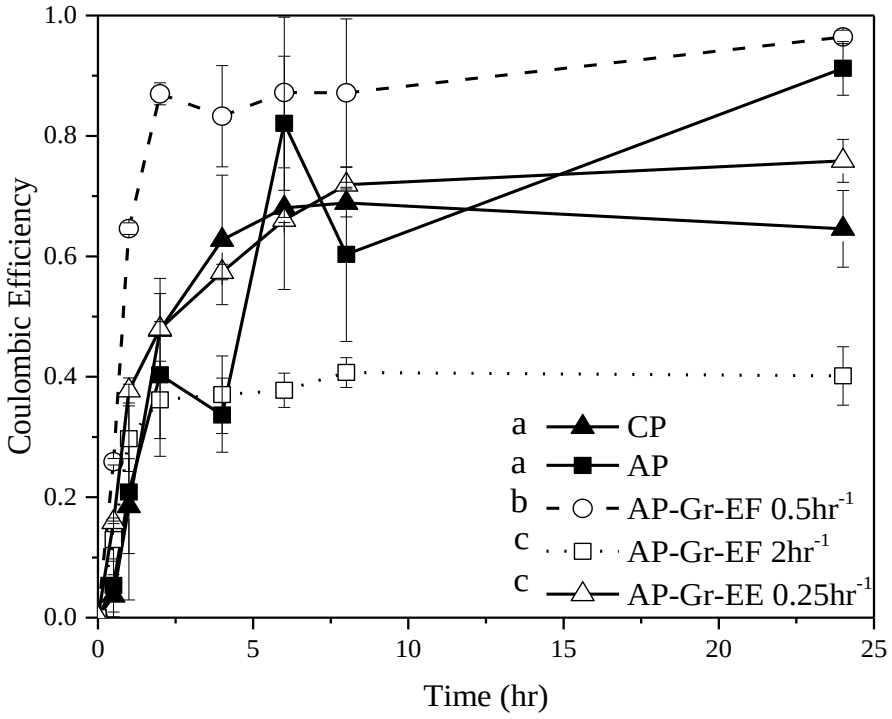

Figure 2.7: Coulombic efficiency under constant polarity and alternating polarity.

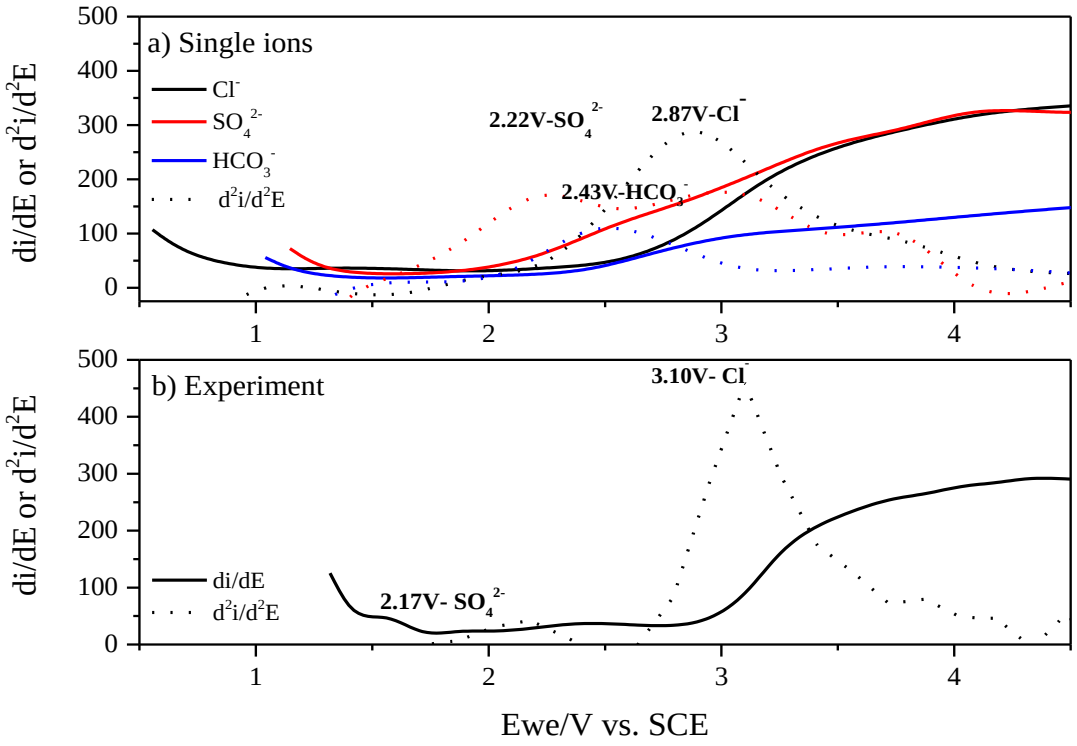

Figure 2.S1: Comparison of cyclic voltammetry between single ions to experiment

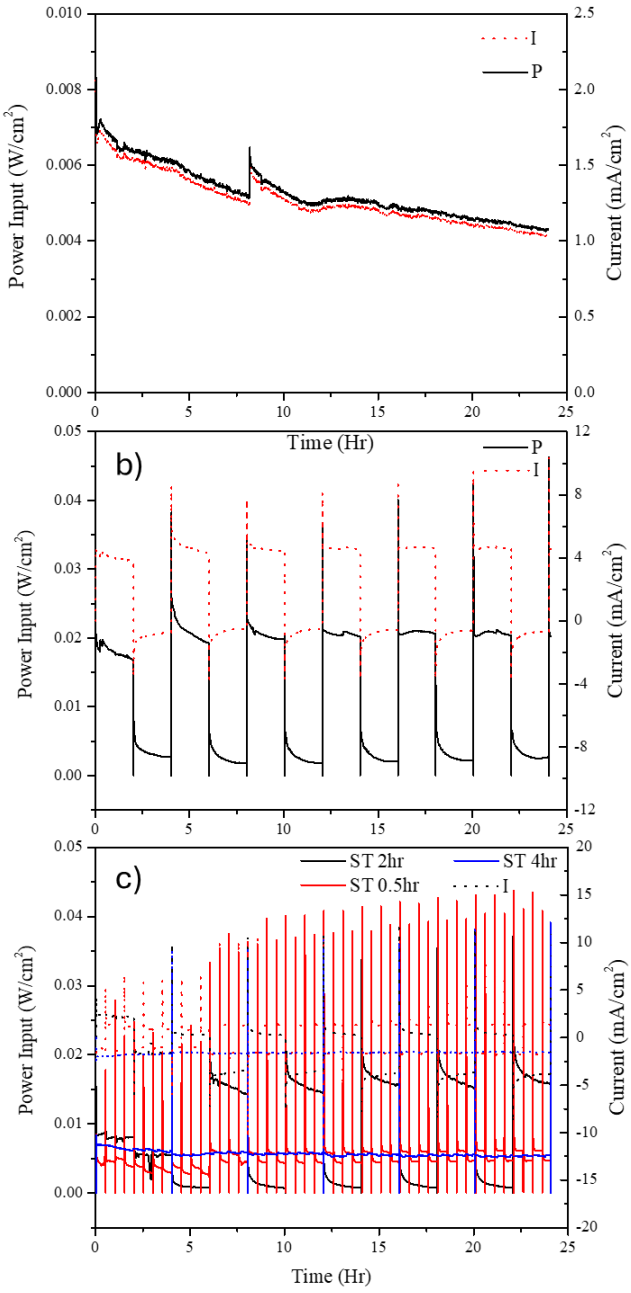

Figure 2.S2: Power input and current change of electrochemical system over time under constant polarity (a), alternating polarity (b) and different exchange frequencies (c). (a) (b)- using BDD&Gr, (c)-using Gr&Gr

CHAPTER III OPTIMIZATION ELECTROCHEMICAL TREATMENT OF N-ALKANE IN PETROLEUM PRODUCED WATER

Abstract

Prolonged application of electrochemical oxidation in high-salinity, high-hardness petroleum produced water is often limited by performance deterioration caused by electrode fouling, particularly due to inorganic scaling under alkaline conditions at the cathode. To address this challenge, a novel strategy of alternating polarity was tested to alleviate scale formation and subsequently improve electrochemical degradation efficiency. Batch experiments were first conducted to optimize applied voltages (2, 4, and 5 V) and electrode configurations (anode/cathode: BDD/BDD, BDD/Graphite, Graphite/Graphite) using n-docosane as a model n-alkane. Results showed that voltages above 4 V initiated effective degradation of n-docosane, primarily due to the formation of strong oxidative species such as free chlorine and reactive radicals. Graphite electrodes exhibited a synergistic effect of adsorption and oxidation: their strong affinity for n-docosane enhanced interfacial pollutant accumulation, increasing the likelihood of subsequent oxidation by electrochemically generated oxidants. This dual function highlights graphite as a promising and cost-effective electrode material. Further tests in a semi-continuous system demonstrated that alternating polarity resolved the performance deterioration due to electrode fouling under constant polarity and improved overall removal efficiency from 72.0% under constant polarity to 85.7% under alternating polarity by accelerated first-order decay kinetic and refreshed active sites for both adsorption and oxidation. These results indicate that alternating polarity is an effective and scalable approach to mitigate electrode fouling, sustain EO performance, and advance the treatment of saline and hard produced waters.

Key words: electrochemical oxidation; n-docosane; electrode fouling; alternating polarity

1. Introduction

The rapid growth of the oil and gas industry has led to the generation of large volumes of petroleum produced water (PPW), one of the most abundant and environmentally challenging effluents, particularly in offshore oil and gas production (Beni et al., 2023). PPW is chemical complexity, containing extremely elevated concentrations of inorganic salts, petroleum hydrocarbons, surfactants, heavy metals, and persistent organic pollutants such as phenols, polycyclic aromatic hydrocarbons (PAHs), and n-alkanes (Wei et al., 2019). Reported salinity levels range from 100 to 400,000 mg/L, far exceeding that of seawater (approximately 35,000 mg/L), and improper disposal or inadequate treatment of PPW can result in severe ecotoxicological impacts (Abdalrhman and Gamal El-Din, 2020). Therefore, the safe treatment and reuse of PPW remain critical for environmental protection and regulatory compliance (Mansour et al., 2024; Zhao et al., 2024).

Conventional treatment methods such as gravity separation, coagulation/flocculation, membrane filtration, and biological processes are often inadequate, especially under field conditions where emulsified and low-biodegradability compounds are present (Mokif et al., 2022; Narayan Thorat and Kumar Sonwani, 2022; Varjani et al., 2020). In recent years, electrochemical oxidation (EO) has emerged as a promising advanced treatment technology due to its ability to mineralize a broad spectrum of organic contaminants through the in-situ generation of strong oxidants such as hydroxyl radicals and active chlorine species (Abdalrhman and Gamal El-Din, 2020; Gargouri et al., 2014; Zhao et al., 2024). However, the performance of EO is strongly influenced by the physicochemical characteristics of the treated wastewater (Abdalrhman and Gamal El-Din, 2020; Bian et al., 2019). Conditions that limit effective interactions between target pollutants and in situ generated oxidants can significantly compromise treatment efficiency. Previous studies have shown that organic fouling caused by aromatic compounds is largely dictated by the anode potential, which governs the electrode's thermodynamic behavior and promotes the formation of passivating polymeric films from reactive intermediates (Abdalrhman and Gamal El-Din, 2020). The presence of chloride has been shown to mitigate this issue

by suppressing polymeric film formation through the generation of active chlorine species (e.g., Cl• and Cl_2) via anodic oxidation. By contract, inorganic fouling on the cathodic electrode is primarily caused by the precipitation of carbonate and hydroxide salts under locally alkaline conditions remain the main issue that control the performance of electrochemical system (Eq1) (Chow and Pham, 2021; Severin and Hayes, 2019). Similar inorganic cathode fouling also observed in electrocoagulation and water softening, which strongly promoted by the elevated hardness, has emerged as a critical challenge, leading to decreased reactor efficiency and long-term operational instability (Chow et al., 2021; Chow and Pham, 2021).

Several fouling mitigation strategies have been investigated, including chemical dosing, ultrasound, and mechanical scrubbing. alternating polarity has received considerable attention due to its ability to remove electrode fouling in situ without the need for additional chemicals or physical cleaning (Bian et al., 2019). By periodically reversing the electrode polarity, this approach effectively neutralizes localized alkaline conditions at the cathode, thereby inhibiting the formation of scaling precipitates. Besides mitigating fouling, alternating polarity extends its application to enhance biogas production in methanogenic reactors and promote the degradation of recalcitrant compounds in microbial fuel cells through pathway regulation. Recently, alternating polarity also showed enhanced electrochemical pollutant degradation on per- and polyfluoroalkyl substances and antibiotics by generating additional active sites and altering electrostatic interactions. While the performance of alternating polarity depends on solution chemistry, electrode material and configuration, and operating parameters such as current density and exchange frequency. For instance, Chow et al. (2021) demonstrated that Faradaic efficiency (the coagulant production efficiency per unit of electric charge passed through the system) is strongly dependent on electrode material and on the frequency of alternating polarity, rather than being simply improved by higher current density. Based on these findings, the integration of alternating polarity into EO systems represents a promising strategy to mitigate electrode fouling and enhance degradation efficiency in the treatment of PPW (Bian et al., 2019; Chow et al., 2021; Yao et al., 2023). Therefore, this study aims to systematically evaluate alternating polarity-assisted electrochemical

systems for mitigating electrode fouling and degrading n-alkane (n-docosane) in PPW. Optimal operating voltage and electrode configurations were determined using batch electrochemical reactors, while long-term performance was assessed in a semi-continuous setup. Key performance indicators, including removal efficiency, oxidant generation and effluent pH were measured to comprehensively characterize system behavior. The results are expected to support the development of more sustainable and resilient EO technologies for complex wastewater treatment applications.

2. Methode and material

2.1 Water composition

Simplified produced water containing 84 g/L NaCl, 8.4 g/L $NaHCO_3$ and a concentration of 4 g/L n-docosane (3400 mg/L TOC) was introduced into the batch reactor. Synthetic produced water was prepared for semi-continuous reactor using analytical grade reagents: 68 g/L NaCl, 21.5 g/L $CaCl_2$, 2 g/L $MgSO_4$, and 1 g/L $CaCO_3$ (Table 1). The pH was adjusted to 6.5 by adding 0.5 mL of 1 M H_2SO_4 per liter of solution. This resulted in a total alkalinity of 300 mg/L as $CaCO_3$ and a total hardness of 21,900 mg/L as $CaCO_3$, primarily contributed by calcium (Table 1). Due to the limited solubility of n-docosane in water, a higher concentration of 10 g/L (8500 mg/L TOC) was employed in the semi-continuous reactor to facilitate better mixing.

2.2 Reactor and electrochemical configuration

Electrochemical degradation experiments were conducted in both batch and semi-continuous reactors. Batch tests, each with a working volume of 100 mL, were performed over varying reaction times to investigate degradation kinetics. Based on the batch results, the semi-continuous was operated at a hydraulic retention time (HRT) of 48 hours in order to achieve an around 90% degradation of the n-docosane. The semi-continuous maintained the same geometric configuration as the batch system.

Each reactor was equipped with two parallel electrodes spaced 10 mm apart. Two types of electrodes were evaluated: a boron-doped diamond (BDD) electrode supported on a niobium substrate (BDD/Nb 2500ppm neoCoat, La Chaux-de-Fonds, Switzerland), and a graphite electrode (9121K64, McMaster-Carr, Elmhurst, IL, USA). BDD electrodes are widely recognized for their ability to generate strong oxidizing species—such as

hydroxyl radicals, sulfate radicals, and free chlorine, while minimizing oxygen evolution through water electrolysis (Eq. 1) (Wang and Xu, 2012). In contrast, graphite electrodes serve as a cost-effective, electrochemically inert alternative and are commonly employed in environmental applications (Sivodia and Sinha, 2020).

$$2H_2O \rightarrow 4e^- + 4H^+ + O_2 \qquad \textit{Equation 1}$$

For the batch experiments, various applied voltages (2, 4, and 5 V) were tested, and electrode configurations (BDD/BDD, BDD/Graphite, and Graphite/Graphite) were evaluated specifically at 4 V. It is important to note that n-docosane is practically insoluble in water, therefore, the compound was preheated to 45 °C before each experiment to ensure complete liquefaction and was maintained at this temperature throughout the procedure. However, the resulting mixture was not a true homogeneous solution but rather a two-phase system. As a result, time-resolved sampling from a single batch was not feasible due to potential inconsistencies in phase distribution. To ensure accuracy and reproducibility, each batch experiment was performed independently using a freshly prepared mixture. This approach minimized variability caused by the heterogeneous distribution of n-docosane and ensured that each measurement reflected the degradation behavior at a specific time point under consistent experimental conditions.

For the semi-continuous experiments, 48hr HRT was achieved by replacing 50 mL of solution with 50 mL of 10 g/L n-docosane solution every 24 hours. Two types of electrode polarity configurations (constant polarity and alternating polarity) were evaluated under an applied voltage of approximately 4 V. A corresponding constant current mode was used to ensure stable electrochemical conditions throughout the tests since the absolute current need to keep below 1.0 A. Different polarity conditions were induced by a BioLogic SP-150eZ potentiostat (BioLogic, Seyssinet-Pariset, France). Constant polarity established a constant anodic and cathodic conditions for BDD and graphite electrode configuration respectively (BDD/Gr). Alternating polarity periodically exchanged electrodes from anodic to cathodic conditions for graphite and graphite configuration (Gr/Gr) and back again, where the frequency was referred to as the

exchange frequency, 0.5 hr^{-1} exchange frequency was chosen by previous result. At the end of the experiment, extract the electrodes to determine the adsorption.

2.3 n-docosane adsorption isotherm and kinetics

Preliminary tests confirmed that n-docosane was stable when heated at 45 °C, with nearly 100% recovery in the absence of electrodes (Fig. 3.1A). However, when electrodes were present without current, most of the compound was depleted from the bulk solution. Extraction revealed that n-docosane was primarily adsorbed onto the electrodes, with graphite retaining the largest fraction (~75%) (Fig. 3.1B&C). These findings indicate a strong affinity of graphite for n-docosane.

To further evaluate the equilibrium adsorption capacity of graphite for n-docosane and to elucidate the underlying adsorption mechanism, isotherm experiments were conducted at 45 °C. A series of *n*-docosane stock solutions were prepared by adding 0.05, 0.1, 0.5, 1.0, and 1.2 g of *n*-docosane to 100 mL of synthetic produced water, yielding concentrations of 0, 0.5, 1, 5, 10, and 12 g/L. A pre-weighed amount of graphite was then half submerged to each solution. The beakers were placed in a temperature-controlled orbital shaker and agitated at 150 rpm for 8 hours to ensure the equilibrium was reached. After equilibration, the residual concentrations of *n*-docosane in the solutions were quantified as described in the analytical methods.

Adsorption kinetics experiments were conducted at 45 °C to evaluate the time-dependent behavior of n-docosane adsorption onto graphite and to identify potential rate-limiting steps and underlying adsorption mechanisms. A solution with an initial concentration of 10 g/L was prepared by dissolving 1 g of n-docosane in 100 mL of synthetic produced water, followed by gentle heating and stirring to ensure complete dissolution. Pre-weighed graphite was then half submerged to the solution. The beakers were subsequently placed in a temperature-controlled orbital shaker set to 150 rpm and maintained at 45 °C throughout the experiment. Samples were collected and the residual concentration of n-docosane was quantified at 0.5, 1, 2, 4, 6, 8, and 24 hours according to the analytical methods.

2.4 Analytical method

n-Docosane was first extracted out of the solution into hexane and measured in the hexane phase using a gas chromatograph. For gas chromatography a non-polar column was used in combination with an FID detector, which had a temperature set to 400ºC to ensure that n-docosane was in the vapor phase during detection. To create a timely gas chromatography (GC) run a temperature profile was chosen such that 40ºC was held for 3 minutes to pass the hexane through, then the temperature was ramped to final temperature of 230ºC to drive out the n-docosane within 13 minutes. This procedure was able to separate hexane and docosane for easy quantification.

Water quality parameters, such as pH and chloride, were monitored over the course of each experiment. The potential oxidant reagent was carried out by cyclic voltammetry in this system (Eq. 2-5). Because of extremely high amounts of Cl- (~55,000 mg/L), so free chlorine was considered as the main oxidant reagent, which was colorimetrically measured using the standard DPD method as previously described (Zheng et al., 2015). Electrochemical conditions, i.e., applied voltage or current, were set and actively monitored using a BioLogic SP-150eZ potentiostat.

$$2Cl^- \rightarrow Cl_2 + 2e^- \qquad \textit{Equation2}$$

$$SO_4^{2-} \rightarrow SO_4 \cdot^- + e^- \qquad \textit{Equation 3}$$

$$2H_2O + 2e^- \rightarrow H_2 + 2OH^- \qquad \textit{Equation 4}$$

$$OH^- \rightarrow OH \cdot^- + e^- \qquad \textit{Equation 5}$$

2.5 Data Analysis

To evaluate the adsorption behavior of n-docosane onto graphite, experimental equilibrium data were fitted using the Langmuir isotherm model, which assumes monolayer adsorption on a homogeneous surface with a finite number of identical sites (Wang and Guo, 2020; Zhu et al., 2019a). The nonlinear form and linearized form of the Langmuir equation are expressed as:

$$q_e = Q^0 \frac{bC_e}{1 + bC_e} \qquad \textit{Equation 6}$$

$$\frac{1}{q_e} = \left(\frac{1}{Q^0 b}\right)\left(\frac{1}{C_e}\right) + \frac{1}{Q^0} \qquad \textit{Equation 7}$$

Where q_e is the number of moles (or sometimes mass) of adsorbed per unite mass of adsorbent, and Q^0 is the number of moles (or sometimes mass) of adsorbate adsorbed per unit mass od adsorbent at complete surface coverage, and C_e is the (equilibrium) solute concentration, and b is Langmuir constant.

The time-dependent adsorption of n-docosane onto graphite was analyzed using the pseudo-second-order kinetic model, which assumes that chemisorption is the rate-limiting step. The nonlinear form and linearized form of the pseudo-second-order kinetic model are expressed as:

$$q_t = \frac{{q_e}^2 kt}{1 + q_e kt} \qquad \textit{Equation 8}$$

$$\frac{t}{q_t} = \frac{1}{k{q_e}^2} + \frac{1}{q_e} t \qquad \textit{Equation 9}$$

Where q_t is the adsorption capacity at time t, and k is second-order rate constant.

One potential concern with waters with high salinity and hardness is that if pH is allowed to increase, scaling can readily occur. As seen earlier, with the potential for electrolysis of the water to occur hydroxide ions can increase the pH (Eq. 4), leading to the event of scaling within the reactor which may impede treatment efficacy. As such the electrode fouling rate was used to describe the formation of electrode scales (Eq. 10).

$$\text{Electrode fouling rate } (\text{g}/m^2 \cdot \text{day}) = \frac{M_{t-} M_{t0}}{A * (t - t_0)} \qquad \textit{Equation 10}$$

Where M_t was the mass of the electrode at time t in grams, M_{t0} was the mass of the electrode initially in grams, and A was the surface area of the electrode exposed in the reactor in m^2.

3. Results

3.1 Adsorption characteristics of n-docosane onto graphite

3.1.1 Adsorption isotherm

The adsorption of n-docosane onto graphite at 45 °C was well described by the Langmuir isotherm model (Fig. 3.2), which assumes monolayer adsorption on a surface with uniform energy sites and no lateral interactions between adsorbed molecules. The model exhibited an excellent fit to the experimental data with a correlation coefficient of

$R^2 = 0.9904$. Based on the linearized form of the Langmuir equation, the key model parameters were determined: the maximum adsorption capacity Q^0 was calculated to be 0.11 g n-docosane/g graphite, and the Langmuir constant b was 3.36 L/g. The relatively high Q^0 value reflects the strong adsorption affinity of n-docosane for the graphite surface. Furthermore, the asymptotic trend of the isotherm curve at high equilibrium concentrations supports the concept of site saturation, indicating that monolayer coverage was achieved under the experimental conditions.

Although the Freundlich model, which assumes heterogeneous surface energies and multilayer adsorption, also produced a relatively good fit ($R^2 = 0.9813$), its calculated Freundlich constant n was 0.39, indicating unfavorable adsorption behavior. In general, an n value less than 1 suggests that adsorption becomes less efficient as the concentration increases, which contradicts the observed saturation trend. Therefore, the Langmuir model not only provided a better statistical fit but also yielded parameters more consistent with the physical nature of the system. These findings suggest that n-docosane adsorption on graphite follows a monolayer adsorption mechanism, likely dominated by van der Waals interactions on a relatively uniform surface.

3.1.2 Adsorption kinetics

The adsorption kinetics of n-docosane onto graphite at 45 °C were evaluated using both pseudo-first-order and pseudo-second-order kinetic models to better understand the adsorption mechanism. As shown in Fig. 3.3, the pseudo-second-order model provided an excellent fit to the experimental data, with a correlation coefficient of $R^2 = 0.9957$ compared to the pseudo-first-order model with $R^2 = 0.839$, and an equilibrium adsorption capacity q_e of 0.11 g n-docosane/g graphite, which is consistent with the Langmuir monolayer adsorption capacity, showing all sited being taken when it reach equilibrium. The corresponding rate constant k was 60.95, indicating a rapid adsorption process that reached equilibrium within approximately 6 hours. Overall, the superior fit and physically meaningful parameters obtained from the pseudo-second-order model suggest that the adsorption of n-docosane onto graphite follows a mechanism dominated by surface-controlled physisorption, likely through van der Waals interactions, rather than simple mass transfer or diffusion processes described by the pseudo-first-order model.

3.1.3 The impact of fouling on adsorption

To investigate how the accumulation of precipitates affects the adsorption performance of graphite, the equilibrium adsorption capacity was measured under different levels of surface precipitation. Time-resolved precipitation was carried out under batch electrochemical conditions. A 10 g/L solution of *n*-docosane in synthetic produced water was pre-heated to ensure dissolution and then mixed with a known mass of graphite (partially pre-weighed to include deposited precipitates). After 8 hours of contact at 45 °C, the residual *n*-docosane concentration in the solution was quantified, and the adsorption amount onto the graphite was calculated by mass balance.

As shown in Fig. 3.4, the experimentally measured q_e values exhibited a non-linear response to increasing precipitation mass. At low precipitation levels (<100 g/m²), q_e dropped significantly, indicating that early-stage precipitation likely blocked active sites or reduced surface accessibility. Interestingly, as precipitation increased beyond 150 g/m², and then gradually recovered and eventually surpassed the initial values at >300 g/m², suggesting that the deposited layer may start contributing additional adsorption interfaces or modifying surface properties favorably. To further interpret this trend, the Langmuir model was applied to the q_e data to derive the theoretical maximum adsorption capacity Q^0. A similar trend was observed in Q^0, reinforcing the hypothesis that excessive precipitation can structurally or chemically modify the interface to enhance n-docosane adsorption. However, the enrichment induced by precipitation represents a limited fixation effect rather than actual degradation, and the effective removal of pollutants remains primarily dependent on electrochemical reactions.

3.2 Degradation performance in batch reactor

3.2.1 Degradation performance under different voltages

In electrochemical oxidation systems, the applied voltage is a critical parameter that governs the generation of oxidative species and determines the overall degradation efficiency. To optimize voltage for the electrochemical treatment of alkanes, batch experiments were conducted at 2.0 V, 4.0 V, and 5.0 V using a BDD/graphite (BDD/Gr) electrode configuration. Reactions were monitored over time to evaluate the pseudo-first-order degradation behavior of n-docosane under each condition.

As shown in Fig. 3.5, the lowest degradation was observed at 2.0 V, where the normalized concentration (C/C_0) remained at 0.625 after 6 hours. In contrast, 4.0 V and 5.0 V showed significantly enhanced degradation, with C/C_0 values of 0.34 and 0.28, respectively. The corresponding pseudo-first-order rate constants were calculated as 0.086 hr^{-1} for 2.0 V, 0.167 hr^{-1} for 4.0 V, and 0.230 hr^{-1} for 5.0 V. These results demonstrate that higher applied voltages promote faster degradation, likely due to increased generation of reactive oxidative species such as hydroxyl radicals (.OH). Although 5.0 V exhibited the highest degradation efficiency, the difference in performance compared to 4.0 V was not substantial. Given this, 4.0 V may represent an optimal balance point between treatment effectiveness and energy consumption.

In addition to degradation, other system responses also reflected voltage-dependent behavior. The pH of the reactor solution increased with applied voltage, rising from 8.68 at 2.0 V to 9.05 at 4.0 V and 9.49 at 5.0 V. This shift toward alkalinity is likely due to hydroxide ion (OH^-) generation at the cathode. However, more alkaline conditions at higher voltages may accelerate precipitation or scaling on the electrode surface, potentially affecting long-term system stability.

Furthermore, free chlorine (Cl_2) generation was positively correlated with voltage. Negligible free chlorine was detected at 2.0 V, consistent with cyclic voltammetry results that indicated chlorine evolution does not occur below ~3.1 V. At 4.0 V and 5.0 V, free chlorine concentrations increased significantly, with the highest levels observed at 5.0 V, exceeding 1000 ppm by the end of the 6-hour treatment. However, once free chlorine concentrations surpassed ~1000 ppm, increased variability was observed in the measurements at 5.0 V. This instability is likely associated with secondary reactions involving Cl_2, such as disproportionation, volatilization. These pathways can consume free chlorine and reduce its steady-state concentration.

3.2.2 Degradation performance under different electrode configurations

The configuration of electrodes plays a crucial role in determining the degradation performance of n-docosane in electrochemical systems. Experiments were conducted using three electrode pairings: BDD/BDD, BDD/graphite (BDD/Gr), and graphite/graphite (Gr/Gr), under otherwise identical conditions (Fig. 3.6).

The electrode configuration was found to significantly influence the degradation kinetics of *n*-docosane. When considering only the oxidative degradation pathway, the BDD/Gr system exhibited the highest pseudo-first-order rate constant of 0.167 hr^{-1}, followed by Gr/Gr at 0.106 hr^{-1}, and BDD/BDD at 0.070 hr^{-1}. These results indicate that coupling graphite with BDD can enhance the oxidation rate, likely due to improved interfacial electron transfer or electrocatalytic effects at the graphite cathode.

However, analysis of the relative concentration (C/C_0) revealed that the Gr/Gr configuration achieved the lowest final C/C_0 value of 0.30. This rapid initial decrease is primarily attributed to the strong adsorption of *n*-docosane onto the graphite surface at the beginning of the experiment, which significantly reduced its concentration in solutions. This observation highlights the considerable potential of graphite to facilitate *n*-docosane removal through adsorption.

When adsorption was considered, the total removal efficiency further improved. In the Gr/Gr system, the final C/C_0 decreased from 0.30 (oxidation only) to 0.05, and the corresponding observed first-order rate constant increased from 0.106 hr^{-1} to 0.335 hr^{-1}. A similar trend was observed in the BDD/Gr system, where the C/C_0 decreased from 0.34 to 0.166, and the observed rate constant rose from 0.167 hr^{-1} to 0.221 hr^{-1}. In contrast, no significant change was observed in the BDD/BDD configuration, as BDD lacks adsorption capacity.

These findings demonstrate that graphite electrodes not only enhance oxidation rates when coupled with BDD, but also significantly contribute to the overall removal of n-docosane through adsorption. As a considerably more cost-effective alternative, the Gr/Gr configuration exhibited strong performance in both oxidative degradation and adsorption, highlighting its potential for practical applications in electrochemical treatment systems.

The pH evolution of the reactor solution varied slightly depending on the electrode configuration. In all cases, a gradual increase in pH was observed throughout the 6-hour electrolysis period, indicating cathodic generation of hydroxide ions (OH^-) as a common phenomenon across systems. Among the tested configurations, the Gr/Gr system exhibited the most rapid increase in pH during the initial stage (0–2 hr), reaching

approximately 9.2, compared to ~9.0 for BDD/Gr and ~8.8 for BDD/BDD. This could be attributed to the surface properties of graphite, which may promote faster electron transfer and water reduction at the cathode, thereby accelerating OH^- accumulation. After 6 hours, the final pH values for all systems converged between 9.3 and 9.5, suggesting that despite the early differences, the systems eventually reached similar alkaline states. These results imply that graphite-containing electrodes, particularly Gr/Gr, may induce a stronger initial local alkalinity, which could influence factors such as precipitation, radical speciation, or adsorption equilibria during treatment.

The generation of free chlorine (Cl_2) varied notably across different electrode configurations. In the initial 2 hours, all systems exhibited a rapid increase in Cl_2 concentration, consistent with active anodic oxidation of chloride ions (Cl^-). However, the extent and stability of free chlorine accumulation differed between electrode pairs. The Gr/Gr system produced the highest Cl_2 concentration at 2 hours (~800 ppm), followed by BDD/BDD and BDD/Gr at similar levels (~600 ppm). This initial peak in the Gr/Gr system may be attributed to the high surface area of graphite and its catalytic activity toward Cl^- oxidation. However, after reaching the peak, the Cl_2 concentration in the Gr/Gr system gradually declined to ~550 ppm by 6 hours, suggesting possible chlorine loss due to volatilization, adsorption onto graphite, or secondary reactions with organic species. In contrast, the BDD/Gr system showed a steady and continuous increase in Cl_2 concentration, eventually surpassing the other configurations and reaching ~800 ppm at the 6-hour mark. This trend may reflect sustained Cl^- oxidation by the BDD anode with less chlorine loss, supported by the presence of a graphite cathode. The BDD/BDD system maintained relatively stable chlorine levels throughout, suggesting a balance between production and loss mechanisms. These results suggest that while graphite electrodes may initially enhance chlorine generation, they also introduce greater variability due to secondary consumption or adsorption. BDD-based systems offer more stable and sustained chlorine production, which could be advantageous for applications relying on indirect oxidation mechanisms.

3.3 Degradation performance in semi-continuous reactors under different electrode polarity

The semi-continuous experiment was operated for 2.5HRT for about 120 hours in total, where each experiment had an applied voltage of about 4.0V. For constant polarity, it was anticipated that an estimated 88.9% degradation of n-docosane with electrode configuration of BDD/Gr based on the first order decay rate of $0.167hr^{-1}$. And for alternating polarity, it was anticipated that an estimated 83.6% degradation of n-docosane with electrode configuration of Gr/Gr based on the first order decay rate of $0.106hr^{-1}$.

3.3.1 Degradation performance under constant polarity

Under constant polarity operation in the semi-continuous system, of the 3.01 g of *n*-docosane introduced, only 0.84 g was recovered in effluent, resulting in a total removal of 2.17 g, or 72.1% (Fig. 3.7). Mass analysis revealed that 0.37 g of *n*-docosane was adsorbed onto the electrodes, with 0.36 g attributed to the graphite electrode and only 0.01 g to the BDD electrode (Fig. 3.8). This distinction highlights the dual role of graphite: it not only facilitates oxidation but also contributes substantially to total pollutant removal through adsorption, which showed adsorption may aid in the overall removal of hydrophobic pollutants like *n*-docosane. After accounting for the adsorbed fraction, it was estimated that 1.80 g (equivalent to 59.6% of the original mass) was removed via electrochemical oxidation.

Interestingly, while 72.1% total removal was achieved, it fell short of the ~90% removal predicted from batch reactor results. Time-resolved effluent monitoring further revealed that *n*-docosane concentration dropped to removal rate 59.4% after 24 hours (Fig. 9). Removal peaked at 86.3% at 48 hours (1.4 g/L), aligning closely with batch predictions. However, this efficiency was not sustained—removal declined to 71.4% after 72 hours and further dropped to 58.7% at 120 hours, falling below the 24-hour value.

This reduction in long-term performance coincided with significant mass accumulation on the electrodes, particularly the graphite electrode, which gained 3.64 g after the trial, while the BDD electrode gained only 0.15 g. These masses greatly exceeded the recovered *n*-docosane (0.36 g and 0.01 g, respectively), suggesting that other species—likely inorganic precipitates—were involved. Post-trial observations confirmed severe

surface scaling on the graphite electrode (Fig.7), whereas BDD showed minimal deposits. The deposits were brittle and distinct from the waxy texture of *n*-docosane, implicating mineral scaling, possibly from Ca^{2+} and Mg^{2+} ions in the high-hardness synthetic water. Indeed, pH increased gradually from 6.5 to 7.4 over 120 hours, a range conducive to carbonate or hydroxide precipitation. Notably, scaling was localized to the graphite surface rather than system-wide, suggesting microenvironmental pH shifts or electrochemical effects at the cathode.

Despite this, free chlorine generation—primarily from the BDD anode—continued to increase, reaching 1,800 ppm at 24 hours and over 4,000 ppm by 120 hours, indicating that oxidant production was not significantly hindered by scaling. However, *n*-docosane degradation declined over time, implying that adsorption onto the graphite electrode was a critical step enabling oxidation. Once the electrode surface was obstructed by scale, adsorption and hence oxidation was impaired.

In conclusion, sustained removal of *n*-docosane in continuous systems is limited not by oxidant availability but by electrode fouling. Effective mitigation of cathodic scaling, particularly on graphite electrodes, is essential for the long-term electrochemical treatment of hydrophobic compounds.

3.3.2 Degradation performance under alternating polarity

The n-docosane degradation was examined under alternating polarity with two graphite electrodes and a 0.5 hr^{-1} exchange frequency based on prior results showing minimized precipitation. It was seen that the mass leaving the reactor of n-docosane was only about 14.3% of the n-docosane that was put into the reactor, whereas there was 28.0% of the input n-docosane that was detected in the effluent under constant polarity. This had resulted in about 85.7% removal of n-docosane under alternating polarity, whereas only 72% of the n-docosane was removed when the reactor was under constant polarity (Fig. 3.9). This was notably higher than the BDD/Gr system, likely due to greater adsorption and oxidation capacity of graphite, as demonstrated in batch tests.

For the n-docosane degradation with time, it was observed that relative concentration of n-docosane went down to 0.08 (relative removal 92%) and remain stable, indicating alternating polarity could solve the deterioration of performance caused by electrode

fouling. Meanwhile, electrode precipitation was visibly reduced, but the high current due to graphite's excellent conductivity contributed to electrode corrosion. Thus, the mass of accumulated deposits was not quantified.

In addition to improved degradation performance, the pH profile of the effluent further highlighted the advantages of alternating polarity operation. The pH of the effluent under constant polarity gradually increased from an initial value of 6.6 to 7.3 after 120 hours. In contrast, the effluent pH under alternating polarity remained more stable, ranging narrowly between 6.5 and 6.7 throughout the duration of the experiment, and ultimately ending at a lower value of 6.7. This consistently lower pH under alternating polarity likely results from enhanced redox cycling and ion exchange reactions occurring at the electrodes due to periodic reversal of current direction. Such conditions suppress the localized accumulation of hydroxide ions near the cathode, which otherwise promotes precipitation of sparingly soluble salts such as $CaCO_3$ or $Mg(OH)_2$. The relatively acidic environment under alternating polarity is therefore less conducive to inorganic scaling, offering an operational advantage in high-salinity and high-hardness waters. These findings suggest that alternating polarity not only enhances pollutant removal but also contributes to the mitigation of electrode fouling by stabilizing pH at levels less favorable for precipitate formation.

The generation of free chlorine further reflects these operational differences. Under alternating polarity, the accumulation of free chlorine was significantly faster during the initial 24 hours, reaching up to ~5000 ppm-Cl_2, much higher than the ~2000 ppm-Cl_2 observed under constant polarity. There was a similar trend observed under Gr/Gr configuration in batch test, rapid increase at initial time but stabilized at similar concentration at the end, which means Gr/Gr. So, the 2.5 times increase cannot simply be attributed to Gr/Gr configuration. Alternating polarity promoted uniform current distribution and periodic regeneration of electrode surfaces which also contributed to the rapid increase in free chlorine in the initial 24hr. Over extended operation, the free chlorine concentration under alternating polarity gradually decreased and stabilized between 3000–4000 ppm-Cl_2, while constant polarity maintained a relatively steady concentration around 3500–4000 ppm-Cl_2. This decline under alternating polarity was

primarily attributed to the long hydraulic retention time (48hr), which limited the replenishment of chloride ions and gradually diluted the reactive chloride species in the bulk solution.

In summary, alternating polarity enhanced *n*-docosane degradation, reduced scaling, and stabilized system pH, making it a promising strategy for long-term electrochemical treatment. However, graphite corrosion remains a limitation. Future efforts should focus on identifying highly conductive yet mechanically durable carbon materials to maintain adsorption and oxidation performance under alternating polarity.

4. Discussion

4.1 Higher voltage facilitated the degradation of n-docosane

The batch experiments demonstrated that applying higher voltages (4 V and 5 V) significantly enhanced the degradation efficiency of n-docosane compared to 2 V. This improvement was accompanied by a marked increase in free chlorine (Cl_2) concentration, indicating enhanced anodic activity and oxidant generation under elevated potentials. According to previous studies, Cl^- and SO_4^{2-} undergo electrochemical oxidation at anodic potentials above 3.1 V and 2.17 V, respectively. Hydroxyl radical (•OH) formation on BDD electrodes theoretically occurs at potentials exceeding 2.3 V (Rajasekhar et al., 2021), and chlorine radicals, including Cl• and $Cl_2^{\bullet-}$, can also be produced during electrochemical and advanced oxidation processes (Lei et al., 2020). Higher applied voltages also lead to increased current density, thereby accelerating electrochemical reaction rates and promoting the generation of oxidants (Al-Tameemi et al., 2024; Ingelsson, 2021). In this study, free chlorine was monitored as a representative indicator of oxidant production efficiency. Although Cl_2 and other chlorine-based oxidants (e.g., HOCl) were abundant under chloride-rich conditions, their direct contribution to n-docosane degradation was likely limited due to the chemically inert and nonpolar nature of these compounds (Alsharyani and Muruganandam, 2024; Rajasekhar et al., 2021). Instead, hydroxyl radicals (·OH) and sulfate radicals ($SO_4^{\cdot-}$), potentially generated at high anodic potentials, are more likely to initiate n-alkane oxidation via hydrogen abstraction, producing oxygenated intermediates such as alcohols, aldehydes, and carboxylic acids (Alsharyani and Muruganandam, 2024; Rajasekhar et al., 2021; Zhu et

al., 2019a). However, the high concentration of chloride may also favor side reactions that quench these reactive radicals (Hand and Cusick, 2021). While chlorine-based oxidants may not dominate the primary oxidation pathway of n-docosane, it is worth noting that chlorine radicals (Cl•) have been shown to effectively oxidize n-alkanes via hydrogen abstraction in the gas phase (Jahn et al., 2021). Nonetheless, in liquid-phase electrochemical systems, their contribution is likely restricted due to their short lifetime, strong competition from side reactions, high background Cl^- concentrations, and mass transfer limitations (Boczkaj and Fernandes, 2017; Jahn et al., 2021). Despite these constraints, chlorine-based oxidants should not be entirely disregarded, as they may participate in secondary transformations of oxygenated intermediates or lead to the formation of chlorinated byproducts, potentially altering the degradation pathway.

With increasing voltage, a concurrent rise in effluent pH was also observed. At the cathode, water reduction reactions produce OH^- and H_2, and the enhanced current promotes OH^- accumulation. Since the electrons used in this process are not diverted to competing reactions, OH^- continuously accumulates in the bulk solution, leading to elevated pH. While this pH shift does not interfere with Cl_2 generation, it can create favorable conditions for inorganic scaling on electrode surfaces in high salinity and high hardness systems. Such fouling may compromise long term electrochemical performance, which raises a concern further explored in the semi-continuous experiments.

4.2 Dual role of graphite in electrochemical degradation

The electrode material had a significant influence on the degradation kinetics of *n*-docosane. The pseudo-first-order rate constant increased from 0.070 hr^{-1} for the BDD/BDD configuration to 0.167 hr^{-1} for the BDD/graphite (BDD/Gr) setup, suggesting a synergistic effect between BDD's high oxidative potential and graphite's excellent conductivity and surface interaction properties. Graphite as cathode likely improved mass transfer and enhanced contact between the pollutants and oxidants, thereby accelerating degradation. Interestingly, even the graphite/graphite (Gr/Gr) configuration outperformed BDD/BDD (0.106 hr^{-1} vs. 0.070 hr^{-1}), despite the absence of strong oxidizer hydroxyl radical (•OH) generation typically associated with BDD. This highlights graphite's

intrinsic ability to contribute to electrochemical degradation through strong adsorption affinity and effective electron transfer.

Notably, the Gr/Gr system achieved fastest initial reduction in solution-phase n-docosane concentration. This was attributed to the strong adsorption affinity of graphite, which enabled rapid pollutant accumulation on the electrode surface. Adsorption not only removed n-docosane from the bulk solution but also increased its local concentration at the electrode interface, thereby facilitating more efficient oxidation. This dual mechanism—adsorption followed by electrochemical oxidation—underscores graphite's multifunctional role in pollutant removal. While graphite has a limited ability to generate reactive oxygen species compared to BDD, its superior adsorption and conductivity properties significantly improve overall degradation performance. These results demonstrate that carbon-based electrodes like graphite can significantly enhance degradation efficiency through combined adsorption and electrochemical processes, making them promising candidates for the treatment of hydrophobic organic contaminants in electrochemical treatment.

4.3 Coupled effects of adsorption dynamics and cathodic fouling

The adsorption of n-docosane onto graphite plays a critical role in enhancing its electrochemical degradation in this system. To clarify the underlying mechanism, both equilibrium isotherm and kinetic models were evaluated. The thermodynamic results showed that the adsorption of n-docosane onto graphite at 45 °C was well described by the Langmuir isotherm model, indicating monolayer adsorption on a surface with uniform energy sites and no interaction between adsorbed molecules. The maximum adsorption capacity (Q^0) was determined to be 0.11 g n-docosane/g graphite, reflecting a strong affinity of the hydrophobic compound for the graphite surface.

In terms of adsorption kinetics, the experimental data fit the pseudo-second-order model with high accuracy. This model suggests that the overall adsorption process involves multiple sequential steps, including bulk transport, film diffusion, intraparticle diffusion, and final attachment at active sites. The model is often associated with chemisorption mechanisms, which involve valence forces and electron exchange between the adsorbent and adsorbate. However, graphite is widely recognized as a physical absorbent, where

physisorption governed by van der Waals interactions is typically dominant. The strong fit of the pseudo-second-order model in this case appears to deviate from the expected behavior of typical Langmuir-type systems and is likely due to specific characteristics of the n-docosane–graphite system. For example, long-chain hydrocarbons such as n-docosane may exhibit significant lateral interactions on the graphite surface, causing deviation from ideal monolayer assumptions. In addition, the biphasic nature of n-docosane in aqueous systems, where much of the compound tends to float at the liquid surface, may influence the mass transfer dynamics and surface coverage kinetics. Similar deviations have been reported in previous studies (Kern et al., 2007; Kern and Findenegg, 1980), where pseudo-second-order kinetics were observed for hydrophobic organic compounds interacting with carbon-based materials. These factors together may explain why the pseudo-second-order model better describes the adsorption process in this case. While in electrochemical treatment of high salinity/ hardness wastewater, electrode fouling is a common operational challenge. Experimental analysis of fouling effects revealed a two-stage influence on adsorption behavior. During the initial phase, the accumulation of inorganic precipitates on the graphite surface blocked active adsorption sites, resulting in a measurable reduction in the equilibrium adsorption capacity. As fouling progressed, however, the growing deposit layer began to provide additional attachment surfaces for n-docosane, partially restoring the overall adsorption capacity. Despite this compensatory effect, the adsorbed n-docosane molecules embedded within the fouling layer lost direct contact with the electrode interface, thereby limiting their access to electron transfer pathways. Consequently, these contaminants could no longer undergo direct anodic oxidation and instead depend on the diffusion of reactive species, such as free chlorine and hydroxyl radicals, to reach and degrade them. Thus, although extensive electrode fouling does not severely compromise the total adsorption of n-docosane, it may substantially impair its direct electrochemical oxidation. These findings highlight the critical role of maintaining a clean and accessible electrode surface to sustain oxidation-driven degradation pathways, especially for hydrophobic contaminants in high hardness/salinity systems.

4.4 Advantages and trade-offs of alternating polarity in long-term operation

The critical role of electrode fouling in long-term degradation performance was confirmed in the semi-continuous system operated under constant polarity. Prolonged operation led to significant fouling at the graphite cathode, accompanied by a notable decline in n-docosane removal efficiency. Over time, the effluent pH increased from 6.5 to 7.3, creating favorable conditions for the accumulation of inorganic precipitates. Interestingly, this fouling did not impair the generation of free chlorine, indicating that the indirect oxidation pathway remained largely unaffected. However, the build-up of precipitates hindered direct contact between n-docosane and the electrode interface, thereby reducing the effectiveness of direct electrochemical oxidation and slowing the overall degradation rate. This interpretation is further supported by previous studies, which reported that the first-order degradation rate decreased with increasing electrode fouling.

In contrast, alternating polarity operation in the semi-continuous system effectively mitigated electrode fouling. Throughout the extended treatment period, no significant decline in degradation efficiency was observed. This improvement is primarily attributed to the periodic reversal of anodic and cathodic roles, which neutralizes localized pH gradients and maintains near-neutral conditions at the electrode surfaces, thereby suppressing fouling. Moreover, alternating polarity significantly enhanced free chlorine production during the initial stage, exceeding levels observed under constant polarity operation. Although the Gr/Gr configuration in batch tests was shown to stabilize free chlorine levels more rapidly than BDD/Gr, it did not achieve a higher peak concentration. Thus, the early stage increase under alternating polarity can be attributed to enhanced electron utilization. Unlike constant polarity systems, where chloride is oxidized predominantly at the anode, alternating polarity enables chloride oxidation at both electrodes, effectively doubling the reactive surface and promoting faster Cl_2 formation. Interestingly, after the initial peak, free chlorine concentrations gradually declined to levels comparable to those in constant polarity operation. This reduction may be attributed to the depletion of readily oxidizable chloride species near the electrode surfaces and the limited replenishment rate from the bulk solution. Despite this decline,

degradation efficiency remained high throughout the experiment. This decoupling between oxidant concentration and removal performance is likely a result of the intrinsic characteristics of the Gr/Gr electrode configuration. The strong adsorption capacity of graphite facilitates rapid accumulation of n-docosane at the electrode interface, enhancing the effectiveness of direct oxidation. This mechanism is consistent with batch experiments, where the observed first order degradation rate constant (kobs) for Gr/Gr was notably higher than that for BDD/Gr, highlighting graphite's superior combined adsorption and oxidation performance.

Overall, these findings demonstrate that alternating polarity not only mitigates fouling and enhances early-stage oxidant generation but also maintains long-term degradation efficiency through the synergistic effects of adsorption and oxidation at the graphite electrode. These advantages underscore its value as an operational strategy for treating hydrophobic contaminants in challenging, high-salinity water matrices.

Despite the advantages of alternating polarity, prolonged operation at high current density led to noticeable graphite electrode deterioration, including pitting, mass loss, and fragmentation. This is attributed to the periodic role reversal of electrodes, where graphite alternates between anodic and cathodic states. Under anodic conditions, electrochemical oxidation produces carbon oxides, while cathodic phases generate local alkalinity that promotes surface hydroxylation and delamination. The high conductivity of graphite further accelerates these degradation processes under alternating polarity, resulting in more severe structural damage than in constant polarity systems (Abdalrhman and Gamal El-Din, 2020; Al-Tameemi et al., 2024; Zhao et al., 2024).

These findings underscore the trade-off between improved process efficiency and material durability. While alternating polarity enhances pollutant removal and suppresses fouling, it also imposes greater electrochemical and mechanical stress on electrode materials. Future work should focus on developing more corrosion-resistant carbon-based electrodes or optimizing switching frequency and current density to strike a balance between performance and longevity.

5. Conclusion

This study systematically investigated the electrochemical degradation of n-docosane in high-salinity and high-hardness synthetic produced water using both batch and semi-continuous systems. Through a series of experiments examining applied voltage (2,4,5V), electrode configuration (Anode/Cathode: BDD/BDD, BDD/Gr, Gr/Gr) and electrode polarity (constant polarity, alternating polarity), we identified key factors that govern degradation efficiency and long-term operational stability.

Initial batch tests demonstrated that increasing the applied voltage from 2 V to 4–5 V significantly enhanced degradation efficiency, primarily due to the elevated generation of free chlorine (Cl_2) above applied voltage 3.1V, the dominant oxidant under high-chloride conditions. However, this enhancement came at the cost of intensified hydroxide (OH^-) accumulation at the cathode, resulting in localized alkalinity and a heightened risk of inorganic precipitation, posing challenges for long-term operation.

Another finding from electrode configuration was graphite electrodes exhibited a strong adsorption affinity for n-docosane, enriching pollutant concentration at the electrode interface and thereby facilitating direct electrochemical oxidation. When employed as both anode and cathode, graphite delivered the highest overall removal efficiency, outperforming BDD-based systems due to the synergistic effect of adsorption and oxidation. These results highlight the importance of preserving active electrode sites, as fouling can obstruct both adsorption and oxidation pathways and compromise overall performance.

Long term semi-continuous experiments under constant polarity confirmed that sustained operation led to gradual pH elevation and substantial electrode scaling, particularly on the graphite cathode. This fouling severely limited pollutant–electrode interaction and caused a decline in degradation efficiency over time, validating the concerns observed in batch experiments. While alternating polarity operation effectively mitigated these issues by periodically reversing electrode roles, stabilizing pH, suppressing scale formation, and maintaining high degradation performance throughout extended operation.

Despite these advantages, alternating polarity accelerated graphite corrosion due to repeated exposure to both anodic oxidation and cathodic delamination. This finding

underscores a trade-off between improved fouling resistance and material durability. In conclusion, graphite serves as a cost-effective and high-performance electrode material for the electrochemical treatment of hydrophobic organic contaminants. However, future work should focus on developing more corrosion-resistant carbon-based electrodes and optimizing polarity-switching parameters to balance long-term efficiency with structural integrity under demanding water chemistries.

Table 3.1: Synthetic produced water composition

Ionic species	Concentration (mg/L)
Ca^{2+}	8,100
Na^{+}	27,000
Mg^{2+}	400
Cl^{-}	55,000
SO_4^{2-}	1,600
CO_3^{2-}	0.01M
Hardness	21,900 mg/L as $CaCO_3$
Alkalinity	300 mg/L as $CaCO_3$
pH	6.5

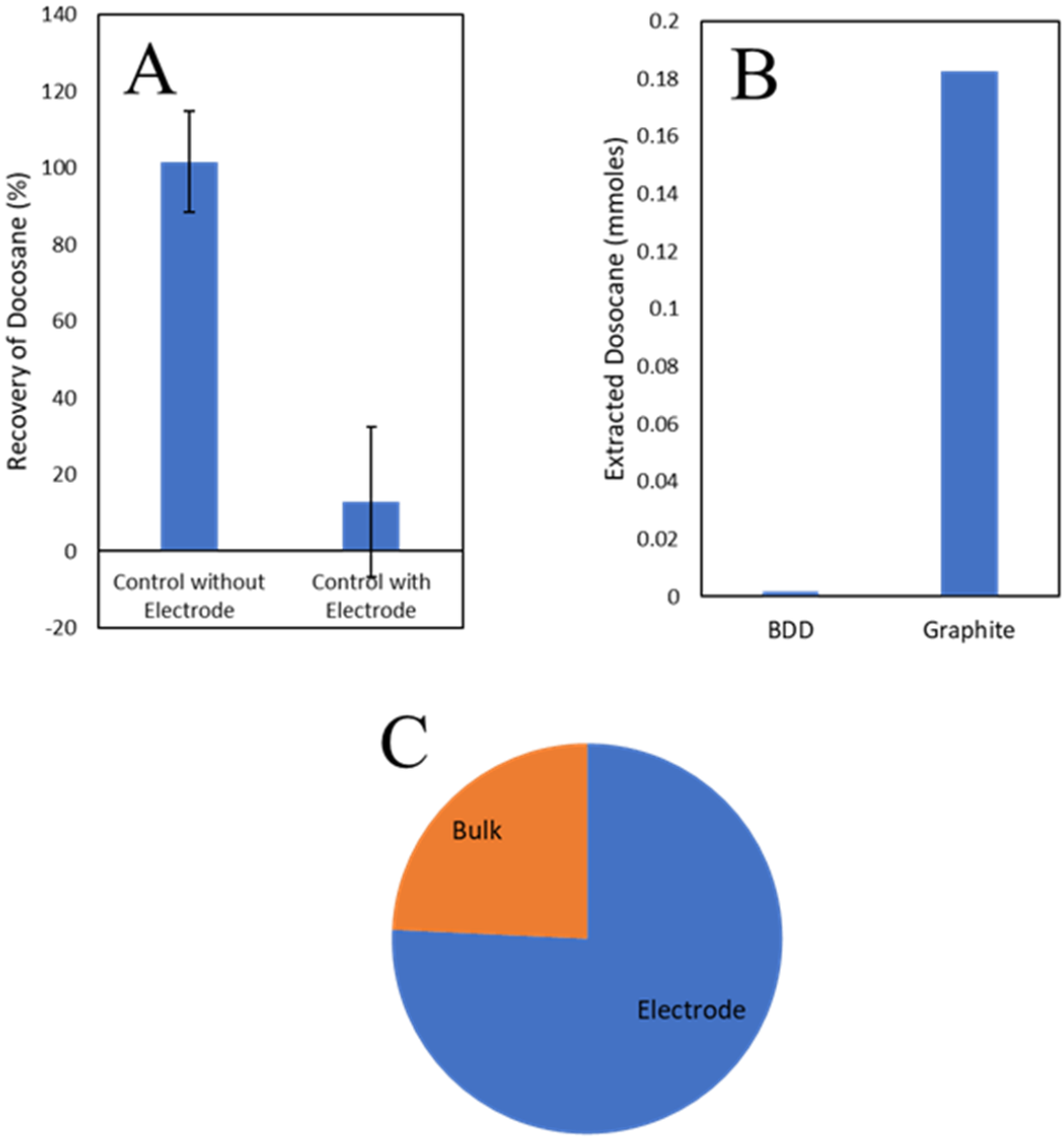

Figure 3.1: Control tests for n-docosane comparing with and without the inclusion of electrodes (A). Further extractions were made with the electrodes to see how much n-docosane was found on BDD and graphite electrodes (B). With extractions from both the bulk solution and electrodes the proportion of docosane could be found for control tests (C)

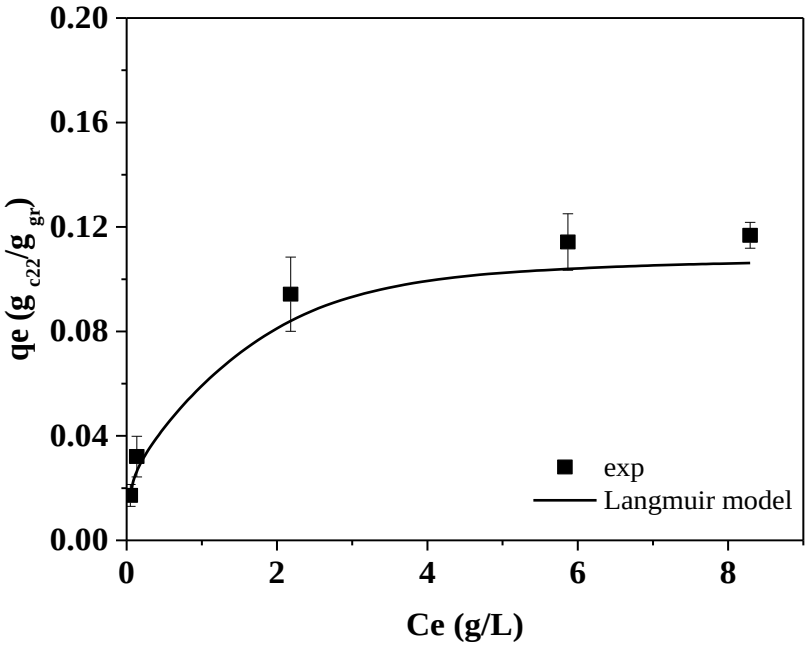

Figure 3.2: n-docosane adsorption and desorption isotherms on the graphite at 45 °C, Langmuir model R^2= 0.9904.

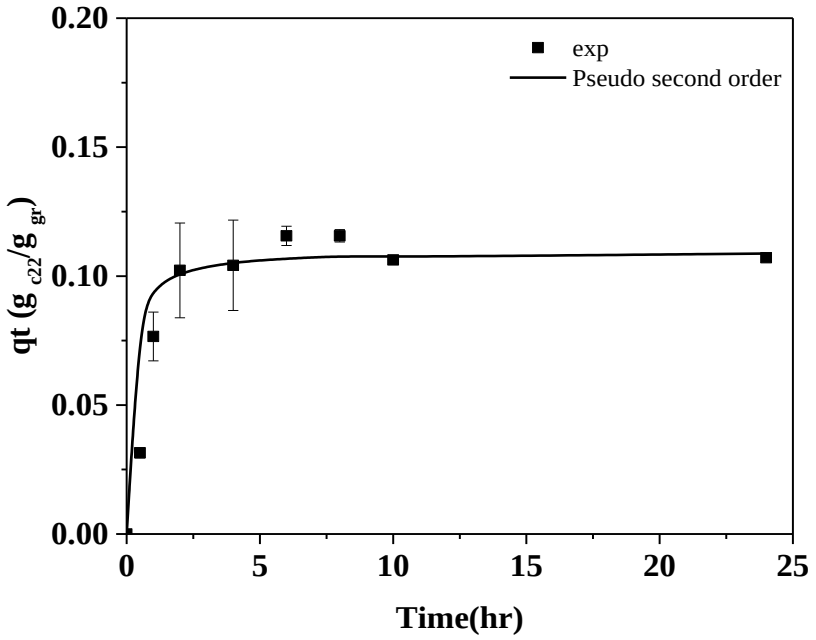

Figure 3.3: n-docosane adsorption kinetics on the graphite at 45°C, pseudo second order R^2= 0.9957.

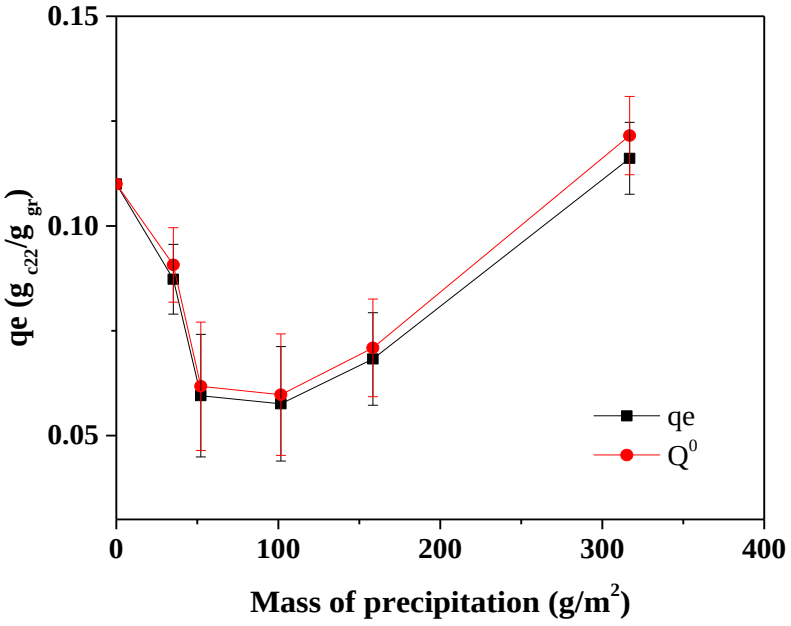

Figure 3.4: The mass of n-docosane adsorption on the graphite at different precipitation accumulated.

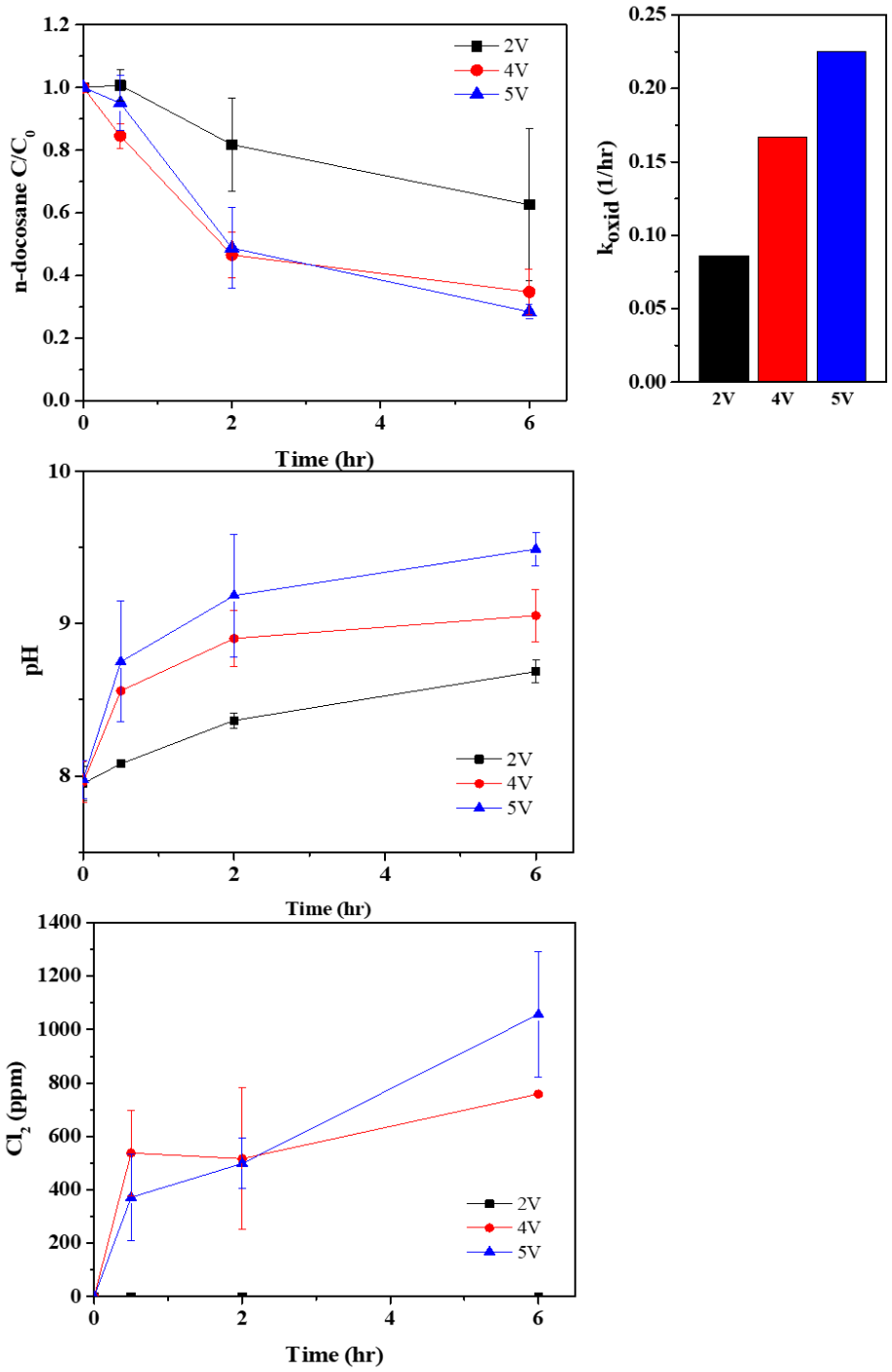

Figure 3.5: Impact that applied voltage and different electrode sets on the electrochemical degradation of n-docosane and the first-order decay constant over different conditions.

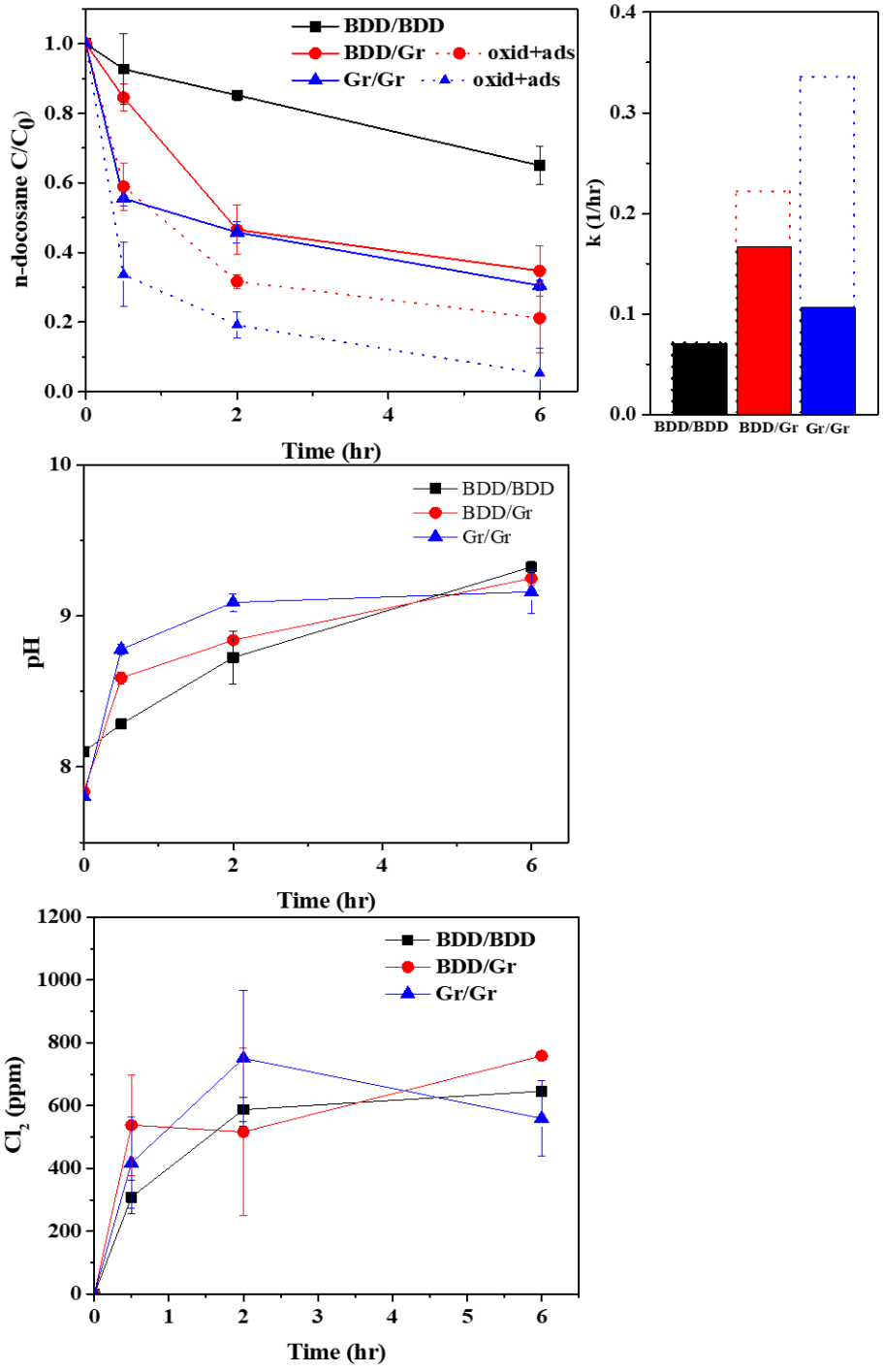

Figure 3.6: Impact that different electrode sets on the electrochemical degradation of n-docosane and the first-order decay constant over different conditions.

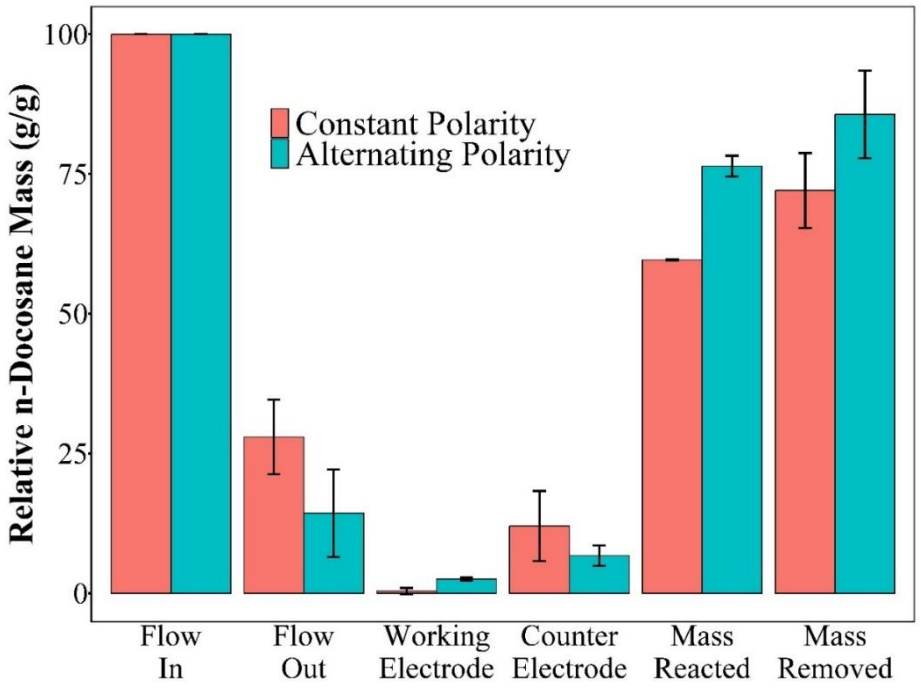

Figure 3.7: Relative n-docosane mass distribution under constant and alternating polarity conditions.

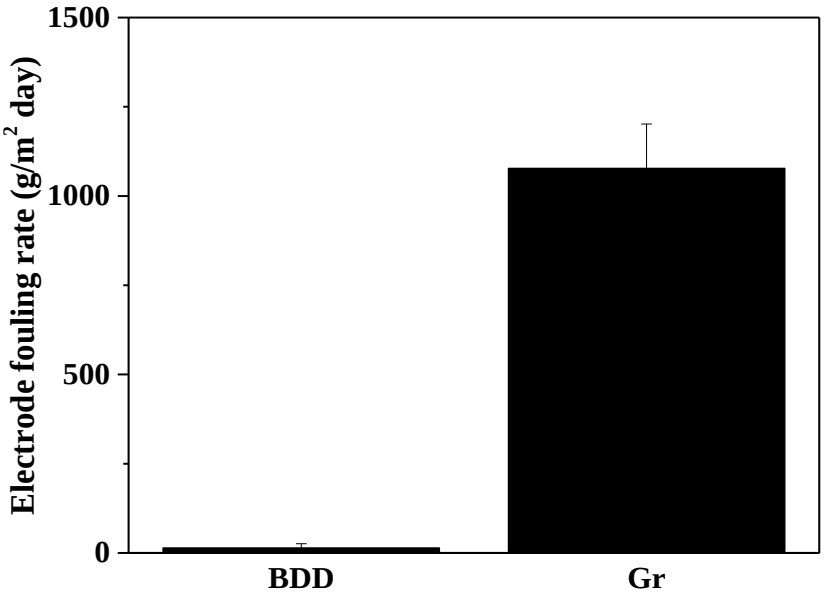

Figure 3.8: Electrode fouling rate under constant polarity

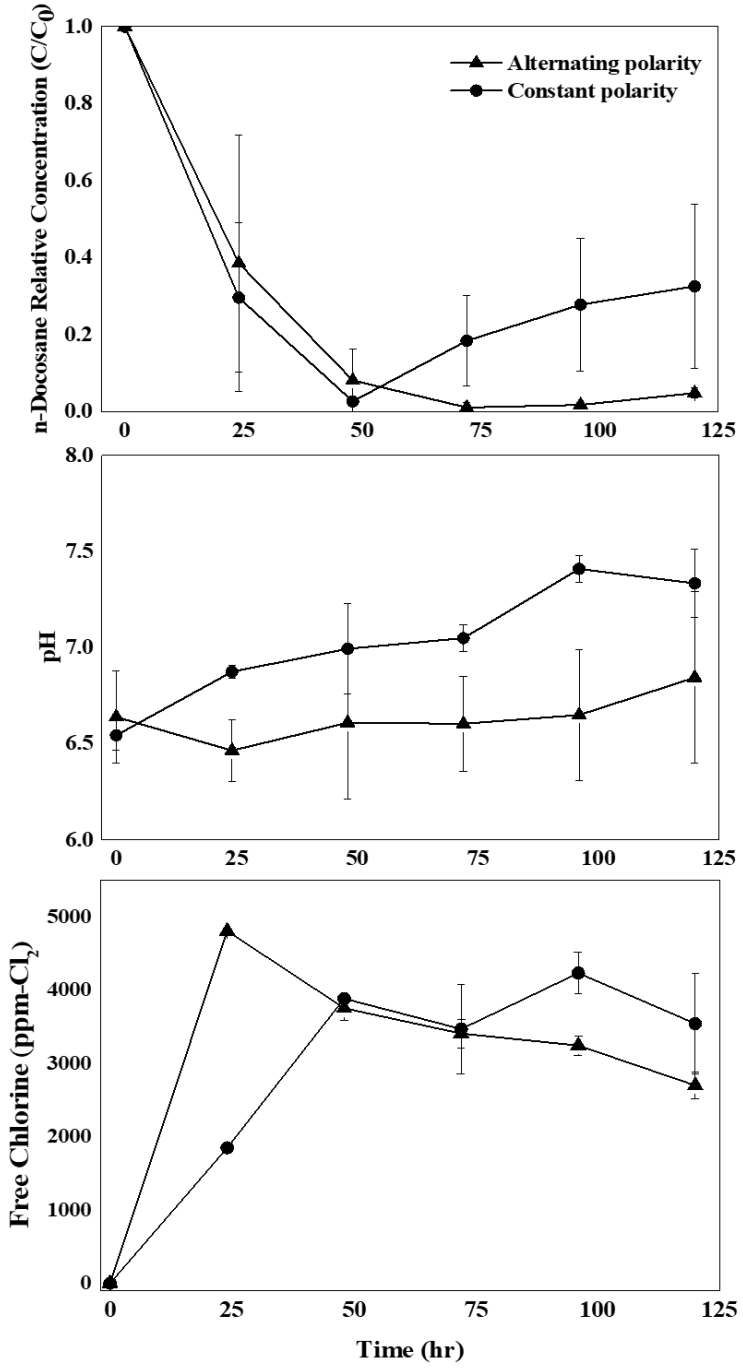

Figure 3.9: Electrochemical reactor performance under different electrode polarities

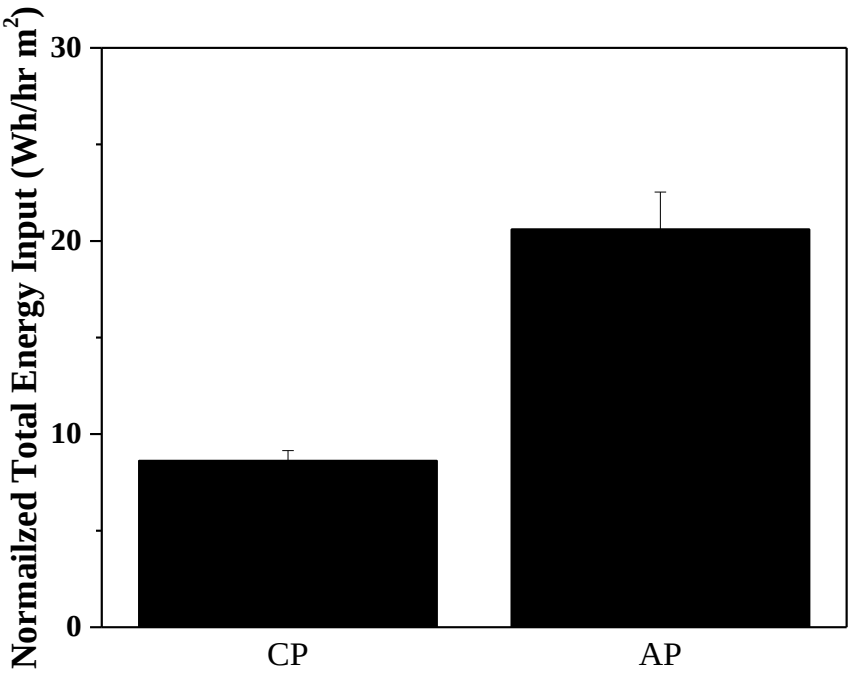

Figure 3.10: Normalized total energy input under different electrode polarities in semi-continuous reactors

CHAPTER IV SUMMARY

This thesis systematically investigated EO to decontaminate organic pollutants in high salinity/hardness wastewater, where electrode fouling critically limited long-term operation. Unlike prior studies, which generally considered fouling control or treatment performance in isolation, this work systematically examined the interplay between these two aspects while also accounting for energy consumption.

In the first part of this study, methylene blue was used as a model compound, different electrode configuration (anode/cathode: BDD/Gr, Gr/Gr), electrode polarity (constant polarity, alternating polarity) and exchange frequency (2 hr^{-1}, 0.5 hr^{-1}, 0.25 hr^{-1}) in alternating polarity have been tested in continuous reactor. Electrochemical reactor performance was assessed through multiple indicators, including pollutant degradation efficiency, production of oxidizing agents, and effluent pH. In addition, energy consumption and coulombic efficiency were calculated to quantify system efficiency and sustainability.

Results showed that long-term experiments revealed that constant polarity operation led to rapid cathodic scaling, a steady decline in removal efficiency, and a decrease in coulombic efficiency. Degradation efficiency remained high during the initial stage but gradually declined after 48 hours, dropping below 90% by 72 hours of continuous operation. The first-order decay rate decreased sharply, from 1.83 min^{-1} at the beginning to 0.933 min^{-1} after 12 hours, indicating a substantial loss of kinetic activity. Notably, this decline occurred even though the production of oxidizing agents showed little variation, suggesting that the performance deterioration was primarily attributable to cathodic fouling and the consequent reduction of effective electrode surface area rather than a shortage of oxidant generation.

In contrast, alternating polarity substantially reduced scale accumulation, maintained stable degradation performance, and improved coulombic efficiency, Specifically, electrode fouling significantly from 201 g/m^2 day to 26 g/m^2 day and the production of oxidation reagent (Cl_2) was 2.8 times higher than constant polarity due to the higher electron utilization (Columbic efficiency), which demonstrate greater pollutant degradation potential. However, this improvement came at the cost of a 122% increase in energy consumption. Substituting graphite for BDD as the anode reduced energy

consumption by 27% while maintaining comparable performance. Substitute BDD to graphite maintained the great performance also decreased the energy consumption 27%. Importantly, the polarity exchange frequency was shown to govern the trade-off between fouling mitigation and energy input. High exchange frequency was effective in stabilizing effluent pH but failed to significantly reduce electrode scaling, leading to increased energy consumption without proportional performance gains. Optimized exchange frequency, particularly around 0.5 hr^{-1}, achieved the best overall outcomes by markedly reducing fouling intensity, enhancing oxidant generation, and sustaining high pollutant removal but higher energy input. While excessively low exchange frequency allowed substantial precipitation to accumulate, thereby lowering fouling-control efficiency even though oxidant production did not decline noticeably. These findings highlight that the design of alternating polarity assisted EO systems must carefully tailor the polarity-exchange frequency to simultaneously achieve fouling control, pollutant degradation, and energy efficiency.

In the second part of this study, n-docosane was selected as a representative n-alkane pollutant in synthetic petroleum produced water (high salinity and high hardness) to evaluate the applicability of alternating polarity-assisted EO under more complex and hydrophobic conditions. Applied voltages (2, 4, and 5 V) and electrode configurations (anode & cathode: BDD & BDD, BDD & Graphite, Graphite & Graphite) were tested under bath reactor. Voltages above 4 V initiated effective degradation of n-docosane, primarily due to the formation of strong oxidative species such as free chlorine and reactive radicals. BDD & Gr electrode configuration exhibited the highest first order decay rate of 0.167 hr^{-1}. Surprisingly, the strong adsorption of n-docosane onto graphite enabled the Gr/Gr electrode configuration to achieve the highest overall removal efficiency, owing to the combined effects of adsorption enrichment and subsequent electrochemical oxidation. Adsorption isotherm and kinetics were employed to study the adsorption behaviors, the maximum adsorption capacity was calculated to be 0.11 g n-docosane/g graphite, and rapid adsorption process that reached equilibrium within approximately 6 hours, early-stage precipitation blocked active adsorption sites while excessive precipitation started to contribute additional adsorption interfaces. A long term

semi-continuous reactor operated at a 48 h HRT was employed to evaluate the alternating polarity (AP)-assisted EO system, with a 2 h exchange interval selected based on the results of the first part. The BDD/Gr configuration was tested under constant polarity, while the Gr/Gr configuration was applied under AP operation due to graphite's strong adsorption affinity for n-docosane.

Under constant polarity, severe electrode fouling markedly hindered degradation performance, as reflected by the decline in n-docosane removal from 71.4% at 72 h to only 58.7% after 120 h. In contrast, AP operation significantly enhanced overall removal efficiency, increasing from 72.0% under constant polarity to 85.7%, and importantly, no obvious decline in degradation efficiency was observed over the extended treatment period. Effluent pH stabilized at a lower level during AP operation. However, the concentration of oxidizing agents, particularly active chlorine, rapidly peaked and then declined, which can be attributed to chloride depletion in the electrolyte. Furthermore, although AP effectively reduced inorganic scaling, the high current densities associated with graphite's excellent conductivity accelerated electrode corrosion, highlighting a potential limitation for long-term operation.

Overall, this work provides new mechanistic and practical insights into the application of electrochemical oxidation for treating high-salinity and high-hardness wastewaters. The results clearly demonstrate that electrode fouling, rather than oxidant generation, is the primary factor limiting long-term performance, and that alternating polarity can effectively mitigate scaling while sustaining pollutant removal. At the same time, the findings reveal important trade-offs: shorter or excessively long exchange intervals compromise either fouling control or energy efficiency, while optimized intervals enhance oxidant production and maintain stable degradation. In addition, the experiments with n-docosane highlight the critical role of electrode material, where graphite offers strong adsorption–oxidation synergy that improves overall removal efficiency but also introduces challenges such as electrode corrosion under high current densities. Taken together, these results emphasize that the sustainable application of alternating polarity–assisted electrochemical oxidation requires an integrated strategy that combines electrode material selection, optimized voltage windows, and carefully tailored polarity-exchange

intervals to simultaneously achieve fouling mitigation, high degradation efficiency, and energy efficiency in complex saline and hardness-rich wastewaters.

CHAPTER V FUTURE WORK

Although this thesis has provided systematic insights into the mechanisms and performance of alternating polarity–assisted electrochemical oxidation for treating high-salinity and high-hardness wastewater, several important limitations remain that warrant further investigation. Building on the present findings, the following areas are recommended for future work:

1. Optimization of Polarity-Exchange Strategies

This study demonstrated that polarity-exchange intervals govern the balance between fouling mitigation, pollutant degradation, and energy consumption. Future work should explore adaptive or dynamic control of polarity-exchange frequency, potentially linked to real-time monitoring of cell voltage, pH, or conductivity. Such feedback-based control systems may allow EO reactors to automatically adjust exchange intervals in response to changes in water chemistry, pollutant loading, or scaling intensity, improving efficiency and stability in practical operation.

2 Advanced Electrode Materials and Configurations

Graphite showed strong adsorption–oxidation synergy but suffered from corrosion under high current densities, while BDD provided stability but at higher cost and lower adsorption capacity. Future research should focus on hybrid electrode designs (e.g., graphite composites, protective coatings, Magnéli phase Ti_4O_7) to combine adsorption capability with enhanced durability. In addition, three-dimensional electrode structures or flow-through porous electrodes should be investigated to improve mass transfer and reduce local fouling while minimizing energy demand.

3 By-product Formation and Mitigation

Although alternating polarity improved pollutant degradation, the production of oxidizing agents such as active chlorine may lead to unwanted by-products (e.g., chlorate, perchlorate, AOX). Future work should evaluate the formation pathways of these by-products under long-term alternating polarity operation, and assess strategies to mitigate them, such as coupling EO with granular activated carbon, sulfate radical processes, or biological post-treatment.

4 Extension to Complex Real Wastewaters

This thesis focused primarily on model pollutants (methylene blue, n-docosane) in synthetic saline and hardness matrices. Future studies should investigate real produced water and other complex industrial effluents, which may contain surfactants, aromatics, heavy metals, and other co-contaminants that influence scaling, adsorption, and oxidant demand. Pilot-scale studies under realistic operating conditions will be critical to evaluate scalability and robustness.

5 Techno-Economic and Environmental Assessment

To transition from laboratory findings to industrial application, future work should conduct comprehensive techno-economic analyses considering electrode lifetime, energy consumption, maintenance frequency, and capital costs. In parallel, life cycle assessment (LCA) should be carried out to evaluate the overall environmental footprint of alternating polarity–assisted EO systems compared to conventional treatments. These assessments will provide a solid basis for evaluating feasibility and guiding scale-up.

In summary, future work should integrate reactor control strategies, advanced electrode development, by-product management, testing in real wastewaters, and techno-economic analysis. Such efforts will enable alternating polarity–assisted EO to evolve from a promising laboratory approach into a reliable, sustainable, and scalable solution for the treatment of high-salinity and high-hardness wastewaters.

REFERENCE

Abdalrhman, A.S. and Gamal El-Din, M. 2020. Degradation of organics in real oil sands process water by electro-oxidation using graphite and dimensionally stable anodes. Chem. Eng. J. 389.

Abdollahi, J., Moghaddam, M.R.A. and Habibzadeh, S. 2025. Uncovering the key determinants of electrode passivation and faradaic efficiency in electrocoagulation: Depassivation and sustainable performance via polarity reversal. Environ. Res., 121889.

Al-Tameemi, H.M., Sukkar, K.A. and Abbar, A.H. 2024. Electrochemical Treatment of Petroleum Refinery Wastewater Using SnO2 and Graphite Anodes. Petroleum Chemistry 64(1), 144-150.

Alnaimat, S., Mohsen, O. and Elnakar, H. 2024. Perfluorooctanoic Acids (PFOA) removal using electrochemical oxidation: A machine learning approach. J. Environ. Manage. 370, 122857.

Alsharyani, A.K. and Muruganandam, L. 2024. Fabrication of zinc oxide nanorods for photocatalytic degradation of docosane, a petroleum pollutant, under solar light simulator. RSC Adv 14(13), 9038-9049.

Anglada, A., Urtiaga, A. and Ortiz, I. 2009. Contributions of electrochemical oxidation to waste-water treatment: fundamentals and review of applications. Journal of Chemical Technology & Biotechnology 84(12), 1747-1755.

Arenas, L.F., De León, C.P. and Walsh, F.C. 2019. Three-dimensional porous metal electrodes: Fabrication, characterisation and use. Current Opinion in Electrochemistry 16, 1-9.

Arias, A.N., de Mello, R., Lobato, J., Motheo, A.J. and Rodrigo, M.A. 2022. Electrolytic removal of volatile organic compounds: Keys to understand the process. J. Electroanal. Chem. 912.

Asaithambi, P., Govindarajan, R., Yesuf, M.B. and Alemayehu, E. 2020. Removal of color, COD and determination of power consumption from landfill leachate wastewater using an electrochemical advanced oxidation processes. Sep. Purif. Technol. 233.

Ates, M. 2011. Review study of electrochemical impedance spectroscopy and equivalent electrical circuits of conducting polymers on carbon surfaces. Prog. Org. Coat. 71(1), 1-10.

Backhurst, J., Coulson, J., Goodridge, F., Plimley, R. and Fleischmann, M. 1969. A preliminary investigation of fluidized bed electrodes. J. Electrochem. Soc. 116(11), 1600.

Bagastyo, A.Y., Radjenovic, J., Mu, Y., Rozendal, R.A., Batstone, D.J. and Rabaey, K. 2011. Electrochemical oxidation of reverse osmosis concentrate on mixed metal oxide (MMO) titanium coated electrodes. Water Res. 45(16), 4951-4959.

Bao, H.J., Wu, M.R., Meng, X.S., Han, H.S., Zhang, C.Y. and Sun, W. 2023. Application of electrochemical oxidation technology in treating high-salinity organic ammonia-nitrogen wastewater. Journal of Environmental Chemical Engineering 11(5).

Barba, S., Villaseñor, J., Rodrigo, M.A. and Cañizares, P. 2017. Effect of the polarity reversal frequency in the electrokinetic-biological remediation of oxyfluorfen polluted soil. Chemosphere 177, 120-127.

Bensalah, N., Ahmadi, M.F. and Martinez-Huitle, C.A. 2021. Electrochemical oxidation of 2-chloroaniline in single and divided electrochemical flow cells using boron doped diamond anodes. Sep. Purif. Technol. 263, 118399.

Bian, Y., Ge, Z., Albano, C., Lobo, F.L. and Ren, Z.J. 2019. Oily bilge water treatment using DC/AC powered electrocoagulation. Environmental Science: Water Research & Technology 5(10), 1654-1660.

Bilińska, L., Gmurek, M. and Ledakowicz, S. 2017. Textile wastewater treatment by AOPs for brine reuse. Process Saf. Environ. Prot. 109, 420-428.

Blasco-Gomez, R., Batlle-Vilanova, P., Villano, M., Balaguer, M.D., Colprim, J. and Puig, S. 2017. On the Edge of Research and Technological Application: A Critical Review of Electromethanogenesis. Int J Mol Sci 18(4).

Boczkaj, G. and Fernandes, A. 2017. Wastewater treatment by means of advanced oxidation processes at basic pH conditions: A review. Chem. Eng. J. 320, 608-633.

Cao, D., Wang, Y. and Zhao, X. 2017. Combination of photocatalytic and electrochemical degradation of organic pollutants from water. Current Opinion in Green and Sustainable Chemistry 6, 78-84.

Cataldo, S., Iannì, A., Loddo, V., Mirenda, E., Palmisano, L., Parrino, F. and Piazzese, D. 2016. Combination of advanced oxidation processes and active carbons adsorption for the treatment of simulated saline wastewater. Sep. Purif. Technol. 171, 101-111.

Chen, W.T., He, X., Jiang, Z.K., Li, B., Li, X.Y. and Lin, L. 2023. A capacitive deionization and electro-oxidation hybrid system for simultaneous removal of heavy metals and organics from wastewater. Chem. Eng. J. 451.

Chow, H., Ingelsson, M., Roberts, E.P. and Pham, A.L.-T. 2021. How does periodic polarity reversal affect the faradaic efficiency and electrode fouling during iron electrocoagulation? Water Res. 203, 117497.

Chow, H. and Pham, A.L.-T. 2021. Mitigating electrode fouling in electrocoagulation by means of polarity reversal: the effects of electrode type, current density, and polarity reversal frequency. Water Res. 197, 117074.

Chuang, Y.H., Chen, S., Chinn, C.J. and Mitch, W.A. 2017. Comparing the UV/Monochloramine and UV/Free Chlorine Advanced Oxidation Processes (AOPs) to the UV/Hydrogen Peroxide AOP Under Scenarios Relevant to Potable Reuse. Environ Sci Technol 51(23), 13859-13868.

Clematis, D. and Panizza, M. 2021. Application of boron-doped diamond electrodes for electrochemical oxidation of real wastewaters. Current Opinion in Electrochemistry 30, 100844.

da Silva Santos, D.H., Xiao, Y., Chaukura, N., Hill, J.M., Selvasembian, R., Zanta, C.L.S. and Meili, L. 2022. Regeneration of dye-saturated activated carbon through advanced oxidative processes: A review. Heliyon 8(8).

Enache, T.A. and Oliveira-Brett, A.M. 2011. Phenol and para-substituted phenols electrochemical oxidation pathways. J. Electroanal. Chem. 655(1), 9-16.

Feng, H., Liao, X., Yang, R., Chen, S., Zhang, Z., Tong, J., Liu, J. and Wang, X. 2023. Generation, toxicity, and reduction of chlorinated byproducts: Overcome

bottlenecks of electrochemical advanced oxidation technology to treat high chloride wastewater. Water Res. 230, 119531.

Fernandes, A., Santos, D., Pacheco, M., Ciríaco, L. and Lopes, A. 2016. Electrochemical oxidation of humic acid and sanitary landfill leachate: influence of anode material, chloride concentration and current density. Sci. Total Environ. 541, 282-291.

Fuladpanjeh-Hojaghan, B., Shah, R.S., Roberts, E.P. and Trifkovic, M. 2023. Effect of polarity reversal on floc formation and rheological properties of a sludge formed by the electrocoagulation process. Water Res. 242, 120201.

Guo, L., Xie, Y.M., Sun, W.Q., Xu, Y.H. and Sun, Y.J. 2023. Research Progress of High-Salinity Wastewater Treatment Technology. Water 15(4).

Guo, N., Wang, Y.K., Tong, T.Z. and Wang, S.G. 2018. The fate of antibiotic resistance genes and their potential hosts during bio-electrochemical treatment of high-salinity pharmaceutical wastewater. Water Res. 133, 79-86.

Haider, M.R., Jiang, W.L., Han, J.L., Mahmood, A., Djellabi, R., Liu, H., Asif, M.B. and Wang, A.J. 2023. Boosting Hydroxyl Radical Yield via Synergistic Activation of Electrogenerated HOCl/H(2)O(2) in Electro-Fenton-like Degradation of Contaminants under Chloride Conditions. Environ Sci Technol 57(47), 18668-18679.

Hand, S. and Cusick, R.D. 2021. Electrochemical Disinfection in Water and Wastewater Treatment: Identifying Impacts of Water Quality and Operating Conditions on Performance. Environ Sci Technol 55(6), 3470-3482.

Hanssen, B.L., Siraj, S. and Wong, D.K. 2016. Recent strategies to minimise fouling in electrochemical detection systems. Rev. Anal. Chem 35(1), 1-28.

He, H.J., Chen, Y.J., Li, X., Cheng, Y., Yang, C.P. and Zeng, G.M. 2017. Influence of salinity on microorganisms in activated sludge processes: A review. Int. Biodeterior. Biodegrad. 119, 520-527.

Hoseinzadeh, E. and Rezaee, A. 2015. Electrochemical degradation of RB19 dye using low-frequency alternating current: effect of a square wave. RSC Advances 5(117), 96918-96926.

Ingelsson, M. 2021. Investigating Electrode Polarity Reversal as a Performance Enhancement Strategy in Electrochemical Water Treatment Processes.

Isaev, A.B., Shabanov, N.S., Magomedova, A.G., Nidheesh, P. and Oturan, M.A. 2023. Electrochemical oxidation of azo dyes in water: a review. Environmental Chemistry Letters 21(5), 2863-2911.

Jahn, L.G., Wang, D.S., Dhulipala, S.V. and Ruiz, L.H. 2021. Gas-phase chlorine radical oxidation of alkanes: Effects of structural branching, NO x, and relative humidity observed during environmental chamber experiments. The Journal of Physical Chemistry A 125(33), 7303-7317.

Jajuli, M.N., Mohamed, N. and Suah, F.B.M. 2020. Electrochemical removal of cadmium from a sulphate solution using a three-dimensional electrode. Alexandria Engineering Journal 59(6), 4237-4245.

Jang, G.G., Castillo, C., Dutta, S., Su, Y.-F., Jun, J., Keum, J.K., Kim, K., Chellam, S. and Tsouris, C. 2024. Performance restoration of iron electrodes by polarity reversal after long-term surface fouling in wastewater electrocoagulation. ACS ES&T Water 4(6), 2390-2402.

Jeong, J., Kim, C. and Yoon, J. 2009. The effect of electrode material on the generation of oxidants and microbial inactivation in the electrochemical disinfection processes. Water Res. 43(4), 895-901.

Jin, H., Yu, Y., Zhang, L., Yan, R. and Chen, X. 2019. Polarity reversal electrochemical process for water softening. Sep. Purif. Technol. 210, 943-949.

Kern, H., Piechocki, A., Brauer, U. and Findenegg, G. (2007) Progress in Colloid & Polymer Science: Lösungen und Adsorption, pp. 118-124, Springer.

Kern, H.E. and Findenegg, G.H. 1980. Adsorption from solution of long-chain hydrocarbons onto graphite: surface excess and enthalpy of displacement isotherms. J. Colloid Interface Sci. 75(2), 346-356.

Lee, J., Von Gunten, U. and Kim, J.-H. 2020. Persulfate-based advanced oxidation: critical assessment of opportunities and roadblocks. Environ. Sci. Technol. 54(6), 3064-3081.

Lei, Y., Lei, X., Westerhoff, P., Zhang, X. and Yang, X. 2020. Reactivity of chlorine radicals (Cl• and Cl2•–) with dissolved organic matter and the formation of chlorinated byproducts. Environ. Sci. Technol. 55(1), 689-699.

Lei, Y., Soares da Costa, M., Zhan, Z., Saakes, M., van der Weijden, R.D. and Buisman, C.J. 2022. Electrochemical phosphorus removal and recovery from cheese wastewater: function of polarity reversal. ACS ES&T Engineering 2(12), 2187-2195.

Li, J., Li, Y., Xiong, Z., Yao, G. and Lai, B. 2019. The electrochemical advanced oxidation processes coupling of oxidants for organic pollutants degradation: a mini-review. Chin. Chem. Lett. 30(12), 2139-2146.

Li, S., Meng, D., Zhang, G. and Yang, F. 2024a. Periodic polarity reversal triggered sequential electrochemical redox of blue TiO2 nanotube arrays for efficient removal of antibiotics and inorganic nitrogen from actual mariculture wastewater. Chem. Eng. J. 499, 156651.

Li, X.Y., Ding, F., Lo, P.S.Y. and Sin, S.H.P. 2002. Electrochemical disinfection of saline wastewater effluent. Journal of Environmental Engineering-Asce 128(8), 697-704.

Li, Y., Zhang, G., Liang, D., Wang, X. and Guo, H. 2024b. Tetracycline hydrochloride degradation in polarity inverted microbial fuel cells: Performance, mechanisms and microbiology. Chemosphere 349, 140902.

Li, Z.S., Gao, X.L., Miao, D.T., Yang, W.L., Xie, Y.Q., Ma, L. and Wei, Q.P. 2021. Effects of process parameters on the degradation of high salinity industrial wastewater. Water Quality Research Journal 56(1), 31-44.

Lin, S.H., Shyu, C.T. and Sun, M.C. 1998. Saline wastewater treatment by electrochemical method. Water Res. 32(4), 1059-1066.

Liu, J., Zhou, M., Zhang, Y., Liu, P., Liu, Z., Xie, Y., Cai, W., Yu, F., Zhou, Q. and Wang, X. 2017. Electrochemical oxidation of carbon at high temperature: principles and applications. Energy & Fuels 32(4), 4107-4117.

Liu, X., You, S., Ma, F. and Zhou, H. 2021a. Characterization of electrode fouling during electrochemical oxidation of phenolic pollutant. Frontiers of Environmental Science & Engineering 15, 1-10.

Liu, X., You, S., Ma, F. and Zhou, H. 2021b. Characterization of electrode fouling during electrochemical oxidation of phenolic pollutant. Frontiers of Environmental Science & Engineering 15(4), 53.

Lu, Y.W., Wang, Y., Liu, Y.R. and Liu, H. 2024. Square-wave alternating voltage driving promotes nanowire-assisted electroporation inactivation and fouling resistance of pathogenic bacteria for water disinfection. Chem. Eng. J. 480.

Luo, T., Peng, Y., Chen, L., Li, J., Wu, F. and Zhou, D. 2020. Metal-Free Electro-Activated Sulfite Process for As(III) Oxidation in Water Using Graphite Electrodes. Environ Sci Technol 54(16), 10261-10269.

Luo, Y.L., Awoyemi, O.S., Gopalan, S., Nolan, A., Robinson, F., Fenstermacher, J., Xu, L., Niu, J.F., Megharaj, M., Naidu, R. and Fang, C. 2023. Investigating the effect of polarity reversal of the applied current on electrochemical degradation of per- and polyfluoroalkyl substances. Journal of Cleaner Production 433.

Mandal, P., Dubey, B.K. and Gupta, A.K. 2017. Review on landfill leachate treatment by electrochemical oxidation: Drawbacks, challenges and future scope. Waste Management 69, 250-273.

Mandal, P., Gupta, A.K. and Dubey, B.K. 2020. Role of inorganic anions on the performance of landfill leachate treatment by electrochemical oxidation using graphite/PbO2 electrode. Journal of Water Process Engineering 33, 101119.

Martínez-Huitle, C.A. and Brillas, E. 2009. Decontamination of wastewaters containing synthetic organic dyes by electrochemical methods: A general review. Applied Catalysis B: Environmental 87(3-4), 105-145.

Martínez-Huitle, C.A. and Brillas, E. 2021. A critical review over the electrochemical disinfection of bacteria in synthetic and real wastewaters using a boron-doped diamond anode. Curr. Opin. Solid State Mater. Sci. 25(4).

Martinez-Huitle, C.A. and Ferro, S. 2006. Electrochemical oxidation of organic pollutants for the wastewater treatment: direct and indirect processes. Chem. Soc. Rev. 35(12), 1324-1340.

Martínez-Huitle, C.A. and Panizza, M. 2018. Electrochemical oxidation of organic pollutants for wastewater treatment. Current Opinion in Electrochemistry 11, 62-71.

Mehrkhah, R., Park, S.Y., Lee, J.H., Kim, S.Y. and Lee, B.H. 2023. Prospective performance assessment of enhanced electrochemical oxidation technology: insights into fundamentals and influencing factors for reducing energy requirements in industrial wastewater treatment. Environmental Technology & Innovation 32, 103336.

Najafinejad, M.S., Chianese, S., Fenti, A., Iovino, P. and Musmarra, D. 2023. Application of electrochemical oxidation for water and wastewater treatment: an overview. Molecules 28(10), 4208.

Ontiveros, R., Diakite, L., Alvarez, M.E. and Coras, P. 2013. Wastewater salinity assessment using near infrared spectroscopy. Water Sci. Technol. 68(4), 879-886.

Panizza, M., Barbucci, A., Ricotti, R. and Cerisola, G. 2007. Electrochemical degradation of methylene blue. Sep. Purif. Technol. 54(3), 382-387.

Panizza, M. and Cerisola, G. 2009. Direct and mediated anodic oxidation of organic pollutants. Chem. Rev. 109(12), 6541-6569.

Periyasamy, S. and Muthuchamy, M. 2018. Electrochemical oxidation of paracetamol in water by graphite anode: effect of pH, electrolyte concentration and current density. Journal of environmental chemical engineering 6(6), 7358-7367.

Pikaar, I., Rozendal, R.A., Yuan, Z., Keller, J. and Rabaey, K. 2011. Electrochemical sulfide oxidation from domestic wastewater using mixed metal-coated titanium electrodes. Water Res. 45(17), 5381-5388.

Qi, H., Sun, X. and Sun, Z. 2021. Porous graphite felt electrode with catalytic defects for enhanced degradation of pollutants by electro-Fenton process. Chem. Eng. J. 403.

Radha, K.V. and Sirisha, K. (2018) Advanced oxidation processes for waste water treatment, pp. 359-373, Elsevier.

Rajasekhar, B., Nambi, I.M. and Govindarajan, S.K. 2021. Investigating the degradation of nC12 to nC23 alkanes and PAHs in petroleum- contaminated water by electrochemical advanced oxidation process using an inexpensive Ti/Sb-SnO2/PbO2 anode. Chem. Eng. J. 404.

Rocha, J.H.B., Gomes, M.M.S., Fernandes, N.S., da Silva, D.R. and Martínez-Huitle, C.A. 2012. Application of electrochemical oxidation as alternative treatment of produced water generated by Brazilian petrochemical industry. Fuel Process. Technol. 96, 80-87.

Salehi, M. 2022. Global water shortage and potable water safety; Today's concern and tomorrow's crisis. Environ. Int. 158, 106936.

Saracco, G., Solarino, L., Aigotti, R., Specchia, V. and Maja, M. 2000. Electrochemical oxidation of organic pollutants at low electrolyte concentrations. Electrochim. Acta 46(2-3), 373-380.

Sarfo, D.K., Kaur, A., Marshall, D.L. and O'Mullane, A.P. 2023. Electrochemical degradation and mineralisation of organic dyes in aqueous nitrate solutions. Chemosphere 316, 137821.

Scialdone, O. 2009. Electrochemical oxidation of organic pollutants in water at metal oxide electrodes: A simple theoretical model including direct and indirect oxidation processes at the anodic surface. Electrochim. Acta 54(26), 6140-6147.

Scialdone, O., Randazzo, S., Galia, A. and Silvestri, G. 2009. Electrochemical oxidation of organics in water: role of operative parameters in the absence and in the presence of NaCl. Water Res. 43(8), 2260-2272.

Shestakova, M. and Sillanpää, M. 2017. Electrode materials used for electrochemical oxidation of organic compounds in wastewater. Reviews in Environmental Science and Bio/Technology 16(2), 223-238.

Shi, H., Wang, Q., Ni, J., Xu, Y., Song, N. and Gao, M. 2020. Highly efficient removal of amoxicillin from water by three-dimensional electrode system within granular

activated carbon as particle electrode. Journal of Water Process Engineering 38, 101656.

Sivodia, C. and Sinha, A. 2020. Assessment of graphite electrode on the removal of anticancer drug cytarabine via indirect electrochemical oxidation process: Kinetics & pathway study. Chemosphere 243, 125456.

Stasinakis, A.S. 2008. Use of selected advanced oxidation processes (AOPs) for wastewater treatment–a mini review. Global NEST journal 10(3), 376-385.

Tian, C., Dai, R., Chen, M., Wang, X., Shi, W., Ma, J. and Wang, Z. 2022. Biofouling suppresses effluent toxicity in an electrochemical filtration system for remediation of sulfanilic acid-contaminated water. Water Res. 219, 118545.

Valdes, H., Saavedra, A., Flores, M., Vera-Puerto, I., Avina, H. and Belmonte, M. 2021. Reverse Osmosis Concentrate: Physicochemical Characteristics, Environmental Impact, and Technologies. Membranes (Basel) 11(10).

Wang, J. and Guo, X. 2020. Adsorption kinetic models: Physical meanings, applications, and solving methods. J. Hazard. Mater. 390, 122156.

Wang, J.L. and Xu, L.J. 2012. Advanced Oxidation Processes for Wastewater Treatment: Formation of Hydroxyl Radical and Application. Crit. Rev. Environ. Sci. Technol. 42(3), 251-325.

Wang, W., Wang, J., Wang, J., Wang, H., Wang, C. and Ji, X. 2024. Enhanced treatment of p-nitrophenol and coking wastewater through electrochemical and electrochemical-ozonation coupling process utilizing a novel Ti4O7 reactive electrochemical membrane anode. Journal of Environmental Chemical Engineering 12(3), 112549.

Yang, X.L., Wang, Q., Li, T., Xu, H. and Song, H.L. 2022. Antibiotic removal and antibiotic resistance genes fate by regulating bioelectrochemical characteristics in microbial fuel cells. Bioresour. Technol. 348, 126752.

Yang, Y. 2020. Recent advances in the electrochemical oxidation water treatment: Spotlight on byproduct control. FRONTIERS OF ENVIRONMENTAL SCIENCE & ENGINEERING 14(5).

Yao, S., Swanson, C.S., Cheng, Z., He, Q. and Yuan, H. 2024. Alternating polarity as a novel strategy for building synthetic microbial communities capable of robust Electro-Methanogenesis. Bioresour. Technol. 395, 130374.

Yu, D., Cui, J., Li, X., Zhang, H. and Pei, Y. 2020. Electrochemical treatment of organic pollutants in landfill leachate using a three-dimensional electrode system. Chemosphere 243, 125438.

Yu, T., Chen, H., Hu, T., Feng, J., Xing, W., Tang, L. and Tang, W. 2024. Recent advances in the applications of encapsulated transition-metal nanoparticles in advanced oxidation processes for degradation of organic pollutants: A critical review. Applied Catalysis B: Environmental 342.

Yuan, R., Wang, Z., Hu, Y., Wang, B. and Gao, S. 2014. Probing the radical chemistry in UV/persulfate-based saline wastewater treatment: Kinetics modeling and byproducts identification. Chemosphere 109, 106-112.

Zhang, H., Bao, S., Xu, H., Zhang, Y., Huang, J., Ding, W., Xin, C. and Chen, B. 2025. Biochar-based polarity reversal bipolar electrochemistry coupled with phytoextraction for rapid remediation of lead and zinc-contaminated soil. Chem. Eng. J. 505, 159495.

Zhang, N., Bu, J., Meng, Y., Wan, J., Yuan, L. and Peng, X. 2020. Degradation of p-aminophenol wastewater using Ti-Si-Sn-Sb/GAC particle electrodes in a three-dimensional electrochemical oxidation reactor. Appl. Organomet. Chem. 34(6), e5612.

Zhao, Y., Chang, C., Ji, H. and Li, Z. 2024. Challenges of petroleum wastewater treatment and development trends of advanced treatment technologies: A review. Journal of Environmental Chemical Engineering 12(5).

Zhao, Y.Y., Zhuang, X.M., Ahmad, S., Sung, S. and Ni, S.Q. 2020. Biotreatment of high-salinity wastewater: current methods and future directions. World J. Microbiol. Biotechnol. 36(3).

Zheng, M., He, C. and He, Q. 2015. Fate of free chlorine in drinking water during distribution in premise plumbing. Ecotoxicology 24(10), 2151-2155.

Zhou, L., Li, X., Zhu, B. and Su, B. 2022. An overview of antifouling strategies for electrochemical analysis. Electroanalysis 34(6), 966-975.

Zhu, C., Qin, X., Li, Y., Gong, H., Li, Z., Xu, L. and Dong, M. 2019a. Adsorption and dissolution behaviors of CO2 and n-alkane mixtures in shale: Effects of the alkane type, shale properties and temperature. Fuel 253, 1361-1370.

Zhu, C., Zhang, Z., Xiao, H., Wei, F., Jiang, B., Xiao, F., Zhou, Y. and Luo, X. 2025. Three-dimensionally electrochemical oxidation technology: Current advances, challenges, and prospects for wastewater treatment. Journal of Environmental Chemical Engineering, 117793.

Zhu, K., Wang, X., Ma, X., Sun, Z. and Hu, X. 2019b. Comparative degradation of atrazine by anodic oxidation at graphite and platinum electrodes and insights into electrochemical behavior of graphite anode. Electrocatalysis 10(1), 35-44.

Zou, J., Peng, X., Li, M., Xiong, Y., Wang, B., Dong, F. and Wang, B. 2017. Electrochemical oxidation of COD from real textile wastewaters: kinetic study and energy consumption. Chemosphere 171, 332-338.

APPENDIX

Methylene blue continuous experiment

Time (hr)	Electrode (A/C)	Polarity	Exchange frequency (hr)	pH	Cl_2 (ppm)	Methylene Blue (Absorbance)
0	BDD/Gr	Constant	N/A	6.51	0.650416	1.157
0.5	BDD/Gr	Constant	N/A	7.12	19.2289	0.075
1	BDD/Gr	Constant	N/A	6.97	199.6469	0.011
2	BDD/Gr	Constant	N/A	7.24	506.9451	0.015
4	BDD/Gr	Constant	N/A	7.71	329.924	0.027
6	BDD/Gr	Constant	N/A	7.44	659.0721	0.047
18	BDD/Gr	Constant	N/A	7.53	533.5559	0.078
24	BDD/Gr	Constant	N/A	7.63	1234.715	0.114
0	BDD/Gr	Constant	N/A	6.37	0.641759	1.169
0.5	BDD/Gr	Constant	N/A	7.19	102.6964	0.017
1	BDD/Gr	Constant	N/A	7.19	304.8208	0.009
2	BDD/Gr	Constant	N/A	7.35	605.6268	0.01
4	BDD/Gr	Constant	N/A	7.54	679.6381	0.006
6	BDD/Gr	Constant	N/A	7.63	633.1032	0.019
8	BDD/Gr	Constant	N/A	7.62	304.1642	0.015
24	BDD/Gr	Constant	N/A	7.49	511.9151	0.031
0	BDD/Gr	Constant	N/A	6.55	0.767276	1.136
0.5	BDD/Gr	Constant	N/A	7.23	216.5266	0.013
1	BDD/Gr	Constant	N/A	7.35	508.2436	0.015

2	BDD/Gr	Constant	N/A	7.46	819.2134	0.009
4	BDD/Gr	Constant	N/A	7.63	596.9706	0.011
6	BDD/Gr	Constant	N/A	7.73	888.4637	0.018
8	BDD/Gr	Constant	N/A	7.7	918.7607	0.034
24	BDD/Gr	Constant	N/A	7.74	628.7751	0.017
0	BDD/Gr	Alternating	2	6.35	0.706682	1.191
0.5	BDD/Gr	Alternating	2	8.06	936.0733	0.02
1	BDD/Gr	Alternating	2	8.19	654.7439	0.018
2	BDD/Gr	Alternating	2	8.33	4775.138	0.011
4	BDD/Gr	Alternating	2	7.94	585.4936	0.021
6	BDD/Gr	Alternating	2	8.41	2844.785	0.044
8	BDD/Gr	Alternating	2	8.19	503.2589	0.035
24	BDD/Gr	Alternating	2	8.22	1026.964	0.083
0	BDD/Gr	Alternating	2	6.79	0.728322	1.178
0.5	BDD/Gr	Alternating	2	7.02	260.6737	0.031
1	BDD/Gr	Alternating	2	7.14	637.4313	0.121
2	BDD/Gr	Alternating	2	7.83	464.3056	0.058
4	BDD/Gr	Alternating	2	8.24	1762.749	0.106
6	BDD/Gr	Alternating	2	8.03	1178.449	0.127
8	BDD/Gr	Alternating	2	8.1	2667.331	0.077
24	BDD/Gr	Alternating	2	8.2	2199.892	0.045
0	BDD/Gr	Alternating	2	6.63	0.719666	1.176
0.5	BDD/Gr	Alternating	2	6.99	135.1575	0.038
1	BDD/Gr	Alternating	2	7.08	365.4148	0.023

2	BDD/Gr	Alternating	2	7.32	583.9861	0.018
4	BDD/Gr	Alternating	2	8.17	1741.108	0.015
6	BDD/Gr	Alternating	2	8.25	1503.06	0.012
8	BDD/Gr	Alternating	2	8.05	2814.488	0.021
24	BDD/Gr	Alternating	2	8.23	2961.645	0.05
0	Gr/Gr	Alternating	2	6.75	0.706682	1.239
0.5	Gr/Gr	Alternating	2	9.19	814.8853	0.042
1	Gr/Gr	Alternating	2	8.56	1252.028	0.063
2	Gr/Gr	Alternating	2	8.7	1550.67	0.081
4	Gr/Gr	Alternating	2	8.59	1836.327	0.077
6	Gr/Gr	Alternating	2	8.11	2013.781	0.061
8	Gr/Gr	Alternating	2	7.87	2217.204	0.079
24	Gr/Gr	Alternating	2	8.1	2624.05	0.064
0	Gr/Gr	Alternating	2	6.88	1.126512	1.323
0.5	Gr/Gr	Alternating	2	8.84	503.2589	0.085
1	Gr/Gr	Alternating	2	8.58	853.8386	0.078
2	Gr/Gr	Alternating	2	8.58	962.0422	0.085
4	Gr/Gr	Alternating	2	7.81	866.823	0.094
6	Gr/Gr	Alternating	2	8.34	1992.141	0.077
8	Gr/Gr	Alternating	2	7.8	1970.5	0.072
24	Gr/Gr	Alternating	2	7.53	1935.875	0.083
0	Gr/Gr	Alternating	2	6.52	1.256356	1.335
0.5	Gr/Gr	Alternating	2	7.73	1801.702	0.057
1	Gr/Gr	Alternating	2	7.66	2628.378	0.059

2	Gr/Gr	Alternating	2	7.8	3238.646	0.089
4	Gr/Gr	Alternating	2	9.11	1888.265	0.092
6	Gr/Gr	Alternating	2	9.27	2234.517	0.079
8	Gr/Gr	Alternating	2	7.95	1310.458	0.083
24	Gr/Gr	Alternating	2	8.2	1723.796	0.105
0	Gr/Gr	Alternating	0.5	6.75	0.715338	1.212
0.5	Gr/Gr	Alternating	0.5	6.97	261.9722	0.098
1	Gr/Gr	Alternating	0.5	7.26	379.2649	0.043
2	Gr/Gr	Alternating	0.5	7.2	403.9353	0.1
4	Gr/Gr	Alternating	0.5	7.28	410.4275	0.031
6	Gr/Gr	Alternating	0.5	7.39	578.7923	0.082
8	Gr/Gr	Alternating	0.5	7.33	563.6438	0.093
24	Gr/Gr	Alternating	0.5	6.89	377.5336	0.027
0	Gr/Gr	Alternating	0.5	6.75	0.927417	1.195
0.5	Gr/Gr	Alternating	0.5	7.32	456.3059	0.071
1	Gr/Gr	Alternating	0.5	7.19	465.395	0.064
2	Gr/Gr	Alternating	0.5	7.46	633.7598	0.078
4	Gr/Gr	Alternating	0.5	7.21	521.6608	0.016
6	Gr/Gr	Alternating	0.5	7.24	595.2393	0.083
8	Gr/Gr	Alternating	0.5	7.37	556.7188	0.023
24	Gr/Gr	Alternating	0.5	7.41	598.269	0.098
0	Gr/Gr	Alternating	0.5	6.68	0.797573	1.195
0.5	Gr/Gr	Alternating	0.5	8.12	338.1475	0.071
1	Gr/Gr	Alternating	0.5	8.28	525.989	0.064

2	Gr/Gr	Alternating	0.5	7.84	545.0328	0.078
4	Gr/Gr	Alternating	0.5	7.8	509.9748	0.016
6	Gr/Gr	Alternating	0.5	7.65	467.559	0.083
8	Gr/Gr	Alternating	0.5	7.65	562.7782	0.023
24	Gr/Gr	Alternating	0.5	7.44	619.9097	0.098
0	Gr/Gr	Alternating	4	6.6	1.204418	1.251
0.5	Gr/Gr	Alternating	4	8	762.9475	0.129
1	Gr/Gr	Alternating	4	7.97	1161.137	0.044
2	Gr/Gr	Alternating	4	7.86	1187.106	0.048
4	Gr/Gr	Alternating	4	10.02	1442.466	0.118
6	Gr/Gr	Alternating	4	8.88	1654.545	0.037
8	Gr/Gr	Alternating	4	8.23	1775.733	0.021
24	Gr/Gr	Alternating	4	8.04	3052.536	0.089
0	Gr/Gr	Alternating	4	6.7	2.22586	1.528
0.5	Gr/Gr	Alternating	4	7.14	732.6505	0.123
1	Gr/Gr	Alternating	4	7.2	914.4326	0.172
2	Gr/Gr	Alternating	4	7.21	1277.997	0.19
4	Gr/Gr	Alternating	4	7.51	1524.701	0.115
6	Gr/Gr	Alternating	4	7.64	1628.576	0.12
8	Gr/Gr	Alternating	4	7.58	1745.436	0.093
24	Gr/Gr	Alternating	4	7.53	1606.936	0.137
0	Gr/Gr	Alternating	4	6.74	1.252028	1.193
0.5	Gr/Gr	Alternating	4	7.6	1109.199	0.087
1	Gr/Gr	Alternating	4	7.57	1632.905	0.138

2	Gr/Gr	Alternating	4	7.47	2321.08	0.08
4	Gr/Gr	Alternating	4	7.53	1342.919	0.127
6	Gr/Gr	Alternating	4	8.01	819.2134	0.079
8	Gr/Gr	Alternating	4	9.07	1009.652	0.038
24	Gr/Gr	Alternating	4	9.25	762.9475	0.183

Precipitation accumulation in methylene blue experiment

	Electrode	initial(g)	after(g)	precipitation weight/g	Electrode surface/cm2
DC	C	4.9938	5.4321	0.4383	0.001192002
	C	4.2815	4.7077	0.4262	0.001021978
AC	A	11.0078	11.0406	0.0328	0.00132653
	A	11.0529	11.1074	0.0545	0.001331965
	A	10.9246	10.948	0.0234	0.001316504
	C	7.2304	7.3201	0.0897	0.00172587
	C	6.2524	6.3195	0.0671	0.001492425
	C	7.279	7.3765	0.0975	0.00173747
AC-Gr-ST2	A	8.1521	8.1526	0.0005	0.001945876
	C	5.2186	5.3321	0.1135	0.001245661
	C	7.9366	8.062	0.1254	0.001894437
	A	5.0356	5.0359	0.0003	0.001201979
AC-Gr-ST4	C	7.3084	7.3432	0.0348	0.001744488
	A	6.2915	6.4182	0.1267	0.001501758
	C	5.0258	5.0913	0.0655	0.00119964
	A	7.9354	8.057	0.1216	0.001894151

	C	4.9867	5.1152	0.1285	0.001190307
	A	7.9461	8.1374	0.1913	0.001896705
AC-Gr-ST0.5	C	7.3443	7.4894	0.1451	0.001753057
	A	6.2963	6.361	0.0647	0.001502904
	C	7.1456	7.4527	0.3071	0.001705628
	A	4.9099	5.1624	0.2525	0.001171975
	C	5.4505	5.6345	0.184	0.001301014
	A	4.8576	5.0356	0.178	0.001159491

Free chlorine standard curve

Cl_2 Conc. (ppm)	**Absorbance**
8.4	1.878
4.2	1.231
0.42	0.14
0.105	0.042
8.4	1.954
4.2	1.078
0.42	0.132
0.105	0.031
8.4	1.973
4.2	0.858
8.4	1.967
4.2	0.972

n-docosane standard curve

C22 Conc (M)	GC Time	GC Area	GC Height
1.00226E-05	10.989	31.9	10.5
1.00226E-05	10.989	29.4	9.7
1.00226E-05	10.988	33.7	11
5.05318E-05	10.989	152.5	49.9
5.05318E-05	10.987	154.7	49
5.05318E-05	10.988	143.7	48.2
0.000509912	10.996	1609.4	494.1
0.000509912	10.996	1586.4	477
0.000509912	10.994	1668.6	497.4
0.056372944	11.235	148273	14919.3
0.056372944	11.246	169946.7	15481.7
0.056372944	11.273	207075.2	16691.6

n-docosane semi-continuous experiments

Time (hr)	Electrode (A/C)	Polarity	exchange frequency (hr)	n-docosane inffluent (g/L)	pH	Cl_2 ppm	n-docosane effluent (g/L)
0	BDD/Gr	Constant	N/A	10.089	6.49	0.36043	10.089
24	BDD/Gr	Constant	N/A	10.028	6.9	1836.327	4.349485425
48	BDD/Gr	Constant	N/A	10.008	7.16	3900.852	0.361924461
72	BDD/Gr	Constant	N/A	10.028	7.1	3035.223	1.024644867
96	BDD/Gr	Constant	N/A	10.066	7.36	4433.214	1.573736882
120	BDD/Gr	Constant	N/A	10.066	7.46	4030.697	1.773259316

BDD absorbed mass 0.023g n-docosane					Gr absorbed mass 0.497 g n-docosane		
0	BDD/Gr	Constant	N/A	10.02	6.6	0.135367	10.02
24	BDD/Gr	Constant	N/A	10.042	6.85	1857.968	1.598460837
48	BDD/Gr	Constant	N/A	10.076	6.83	3866.227	0.190625095
72	BDD/Gr	Constant	N/A	10.004	7	3900.852	2.672456274
96	BDD/Gr	Constant	N/A	10.108	7.46	4030.697	4.052011153
120	BDD/Gr	Constant	N/A	10.108	7.21	3052.536	4.813505703
BDD absorbed mass 0.0003g n-docosane					BDD absorbed mass 0.23g n-docosane		
0	Gr/Gr	Alternating	2	9.983	6.47	0.628775	9.983
24	Gr/Gr	Alternating	2	10.15	6.35	4835.732	6.304969624
48	Gr/Gr	Alternating	2	10.028	6.33	3870.555	1.405961741
72	Gr/Gr	Alternating	2	9.992	6.78	3268.943	0.215960235
96	Gr/Gr	Alternating	2	10.104	6.89	3147.755	4.089230306
120	Gr/Gr	Alternating	2	10.088	7.16	2572.112	0.408564543
144	Gr/Gr	Alternating	2	10.088	7.28	1347.247	1.637282723
Gr1 absorbed mass 0.115g n-docosane					Gr2 absorbed mass 0.129g n-docosane		
0	Gr/Gr	Alternating	2	10.056	6.81	0.364758	10.056
24	Gr/Gr	Alternating	2	10.086	6.58	4775.138	1.520346438
48	Gr/Gr	Alternating	2	10.06	6.89	3632.507	0.238508812
72	Gr/Gr	Alternating	2	10.062	6.43	3545.945	0.014071396
96	Gr/Gr	Alternating	2	10.072	6.41	3338.194	0.185350203
120	Gr/Gr	Alternating	2	10.008	6.53	2823.144	3.13527941
144	Gr/Gr	Alternating	2	10.008	7.75	1957.515	0.580515138
Gr1 absorbed mass 0.191g n-docosane					Gr2 absorbed mass 0.283g-n-docosane		

Precipitation accumulation under constant polarity in n-docosane semi-continuous experiment

Experiment No.	Electrode	initial (g)	After (g)	Experiment No.	Electrode	initial (g)	After (g)
No.1	BDD	11.0739	11.1672	No.2	BDD	11.0753	11.2806
	Griphtate	6.4859	9.8095		Griphtate	6.1139	10.0836

n-docosane adsorption kinetics

`	Exp1 (qt g-n-docosane/g-Gr)	Exp1 (qt g-n-docosane/g-Gr)
0	0	0
0.5	0.0328328	0.030079
1	0.0832905	0.087025
2	0.0892388	0.115182
4	0.0917879	0.116586
6	0.1129502	0.116268
8	0.1139056	0.1173

n-docosane adsorption isotherm

Exp1(Ce)	Exp1(qe)	Exp2(Ce)	Exp2(qe)
0.058247	0.020171	0.041482	0.01426183
0.084576	0.026573	0.186483	0.037575847
1.934231	0.104278	2.427552	0.084204506
7.580214	0.114573	4.155581	0.129875985
8.020151	0.126297	8.564106	0.119301874

VITA

Chenyang Wang grew up in Xingtai, Hebei, China. She obtained her Bachelor of Engineering in Environmental and Ecological Engineering from Hengshui University, China, in June 2019. She then pursued her graduate studies at the Chinese Academy of Sciences, where she received the Master of Science in Engineering (Environmental Science) in June 2022. In September 2023, she began her graduate research at the University of Tennessee, Knoxville, as a Master's Candidate in Environmental Engineering in the Department of Civil and Environmental Engineering. She expects to complete the requirements for the Master of Science degree in Civil Engineering at the University of Tennessee in December 2025.